

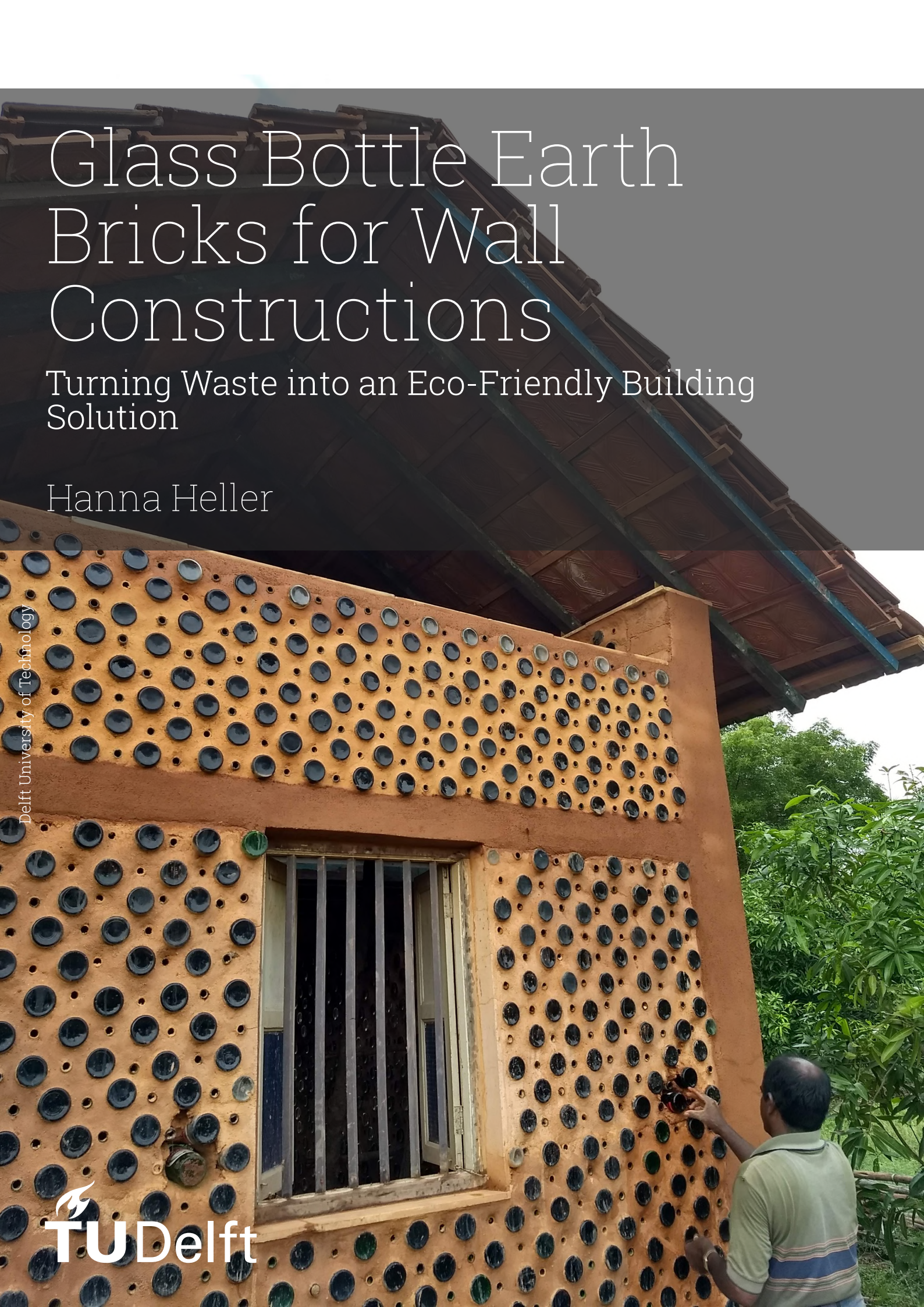
Glass Bottle Earth Bricks for Wall Constructions

Turning Waste into an Eco-Friendly Building Solution

Hanna Heller

Delft University of Technology

 TU Delft



Glass Bottle Earth Bricks for Wall Constructions

Turning Waste into an Eco-Friendly Building
Solution

by

Hanna Heller

Student Name	Student Number
Hanna Heller	4723325

Author: H. (Hanna) Heller
Master Student Building Engineering, Structural Design - TU Delft

Chairman: Prof. dr. ir. P.C. (Christian) Louter
Supervisors: Ir. H. (Hoessein) Alkisaie
Dr. C. (Clarissa) Justino de Lima
Ir. C. (Chris) Noteboom

Project Duration: June, 2023 - April, 2024
Faculty: Faculty of Civil Engineering and Geosciences, Delft

Cover: beer bottle house Miracle, Ousteri Lake Tamil Nade
built by Dilip Patel

Preface

I have a profound interest in innovative and sustainable construction methods. Finding solutions that enhance our living environments and promote sustainability is what truly excites me. During a conversation with H. Alkisaiei, he introduced me to the concept of repurposing glass bottles as a viable building material. The idea of using them in wall constructions immediately intrigued me. Initially, I delved into understanding the complexities of re-purposing glass bottles as a building material, occasionally incorporating them into traditional earthen building techniques. It became clear that there was a lack of engineering research in this area, presenting several challenges. I explored how others were using glass bottles in wall constructions and examined the difficulties they encountered, particularly regarding the irregular shapes of the bottles and the issues with mortar adhesion. Recognizing the need for a solution, the idea was formed of creating a mold to encase the bottles, allowing for the pouring of a liquid earth based mortar to bind the bottles together. Thus, the focus of my thesis emerged: Glass Bottle Earth Bricks for Wall Constructions.

Throughout my research journey, I had the honor of engaging with individuals from diverse backgrounds, including engineers and non-engineers, all of whom shared a keen interest in discussing, exchanging insights, and offering invaluable assistance. I would like to express my sincere gratitude to each of them for their contributions. Special thanks are due to Professor Dr. Ir. P.C. Louter for his role as my chairman and for his expertise in structural glass. I am grateful to Ir. C. Noteboom for his collaborative thinking and constructive feedback. I extend my appreciation to Ir. H. Alkisaiei for his guidance in problem-solving throughout the process. Furthermore, I am grateful to the team at American Glass Research (AGR), particularly Dr. de Lima, for her insightful contributions, assistance with contacts, and expertise in container glass. I also wish to acknowledge Senior Scientist P. de Haan for his valuable insights and all the information he thought. I extend my gratitude to Maiko van Leeuwen for his invaluable guidance in the lab and his concrete knowledge. Special thanks also go to Ton Blom for his assistance with the labor-intensive testing. I am appreciative of Dr. Y. Khulshreshtha for sharing insights on earth buildings, and Dr. A. M. Matos for her expertise in Self-Compacting Earth-Based Composites. I deeply thankful to my parents, Urs and Gracia, as well as my grandparents, Liliane and Cristian, and Ruth and Hans-Rudolf, for their steadfast support, both financially and emotionally. To my friends, I am grateful for your steadfast encouragement throughout this journey.

Ultimately, this journey led to the development of a unique approach to sustainable construction, one that garnered interest and collaboration from diverse experts and enthusiasts alike.

*Hanna Heller
Delft, April 2024*

Abstract

Brazil has a low percentage of recycled container glass due to multiple factors, such as inadequate waste collection and recycling infrastructure, low public awareness about recycling's significance, and insufficient laws to promote it. In addition, the country faces high levels of homelessness and inadequate housing. As a result, an increasing number of builders are exploring repurposing glass bottles as a construction material for walls, occasionally incorporating them into traditional earthen building techniques. Therefore, this thesis investigates the potential of re-purposing glass container bottles for the construction of structural load-bearing walls for affordable housing in Brazil while at the same time reduce pollution, enhance aesthetics, and promote environmental friendliness. Together in collaboration with *AGR American Glass Research* and Delft University of Technology, this thesis investigates the structural feasibility of re-purposing glass bottles in glass bottle earth bricks for wall constructions. The main research question is formulated as follows:

How can the structural feasibility of re-purposing beer bottles in Glass Bottle Earth Bricks (GBEB) for wall constructions be ensured?

The report consists of four parts, which are created for each research area: state of the art, experimental investigations, numerical investigations, and finally the discussion, conclusion and recommendations section.

The literature review underscores a rising trend of incorporating glass bottles into earth-based constructions, driven by their shared advantages of environmental friendliness and affordability. Nevertheless, challenges emerge in connecting glass bottles when constructing walls with mortar due to their irregular shapes. To enhance construction efficiency and quality, innovative methods entail pouring mortar between the bottles rather than applying it manually. This approach is complemented by creating bricks using molds where the bottles are placed inside, facilitating easier stacking and faster execution. The direct integration of glass bottles into bricks further expedites the process. Prefabricating these blocks with pre-placed glass bottles in controlled environments further optimizes efficiency.

During experimental investigations, a self-compacting earth-based mortar mixture is formulated using local Dutch soil from Emmen. Five different mixture designs are explored, utilizing both artificial and natural soil. The mechanical properties of the earth-based mortar mixtures are evaluated through compressive and flexural strength tests, as well as a mini slump flow test to assess workability. The selected earth mixture is anticipated to achieve an average compressive strength of 12.1 MPa after 28 days, an average flexural strength of 3.67 MPa after 7 days, and a flow diameter of 23.05 mm.

Subsequently, a prototype brick containing a horizontally aligned longneck beer bottle is produced, revealing a compressive strength ranging between 8.21 and 11.40 MPa after 28 days of casting.

Upon failure, a fracture analysis indicated that the origin of failure lies at the bottom of the beer bottle, with breaking stresses at failure measuring 608 kg/cm² and 431 kg/cm² for two samples. Results from SEM-EDS analyses reveal iron and aluminium residue at the fracture origin. The earth mortar casted around the bottle showcases a similar composition, suggesting that scratches were likely introduced during brick manufacturing by the earth mixture.

Additionally, an initial evaluation of thermal behavior of the Glass Bottle Earth Brick (GBEB) indicates that the mortar acts as a heat sink, with no observed temperature rises on the unexposed side of the brick after reaching asymptotic temperature. This suggests that the GBEB could contribute to thermal comfort.

Through numerical investigations employing Finite Element Methods (FEM), a comprehensive under-

standing of stress propagation and behavior within a Glass Bottle Earth Brick is achieved. The study reveals that varying the Poisson's ratio and elastic modulus of the earth-based mortar affects peak stresses, particularly at the bottom of the bottle, with higher values resulting in increased stress levels.

While alterations in friction due to glass abrasion and earth composition do not significantly impact stress levels, modeling the brick with the bottle from laboratory experiments aligns with expected peak stresses. However, the Finite Element Method (FEM) model's simplification disregards knurls, the ribbed patterns commonly present on the outer bottom surface of the bottle. Simplifying the model by removing the knurls lowers the computational complexity but potentially overestimating the strength of the GBEB. This underscores the importance of considering knurls to accurately predict peak stresses.

Further investigations explore the optimal arrangement of bottles within bricks, highlighting that alternating bottle placement leads to a more symmetrical stress distribution over the bottle length. However, not alternating the bottles opening, showcase a symmetrical reaction forces over the length the wall. Nevertheless, these asymmetric properties could be counterbalanced by alternating the succeeding row of the GBEB. Both variations exhibit closely comparable peak stresses, making it challenging to choose a favorite bottle arrangement. With these insights, a case study demonstrates the feasibility of constructing low-rise buildings using GBEB masonry units. Assumptions and simplified calculations suggest the potential for constructing a four-story building with limited wall lengths based on these findings.

Based on these findings, it is inferred that re-purposing glass bottles for constructing structural walls capable of supporting small-scale structures is feasible. However, since this represents a novel building approach, it demonstrates potential while also highlighting the need for further investigation and clarification. Increasing the number of samples tested and expanding the range of factors examined can enhance confidence and gain insights in the material results and assumptions made.

Contents

Preface	i
Abstract	ii
Nomenclature	xiii
1 Introduction	1
1.1 Problem Statement	1
1.2 Main Research Question and Sub-questions	2
1.3 Research Methodology	2
1.4 Research Objective	2
1.5 Report Outline	3
State of the Art	4
2 Relevant Case Studies & Building Techniques	5
2.1 WOBO house	5
2.1.1 Construction	5
2.2 Bottle Building by artlife	6
2.2.1 Collection of bottles	6
2.2.2 Preparation of the bottles	6
2.2.3 Construction	6
2.2.4 Repairs	7
2.3 Wat Pa Maha Chedi Kaew: Temple of a Million Bottles	7
2.3.1 Construction	7
2.3.2 Bottle configurations	7
2.4 Beer Bottle House in Tamil Nadu, India	8
2.4.1 Construction	8
2.4.2 Takeaways	8
2.5 Common Raw Earth Building Techniques in Brazil	9
2.5.1 Construction	9
2.5.2 Construction pathology's and repairs	10
2.5.3 Considerations Beyond Interviews and Blogs: Key Insights to Remember	10
3 Glass Pollution & Resource Constraints	14
3.1 Hollow Glass Market of Brazil	14
3.1.1 Production of glass packaging	14
3.1.2 Glass consumption and discard	15
3.2 Recycling and Reusing Glass Waste	15
3.2.1 Recycling of glass waste in Brazil	15
3.2.2 Influencing factors of recycling glass waste	18
3.2.3 The role of informal actors in glass waste management	18
4 Characteristics of the Longneck Beer Bottle	20
4.1 Physical Characteristics	20
4.1.1 Geometrical characteristics	20
4.1.2 Coatings	21
4.2 Knurls	22
4.3 Mechanical Characteristics	23
4.3.1 Surface and Defects: Abraded Bottle Strength	23

4.4	Stress Distribution of Glass Bottles under Loading	23
4.4.1	Glass bottle under vertical load	23
5	Key Insights from the State of the Art and its Influence on the Research	25
5.1	Barriers to Repurpose Glass Bottles in Earth Based Buildings	25
5.1.1	Underdeveloped building techniques	25
5.1.2	Underdeveloped and limited building codes	25
5.1.3	Challenges and knowledge gap	28
5.2	Opportunities For Innovation when Repurposing Glass Bottles In Earth Based Buildings	29
5.2.1	Poured earth: self-compacting earth-based mortar	29
5.2.2	Reflection on case studies	32
5.2.3	Sustainable building material	32
5.2.4	Indoor performance	33
5.2.5	Indirect opportunities	33
5.3	Glass Bottle Earth Brick: The Concept	34
5.3.1	List of requirements	34
5.3.2	Manual handling	35
	Experimental Investigations	37
6	Self-Compacting Earth-Based Mortar	38
6.1	Introduction	38
6.2	Materials	38
6.2.1	Materials list	38
6.2.2	Soil	39
6.2.3	Binders	41
6.2.4	Clay	42
6.2.5	Cement	42
6.2.6	Limestone filler	43
6.2.7	Silt	43
6.2.8	Organic materials	43
6.3	Experimental Methods	44
6.3.1	Experimental program	44
6.3.2	Mixture design	44
6.3.3	Characteristics of fresh mortar: mini cone test	46
6.3.4	Flexural bending test	46
6.3.5	Compressive strength test	47
6.4	Results of Earth Based Mortar (EBM)	47
6.4.1	Self-compactability	47
6.4.2	Mechanical Performance	47
6.5	Discussion	53
6.5.1	Mixture design and self-compactability	53
6.5.2	Mixture design and mechanical performance	54
6.5.3	Compatibility with existing standard (NZS)	54
7	Longneck Beer Bottle Casted in Earth Based Mortar	56
7.1	Introduction	56
7.2	Materials	56
7.3	Compressive Strength Test	57
7.3.1	Experimental program	57
7.3.2	Results	57
7.3.3	Conclusion and discussion	59
7.4	Fracture Analysis	59
7.4.1	Experimental program	59
7.4.2	Results	59
7.4.3	Conclusion and discussion	60
7.5	Thermodynamics of the Brick as a Result of Sunlight Exposure	62
7.5.1	Experimental program	62

7.5.2	Results	63
7.5.3	Discussion and conclusion	64
Numerical Investigations		66
8	Investigations on Stress Concentration of a Longneck Beer Bottle(s) Casted in Earth-Based Mortar	67
8.1	Introduction	67
8.2	Material Properties	68
8.2.1	Material properties of earth-based mortar	68
8.2.2	Material properties of soda-lime container glass	69
8.3	Finite Element Model (FEM)	73
8.3.1	FEM: SolidWorks 2023	74
8.3.2	FEM: DIANA FEA 10.7	75
8.4	Sensitivity Studies	81
8.5	Effect of Knurls	83
8.6	Referring to True Response: FEM Analysis and Laboratory Performance of Bricks	85
8.6.1	FEA: Resistance of the GBEB	85
8.6.2	FEA of Laboratory Performance	87
8.6.3	Longterm resistance of the GBEB	89
8.6.4	Visual comparative analysis: FEM Model versus compression test results	90
8.7	Bottle Arrangement within the Brick	91
8.7.1	alternating vs. non-alternating placement in bricks	91
8.7.2	Influence of horizontal distance between bottles	94
8.7.3	3D FEA: SolidWorks 2023	95
9	Design of Glass Bottle Earth Brick Masonry (GBEB)	99
9.1	Introduction	99
9.1.1	Limit states and load combinations	100
9.1.2	Masonry unit	100
9.2	Case Study: Earth Bottle Brick Masonry Design Using Limit State Method	102
9.2.1	Example three storey load bearing masonry building	103
9.3	Case Study: Final Takeaways	107
Discussion, Conclusions and Recommendations		108
10	Discussion and Conclusion	109
10.1	Discussion	109
10.1.1	Glass Bottles: Exploring Their Role in Wall Configuration Case Studies	109
10.1.2	Interconnecting Glass Bottles: Methods and Load Response in Several Arrangements	110
10.1.3	Limitations and Challenges	110
10.2	Conclusion	111
11	Research Recommendations	113
11.1	Self Compacting Earth Based Mortar	113
11.1.1	Optimizing mixture design	113
11.1.2	Investigating granulometry distribution and soil composition	113
11.1.3	Moisture content influence	113
11.1.4	Alignment with building standards	113
11.2	Glass bottles	114
11.3	Glass Bottle Earth Brick (GBEB)	114
11.3.1	Assumption verification	114
11.3.2	Brick design and optimization	114
11.3.3	Further research	114
References		116
A	Beer bottle Longneck 33 cl, brown, 26 mm Brouwland	120
B	Technical Data Sibelco Deutschland GmbH	122

C SEM-EDS analysis results	125
C.1 Composition of Raw Earth	126
C.2 Composition of Earth Based Mortar	127
C.3 Sample 2: Cleavage Scratch	128
C.4 Sample 2: Next to Cleavage Scratch	129
C.5 Sample 3: Cleavage Scratch	130
D APPROXIMATE TENSILE BREAKING STRESSES OF SODA LIME GLASS (psi)	131
E GBEB: 'Eco'	133
E.1 Technical Drawing	133
E.2 FEM: Principal Stresses	134
E.3 Design Resistance	135
F GBEB: 'Eco-Sturdy'	136
F.1 Technical Drawing	136
F.2 FEM: Principal stresses	137
F.3 Design Resistance	138
G GBEB: 'Sturdy'	139
G.1 Technical Drawing	139
G.2 FEM: Principal Stresses	140
G.3 Design Resistance	141

List of Figures

2.1	WOBO shed on Mr. Heineken's estate in Noordwijk (1963) [16]	5
2.2	glass house (artlife, n.d.) [4]	6
2.3	Wat Pa Maha Chedi Kaew (hippie pants, 2015)	7
2.4	Bottle configurations in Wat Pa Maha Chedi Kaew temple (edited by H. Heller)	8
2.5	Beer bottle house in Tamil Nadu, India [3]	8
2.6	Construction method bottle house in Tamil Nadu, [3]	9
2.7	Cob and Cordwood technique using glass bottles, [39]	9
2.8	Earth based building techniques in Brazil (edited by H. Heller)	11
3.1	Hollow Glass Market in Brazil: Pie chart of production segments by MASSFIX of respectively: beverages, food, pharmaceuticals, cosmetics. [53]	14
3.2	Hollow Glass Market in Brazil: Bar chart of production subdivisions by MASSFIX of respectively: beer, liquor, wine, cachaça, sodas, juices, coffee, other food, pharmaceuticals, cosmetics.[53]	15
3.3	Hollow Glass Market in Brazil: Map of glass consumption within Brazil [53]	18
3.4	Casual loop diagram for stakeholders within the waste management system. Note: The red arrow with a plus symbol denotes a positive cause-and- effect relation, in which two variables change in the same direction; The blue arrow with a minus symbol shows the negative causal influence, in which two variables change in the opposite direction. Double bar (//) indicate lag time between two variables.	19
4.1	Bottle anatomy (Saxco, n.d.)	20
5.1	Precast bottle embedded panel by Mud Hands for a residence in Bangalore	35
5.2	Construction process in a mould by Mud Hands	35
6.1	Granulometry	40
6.2	Sieve analysis Dutch soil originating from Emmen	41
6.3	Pycnometer test with soil from Emmen, the Netherlands	42
6.4	Mini slump flow test (a) and measurement of the flow diameter (b)	46
6.5	Determination of tensile strength: (a) static scheme, loading, and geometry of tested specimens; (b) the view of the specimen ready to test.	46
6.6	Determination of compression strength: (a) static scheme, loading, and geometry of tested specimens; (b) the view of the specimen ready to test.	47
6.7	PCE superplasticizer effect on flow diameter	49
6.8	Slumps of the mini slump flow test	49
6.9	Average flow diameter of Mix ID's A1,A2,A3,N1,N2	50
6.10	Average Flexural Strength after seven days of Mix ID's A1,A2,A3,N1,N2	50
6.11	Average Compressive Strength of Mix ID's A1,A2,A3,N1,N2	51
6.12	Failure mechanisms earth based mortar	51
6.13	Weibull graph of the Compressive Strength of N2 with the linear regression estimator	52
6.14	Weibull graph of the Tensile Strength of N2 with the linear regression estimator	53
6.15	Sp/fines% effect on mechanical strength	54
6.16	w/c effect on mechanical strength	54
7.1	Longneck Beer Bottle Brick Making	57
7.2	Determination of failure and compression strength: (a) static scheme, loading and geometry of tested specimens; (b) specimen ready to test	57
7.3	Images of Failure Around the Heel of the Bottle, Clean Cuts Circled in Red	58

7.4	Images of Failure Along the Height of the Bottle on the Inside	58
7.5	Images of Failure Outside Surface Bottle: Cross-Like Pattern	58
7.6	Location of fracture origin indicated with arrows: Sample 2	59
7.7	Location of fracture origin indicated with arrows: Sample 3	60
7.8	Mirror Measurement - Mirror Diameter of S2 and S3	60
7.9	Sample 2 - Cleavage Scratch under High Magnification	61
7.10	Sample 3 - Cleavage Scratch under High Magnification	61
7.11	SEM-EDS Results: Table with iron (Fe) and aluminium (Al) at fracture origin	61
7.12	SEM-EDS Results: Graph with iron (Fe) and aluminium (Al) at fracture origin	61
7.13	SEM-EDS Analysis Results: earth based mortar (left), raw soil (right)	62
7.14	Test set-up: Sunlight Exposure	63
7.15	Graph Exposed Surface Temperature (outside) EBM_E vs. Not Exposed Surface Temperature (inside) EBM_{NE} , where 6 and 54 represents the age of the brick (days)	63
7.16	Graph Exposed Surface Temperature (outside) Bottom Bottle ($Glass_E$) vs. Not Exposed Surface Temperature (inside) Top Bottle ($Glass_{NE}$)	64
7.17	Crack Pattern Sample 1	64
8.1	comparison of relative strength of soda-lime glass in relationship with load duration: AGR, NEN 2608, EN 16612 and ASTM E1300	72
8.2	Finite Element Method (FEM) SolidWorks: geometry and boundary conditions	74
8.3	Parabolic solid element	74
8.4	Mesh refinement of SolidWorks model: from coarse to fine meshes, with each labeled according to their maximum mesh size	75
8.5	Derivation of 2D simplifications based on 3D model	76
8.6	Geometric properties of 2D model	76
8.7	Geometric properties of 2D model	77
8.8	Modelling Methodology of Alternating vs. Non-Alternating Placement in Bricks using DIANA FEA 10.7	78
8.9	Mesh refinement Model 1 DIANA FEA: Quadratical (first row) and Triangular (second row)	79
8.10	Mesh refinement Model 1 SolidWorks: Voronoi-Delaunay	79
8.11	Graph Convergence Model 1: plane with circular hole	80
8.12	Mesh refinement Model 2 DIANA FEA: Quadratical (first row) and Triangular (second row)	80
8.13	Mesh refinement Model 3 DIANA FEA: Quadratical (first row) and Triangular (second row)	81
8.14	Graph Convergence Model 3: circular hole with disc	81
8.15	Sensitivity study: Poisson's ratio of the Earth Mortar	82
8.16	Sensitivity study: Young's Modulus of the Earth Mortar	83
8.17	Sensitivity study Model 1: Young's modulus EBM stress distribution	83
8.18	Sensitivity study Model 2: Young's modulus EBM stress distribution	83
8.19	Heel impact stress distribution Crescent knurl, W. Hu [36]	84
8.20	Principal stresses of GBEB	86
8.21	Compressive strength of GBEB: comparison of FEA and Laboratory performance	88
8.22	Comparative Analysis: 2D FEM Model versus Physical Compression Test Results	90
8.23	Comparative Analysis: 3D FEM Model versus Physical Compression Test Results	90
8.24	3D bar plot illustrating the distribution of the reaction force [N] for uniform displacement	91
8.25	Distribution of Reaction Forces [N] over the Length of the Brick: Alternating vs. Non-Alternating	92
8.26	Overview of stress plot locations	92
8.27	The relative peak stresses ($\sigma_{peak,bottle}/\sigma_{applied,GBEB}$) from principal stresses (P1, P2, P3) over the length of the bottom bottle on the outside surface (blue)	93
8.28	The relative peak stresses ($\sigma_{peak}/\sigma_{applied}$) from principal stresses (P1, P2, P3) over the length of the bottom bottle on the inside surface (blue)	93
8.29	The relative peak stresses ($\sigma_{peak,bottle}/\sigma_{applied,GBEB}$) from principal stresses (P1, P2, P3) over the length of the bottle on the inside surface (blue)	94
8.30	Principal Stresses P1 for 'large' (left) and 'small' (right) bottle distance, 2D model DIANA FEA	95

8.31	Principal Stresses P2 for 'large' (left) and 'small' (right) bottle distance, 2D model DIANA FEA	95
8.32	Overview of the horizontal distance between bottles ranging from 70 mm up to 300 mm	96
8.33	The relative peak stresses ($\sigma_{peak,glass}/\sigma_{applied,brick}$) from principal stresses (P1, P2, P3) over the length of the bottom bottle on the outside surface (blue) for alternating vs not alternating for different center-to-center distances	96
8.34	The relative peak stresses ($\sigma_{peak}/\sigma_{applied}$) from principal stresses (P1, P2, P3) over the length of the bottom bottle on the inside surface (blue) for different center-to-center distances	97
8.35	The relative peak stresses ($\sigma_{peak}/\sigma_{applied}$) from principal stresses (P1, P2, P3) over the length of the bottle on the inside surface (blue) for different center-to-center distances	97
9.1	Geometry of GBEB: 'Eco' and 'Sturdy'	102
9.2	Floor plan example calculation case study	103
9.3	Cross section at XX	104
C.1	SEM-EDS analysis results with the compositions determined for the earth	126
C.2	SEM-EDS analysis results with the compositions determined for the Earth Based Mortar	127
C.3	SEM-EDS analysis results with the compositions determined for the glass next to the cleavage scratch of sample 2	128
C.4	SEM-EDS analysis results with the compositions determined for the glass next to the cleavage scratch of sample 2	129
C.5	SEM-EDS analysis results with the compositions determined for the Earth Based Mortar	130
D.1	APPROXIMATE TENSILE BREAKING STRESSES OF SODA LIME GLASS (psi)	132
E.1	Orthographic Projection of GBEB 'Eco'	133
E.2	Principal Stresses of GBEB 'Eco'	134
F.1	Orthographic Projection of GBEB 'Eco-Sturdy'	136
F.2	Principal stresses of GBEB 'Eco-Sturdy'	137
G.1	Orthographic Projection of GBEB 'Sturdy'	139
G.2	Principal stresses of GBEB 'Sturdy'	140

List of Tables

1.1	Report Outline	3
2.1	Overview of building techniques superadobe/hyperadobe and cob and cordwood	12
2.2	Overview of building techniques rammed earth and earthen stucco with PET	13
3.1	Estimation of glass production in Brazil by M. Akerman (2023)	16
3.2	Minimum regional and national percentages for the recycling index 2023-2027 [66]	17
3.3	Minimum regional and national percentages for the recycling index 2028-2032 [66]	17
4.1	Geometrical characteristics of longneck beer bottle, 33 cl, by Brouwland	21
5.1	Overview of Building Codes about earth based buildings and scope: Africa, Australia, Brazil, Columbia and Germany [72]	26
5.2	Overview of Building Codes about earth based buildings and scope: India, Kenya, Kyrgyzstan, Nigeria, Peru, Spain, Sri Lanka, Switzerland, Tunisia, Turkey, USA, Zimbabwe [72]	27
5.3	Embodied energy	33
6.1	Material list	39
6.2	Properties Superplasticizer	39
6.3	Specific gravity using Pycnometer	42
6.4	Chemical Analysis of GR-T, red clay powder by Sibelco [28]	43
6.5	Experimental program	44
6.6	Mixture proportions of Earth-Based Mortar	45
6.7	Composition of Artificial Soil of 1585.45 kg/m^3 as used in Table 6.6	45
6.8	Flexural Tensile Strength Test Results	48
6.9	Compressive Strength Test Results after 7 and 28 days of curing	48
6.10	characteristic compressive and tensile strength of EBM, calculation steps linear regression	53
6.11	Comparison Flexural tensile strength according to building code and tests	55
7.1	Sample Geometry of Brick with Longneck Beer Bottle	56
7.2	Results of Compressive Test of Earth Bottle Brick Samples	65
8.1	Material properties of Earth Based Mortar (EBM) as set in FEM Simulation	68
8.2	Load duration factors according to ASTM E1300, calculated to 8/1000 lites probability of breakage	70
8.3	Load duration factors according to the data provided by <i>AGR:American Glass Research</i> , see Appendix D	71
8.4	Comparison of load duration factors for a design load of 50 years: NEN 2608, EN 16612, ASTM E1300 and data by AGR: American Glass Research	72
8.5	Comparison of tensile strength of soda-lime glass for a design load of 50 years according to different standards: EN 16612, NEN 2608 and data by AGR	73
8.6	Material Properties of an abraded Longneck Beer Bottle (severe abrasions) as set in FEM Simulation	73
8.7	Interface properties between glass and earth based mortar: FEM DIANA FEA 10.7	77
8.8	Meshing Properties DIANA FEA: Model 1 plane with circular hole	79
8.9	Meshing Properties Solidworks 2023: Model 1 plane with circular hole.	79
8.10	Meshing Properties DIANA FEA: Model 2 plane with circular hole and ring	80
8.11	Meshing Properties DIANA FEA: Model 3 plane with disc	81
8.12	Heel impact stress indices, W. Hu [36]	84

8.13 FEA Results of Principal Stresses: Referring to Laboratory Performance of Bricks . . .	87
8.14 Failure Probabilities: comparison of FEA and Laboratory performance	89
8.15 Exploring the Impact of Horizontal Bottle Distance: Results from 3D FEM Analysis . . .	98
9.1 Ultimate Limit State (ULS): Load Factors CC2 according to EN 1990	100
9.2 $\Psi_{0;i}$ -factors for buildings according to EN 1990 Table NB.2 - A1.1	100
9.3 Properties of different types of GBEB: 'Eco' and 'Sturdy'	102
9.4 Calculation of the vertical loading on wall C	106
9.5 Stresses wall C and brick strength	107

Nomenclature

Abbreviations

Abbreviation	Definition
AGR	American Glass Research
ASTM	American Society for Testing and Materials
CC2	Consequence Class 2
EN	European Standard
GBEB	Glass Bottle Earth Brick
ISO	International Organization for Standardization
NEN	Dutch Standard
NZS	New Zealand Standard
SCEBM	Self Compacting Earth Based Mortar
SLS	Serviceability Limit State
ULS	Ultimate Limit State

Symbols

Symbol	Definition	Unit
α_{ij}	thermal expansion tensor	[1/K]
γ_G	partial factor for permanent loads	[-]
$\gamma_{Q;1}$	partial factor for variable loads	[-]
ΔT	temperature difference	[K]
ϵ_{ij}	strain tensor	[-]
ρ	density	[kg/m ³]
ν	Poisson's ratio	[-]
$\Psi_{0;i}$	factor for combination of variable load i with the leading variable load	[-]
Φ	capacity reduction factor	[-]
E	modulus of elasticity (Young's Modulus)	[MPa]
f_{ck}	characteristic compressive strength	[MPa]
f_d	design compressive strength	[MPa]

Symbol	Definition	Unit
f_{spe}	the average value of all test results for the set under consideration excluding the suspected abnormal result	[MPa]
f_{spa}	suspected abnormal test result	[MPa]
f'	compressive strength of earth based mortar	[MPa]
G_k	total permanent load	[kN]
m	mass	[kg]
N_{Ed}	the design value of the load	[kN]
N_{Rd}	the design value of the resistance	[kN]
n	number of tests	
$Q_{1;k}$	characteristic value of the leading variable load	[kN]
$Q_{i;k}$	characteristic value of variable load i	[kN]
V	volume	[m ³]
X_a	average test result of a series	
X_s	standard deviation test result of a series	
$X_1, X_2, \dots, X_i \dots X_n$	group of n test results	
x_1, x_2, x_3, x_4	lowest, second lowest, third lowest, fourth lowest test results respectively	

1

Introduction

Unfortunately, there are still many countries where the percentage of recycled glass is low. There are several factors that contribute to this issue, including a lack of proper waste collection and recycling infrastructure, insufficient public awareness about the importance of recycling, and a lack of adequate laws and regulations to promote recycling.

When glass is not recycled, it can be treated in different ways including combustion, landfills and reuse. In Brazil 8.6 million tons of glass is produced annually, of which 300.000 tons get to be recycled [11]. The waste ends up in landfills or is dumped in nature, clogging rivers and polluting the environment.

Another alarming problem Brazil is facing, is the high level of homelessness and inadequate housing. Especially housing for low-income families have drastically decreased. Every one out of fourth Brazilian is homeless or lives in poor housing conditions, with homelessness rates increasing drastically.

As a result, builders are exploring re-purposing glass bottles as a construction material to construct walls, occasionally incorporating them into traditional earthen building techniques. This provides the construction of affordable housing while tackling pollution. In this research, longneck beer bottles as a whole will be repurposed as structural elements in load bearing walls. This while incorporating the glass bottles inside a prefabricated brick. The bottles will be connected to each-other using a self compacting earth based mortar.

1.1. Problem Statement

Informal individuals and communities have been constructing buildings repurposing container glass. In case for walls, mostly a masonry-like method is used where the bottles represent the masonry units which are then connected to each other with a mortar. However, construction pathologies are appearing after some time, resulting from a lack of an engineering approach, building codes and a common familiar construction technique.

This thesis focuses on obtaining the characteristics of a load-bearing wall consisting out of repurposed long neck beer bottles in combination with an earth building technique. The following knowledge gaps will be analysed:

1. How can a load bearing wall be constructed while re-purposing container glass bottles?
2. What should be the configuration of the bottles and how can they be stacked in an efficient way?

3. How do these bottles behave in this type of configuration, what is the strength can be derived?
4. What are the limitations and drawbacks of a wall with repurposed glass bottles?

1.2. Main Research Question and Sub-questions

The following main research question for this thesis will be answered:

How can structural feasibility of re-purposing beer bottles in a Glass Bottle Earth Brick for wall structures be ensured?

In order to formulate an answer to this main question, sub-questions are formulated which are as follows:

- *What specific types of bottles are relevant for this research, and how have they been utilized in case studies focusing on wall configurations?*
- *What method can be employed to interconnect these bottles, and how do they respond to loading within this arrangement?*
- *What are the limitations and challenges of using glass bottles in a structural wall?*

1.3. Research Methodology

To address the initial sub-question, literature research is conducted. Multiple case studies are analysed, focusing on structures re-purposing container glass and raw earth building methods, as well as their hybrid variants. Each case study is examined, exploring construction methodologies, required tools, perceived structural issues, as well as the associated pros and cons. Additionally, an analysis of Brazil's hollow glass market is conducted to gain insights into aspects such as production, recycling, and relevant geographical areas. Furthermore, a relevant container glass bottle is selected for further investigation, in combination with a building technique informed by the findings of the case studies.

The second sub-question will be answered using insights gained from the current state of the art, experimental and numerical investigations. Based on the insights gained from the current state of the art, a building method will be proposed. To understand the mechanical response of these bottles under loading in this configuration, their behavior will be examined including Finite Element Method (FEM) modeling. Upon these findings, laboratory experiments are conducted. This includes the production of samples and analysing their mechanical behaviour by conducting compressive and flexural bending tests.

To answer the last sub-question, the results are reflected on and a conclusion is formed. Also a recommendation for future projects and research will be proposed.

1.4. Research Objective

Following main objectives will be tackled in this thesis:

- Exploring the potential of re-purposing container glass bottles as a building material
- Finding an alignment with current building techniques to derive an innovative yet straightforward building technique
- Structural designing a load bearing wall re-purposing container glass bottles in combination with a raw earth building technique
- Increase knowledge in the mechanical behaviour of container glass bottles in a wall configuration
- Identifying limitations, further research recommendations and possible improvements

This thesis is interesting for following audience:

- Individuals and communities with limited access to conventional building materials and machinery
- Individuals and communities with a desire to create more environmental friendly structures
- Individuals and communities located in areas with low container glass recycling rates
- Individuals and communities drawn to the uniqueness and the aesthetics created when re-purposing container glass in wall structures

1.5. Report Outline

This thesis report is subdivided in four different sections:

1. State of the Art
2. Experimental Investigations
3. Numerical Investigations
4. Discussion, Conclusion and Recommendations

An overview of the report outline is showed in Table 1.1. The table also shows which sections answers the relevant questions 'Q'. Where the acronym 'SQ' stands for sub-question and 'MRQ' stands for main research question.

Table 1.1: Report Outline

Sections	Method	Chapters	Q
<i>State of the Art</i>	Literature Study	2. Relevant Case Studies & Building Techniques	SQ1
		3. Glass Pollution & Resource Constraints	
		4. Characteristics of the Long Neck Beer Bottle	
		5. Key Insights From the State of the Art	
<i>Experimental Investigations</i>	Stevinlab testing	6. Self-Compacting Earth Based Mortar (SCEBM)	SQ2
	AGR experiments	7. Long neck Beer Bottle Casted in SCEBM	
<i>Numerical Investigations</i>	FEM	8. Investigations on Stress Concentrations of Longneck Beer Bottle(s) Casted in SCEBM	
		9. Design of Glass Bottle Earth Brick (GBEB Masonry)	
<i>Discussion Conclusion Recommendations</i>	Review of Results	10. Thesis Discussion, Conclusion and Recommendations	SQ3
			MRQ

State of the Art

2

Relevant Case Studies & Building Techniques

Given the escalating building material prices, growing environmental consciousness, and the pressing need for affordable housing, it comes as no surprise that individuals are exploring unconventional building materials in response to the mounting demand for alternative construction methods. The quest for eco-friendly housing grows, giving rise to an emerging trend known as "earth ships", where individuals construct their own homes using waste materials.

It becomes apparent that certain motivations for construction with glass packaging consistently emerge: environmental friendliness, unique aesthetics, and affordability. These are also reasons why techniques for building with earth are so popular in Brazil, an ancient practice that remains relevant to this day. It is worth noting that a substantial portion, around 30% of the global population, resides in homes made of raw earth [42]. As a result, we sometimes witness the fusion of earth construction techniques with the use of glass bottles. People are experimenting with various methods for building with earth and bottles.

This chapter will delve into these techniques, building motivations, challenges encountered, and overall satisfaction experienced.

2.1. WOBO house



Figure 2.1: WOBO shed on Mr. Heineken's estate in Noordwijk (1963) [16]

During his 1960 world tour of Heineken breweries, Alfred Freddy Heineken was deeply moved when he visited Curaçao. He was struck by the sight of numerous beer bottles littering the beaches. This was in stark contrast to the Netherlands where Heineken bottles were reused at least 30 times and as in Curaçao, the bottles were solely designed for single use. Furthermore, Mr. Heineken observed that many islanders lived in homes constructed from discarded materials. It was during this experience that the concept of the WOBO bottle took shape. [16]

2.1.1. Construction

In collaboration with Dutch architect John Habraken, Mr. Heineken embarked on the development of an innovative bottle that could double as a building brick after being emptied. By 1963, the prototype was successfully created. Two sizes were designed: one for 33cl and another for 50cl.

These bottles were arranged horizontally, with small protrusions on each side, enabling them to be securely connected either dry or using cement and sand mortar with a silicone additive.

Unfortunately, numerous challenges and drawbacks arose, which hindered the realization of the project. Firstly, there were structural and physical limitations. Ventilation requirements necessitated the separation of the roof from the walls. Similar to a greenhouse, the WOBO bottle house is prone to overheating on sunny days, leading to thermal discomfort within the living space.

Apart from the technical difficulties, the WOBO bottle also encountered significant financial and logistical obstacles. Converting production lines to accommodate the unique bottle design incurred substantial costs. Furthermore, the production expenses were considerably higher than those associated with traditional bottles. These factors collectively impeded the widespread adoption and implementation of the WOBO bottle concept. [16]

2.2. Bottle Building by artlife



Figure 2.2: glass house (artlife, n.d.) [4]

Two buildings have been erected, and the construction process has been clearly documented as depicted in reference [4]. The first building, albeit small in size, fulfills the purpose of a storage facility where a variety of bottles are utilized. The second building, on the other hand, has been specifically designed to serve as both an artistic space and a concert venue, accommodating up to 50 individuals. A diverse range of bottles has been employed in this endeavor, including old ashtrays, Japanese glass floats, candy dishes, glass blocks, and wine bottles. Approximately 10,000 bottles have been utilized in the construction of the larger building. Various intricate patterns and artwork have been incorporated to fashion a truly unique aesthetic, as illustrated in image 2.5. It is worth noting that this particular structure holds the distinction of being the first bottle house in the United States to have obtained a building permit.

2.2.1. Collection of bottles

Naturally, the initial course of action involved gathering glass bottles, which posed as the first significant challenge. The builders approached local bars and restaurants for assistance, but soon realized that even this approach proved to be time-consuming and yielded slow results. However, the project gained momentum when the owners decided to explore wineries, where they discovered that a vast number of discarded bottles were being sent to landfills. This allowed them to amass thousands of wine bottles for their bottle house. It is worth noting that the owners were challenged by the weight of the glass bottles, which made transportation a hassle.

2.2.2. Preparation of the bottles

Subsequently, the bottles undergo a thorough cleansing process involving a small amount of chlorine. This serves a dual purpose: to eliminate any potential breeding grounds for mosquito larvae and to effectively remove any residue or grime, including labels. This step holds significant importance, as demonstrated by another case study where the labels were not removed. Regrettably, this oversight led to the labels shrinking and becoming embedded within the mortar during the summer months, ultimately necessitating the demolition of that particular house.

2.2.3. Construction

The foundation of the larger building consists of a 5-inch base with a 20-inch footer, providing a sturdy base for the construction. To establish the framework for the walls, wooden columns and beams are strategically positioned. Subsequently, the bottles are carefully inserted between these wooden elements and secured in place using mortar. The mortar mixture is prepared following the provided instructions, incorporating a quarter cup of ivory dish detergent and one cup of lime. Type S high-strength mortar/stucco mix is utilized, ensuring durability and resilience in the construction process.

2.2.4. Repairs

In the eleven years the building exists, it has endured flooding, winter storms, minor earthquakes, acts of vandalism and even a lighting strike in a nearby tree. Throughout this time, the owner of the building made a noteworthy adjustment by replacing a bottle with one of a different color. This involved carefully breaking the original bottle with a hammer, removing the glass from the wall, and then applying a thin coat of silicone adhesive. A new bottle was then seamlessly inserted into the vacant space, ensuring a seamless integration with the surrounding structure.

2.3. Wat Pa Maha Chedi Kaew: Temple of a Million Bottles



Figure 2.3: Wat Pa Maha Chedi Kaew
(hippie pants, 2015)

The Wat Pa Maha Chedi Kaew, also known as the Wat Pa Maha Chedi Kaeo or the Temple of a Million Bottles, is a Buddhist temple situated in Khun Han, Thailand. The monks became increasingly aware of the detrimental impact that numerous discarded bottles were having on the environment. In response to this issue, Monk Phra Khru Vivek Dharmajahn conceived an ingenious solution to repurpose these bottles within the temple.

By utilizing the collected bottles as decorative and construction materials, the temple was able to save both money and valuable resources. The initiative gained significant traction within the local community, as a call was made for people to contribute their bottles, and many individuals enthusiastically participated in the construction process. This resulted in a remarkable level of community involvement.

The project was initiated in 1984 and has since transformed the Wat Pa Maha Chedi Kaew into a unique and eco-friendly sanctuary.

2.3.1. Construction

The temple encompasses a total of 20 structures, which include a crematorium, multiple prayer rooms, a water tower, bathrooms, and residential accommodations for the monks. Even to this day, the monks continue to gather bottles and remain eager to expand their eco-friendly endeavors. The main building is constructed primarily with bottles from renowned beer brands like Heineken and Singha. However, for ornamental purposes, an array of bottle types and even bottle caps were ingeniously incorporated into artistic creations.

To ensure structural integrity, the bottles are firmly affixed to one another using cement. They serve various purposes throughout the temple, such as forming walls, columns, flooring, and roofing. Additionally, they are ingeniously used for constructing stairs and balustrades, adding a distinctive touch to the temple's design.

It is estimated that an astounding 1.5 million bottles have been utilized in the construction and embellishment of the temple, testifying to the significant scale and impact of this sustainable initiative.

2.3.2. Bottle configurations

The temple stands out not only as a remarkable endeavor in terms of scale, but also due to the innovative configurations of the bottle placements within its walls. While most case studies typically involve bottles being horizontally positioned perpendicular to the wall surface, the builders explored diverse arrangements. A visual representation of these various configurations can be observed in the following images 2.4.

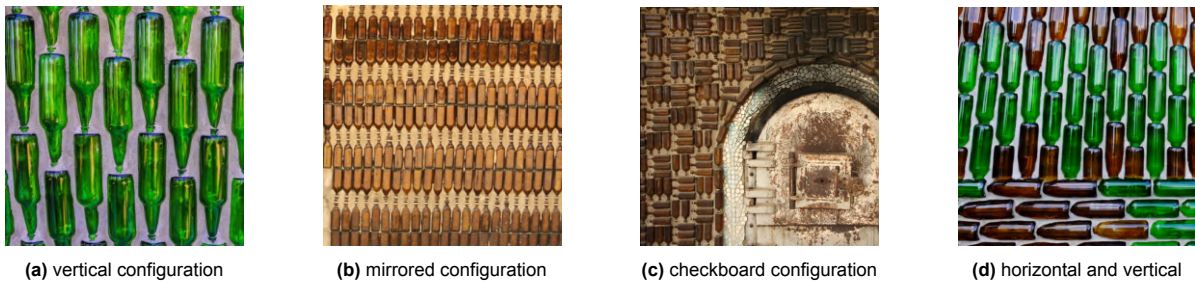


Figure 2.4: Bottle configurations in Wat Pa Maha Chedi Kaew temple (edited by H. Heller)

2.4. Beer Bottle House in Tamil Nadu, India



Figure 2.5: Beer bottle house in Tamil Nadu, India [3]

This magnificent house has been constructed by Mr. Dilip Patel, a graduate in architecture from the United Kingdom who currently resides in India. With a deep appreciation for ecological communities, he has been passionately exploring innovative construction techniques inspired by the international ecological community of Auroville.

Situated in an area notorious for its frequent drinking parties, the surroundings of the house were polluted by an ever-growing litter of bottles. Recognizing the need for change, Mr. Patel took the initiative to organize a cleanup group and began educating the local populace. Motivated by various online sources, he came across the remarkable idea of constructing his very own bottle house. [3]

2.4.1. Construction

The plot for the construction measured three by four meters in size. To establish a solid foundation, a trench of approximately 60 cm deep was excavated and then filled with a mixture of red soil and cement, firmly compacted.

Moving on to the walls, two layers of bottles were carefully arranged in a manner where they were perpendicular to the wall, alternating their orientation. This meant that the bottle openings faced both inward and outward as can be seen in Figure 2.6. The spaces between the bottles were then filled with a mixture of cement and locally sourced soil, serving as mortar to hold them firmly in place.

For the roof, a pitched wooden frame was constructed, upon which Mangalore tiles were laid. To ensure proper ventilation, an open space was intentionally left between the roof and the walls. However, to prevent insects and mosquitoes from entering, this gap was covered with a fine mesh net.

2.4.2. Takeaways

Mr. Dilip Patel predominantly relied on locally available resources throughout the construction process. Despite the scorching heat of the Indian summer, the owner attested that the interior of the house maintains a comfortable temperature.

Furthermore, the owner expressed his personal experience of the construction process as therapeutic and immensely satisfying. Engaging in the creation of this unique bottle house allowed him to connect with the materials and the environment in a profound way. The journey of transforming discarded bottles

into a functional and aesthetically pleasing living space brought a sense of fulfillment and contentment.

Figure 2.6: Construction method bottle house in Tamil Nadu, [3]



2.5. Common Raw Earth Building Techniques in Brazil

Some common earthen building techniques in Brazil are superadobe, hyperadobe, rammed earth, cob, stucco and double stucco filled with PET bottles. As expensive tools are not necessary and construction is relative easy for these techniques, the houses are mostly built by the owners or by a community effort.

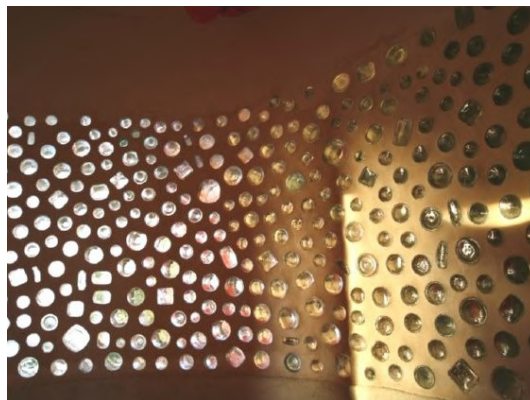
As construction materials are local and inexpensive, builders consider it as a good investment. A study conducted in 2014 compares the building costs of seven houses using earthen building techniques to houses at the same location with similar building patterns. It showed that the earthen houses had a cost of approximately if BRL 310 per m^2 as the average building cost is 670 BRL per m^2 . [13]

While earth based construction techniques have deep roots in a rich tradition, they often lack an engineering approach. One can state that the under-researched nature of these building methods seems inconsistent with its significant relevance.

2.5.1. Construction

The construction methods of superadobe/hyperadobe, Pet-a-pique, rammed earth and cob (opt. with cordwood) are illustrated in Figure 2.8 and detailed in Table 2.1 and 2.2, with information retrieved from [13] [63]. In some references using the cob and cordwood technique, sometimes the use of a bottle can be seen for aesthetic reasons as illustrated in Figure 2.7.

Figure 2.7: Cob and Cordwood technique using glass bottles, [39]



What unites all these building methods is the simplicity and limited nature of the tools required. This accessibility makes these construction techniques suitable for individuals of all backgrounds. This is evident in the projects examined in the literature review, where the builders were often not professional constructors but enthusiastic and creative individuals.

2.5.2. Construction pathology's and repairs

The shortage of skilled builders and construction experts with expertise in earth-based construction can be attributed to the limited availability of knowledge and educational resources dedicated to these specific building methods. This scarcity has led to its relatively low prevalence in the industry. Additionally, building codes for these techniques are underdeveloped and often lacking comprehensive testing for performance evaluation. These factors significantly contribute to the vulnerability of these construction methods to structural issues and other construction-related challenges.

Some construction pathology's showed after some time such as pending walls, cracks, moisture infiltration and peeling of plasters.

Numerous studies have demonstrated the significant influence of clay type and content in soil on water ingress as well as the swelling and shrinking behavior of earth-based construction materials, as cited in references [59][15][58][40]. When an earthen structure undergoes cycles of wetting and drying, resulting in alternating expansion and contraction, it is susceptible to developing cracks. This is what makes earth based constructions sensitive to moist, recommending to avoid direct rain contact.

There is another problem that precludes raw earth buildings in poor conditions and containing holes and cracks: the ideal habitat for insect proliferation. The insect named *Triatoma Infestans* causes the Chagas Disease which is often associated with earth constructions. Besides applying finishes and preventing cracks, some extra ingredients can be added to the earth mix to prevent insect manifestation, such as lime and cement.

Finishes can be qualitative applied to improve the resistance against moisture, also large eaves could protect the building. It is recommended to use predominant plaster for external walls. For the internal wall, a natural coating of cactus sap and flour can be added.

2.5.3. Considerations Beyond Interviews and Blogs: Key Insights to Remember

Below are some points mentioned that recur in blog posts, comments on YouTube videos, or were orally conveyed to me.

- The question if one could pour earth like concrete is a possibility in order to take labor hours down is frequently asked and discussed as conventional production methods for earth building techniques are often very labour intensive.
- Using a hand operated press to produce rammed earth blocks is very labour intensive and you need at least 6 people. (Daniel Gair [blogpost], 2014)
- The production of bricks/blocks has more freedom in time and space than making a wall in-situ.
- The advantage of earth blocks is that they can be produced inside in a better controlled environment and protected from weather factors. Which can also be more comfortable for the constructors.
- Remove the labels from the bottles as they could result in issues when sticking to the mortar.
- When wind blows over the open side of the bottles, they will make a sound.
- Collecting bottles can be a time consuming process.
- The builders are mostly also the owners with a non-professional background, they see themselves as a natural-traditional builder and prefer natural techniques.
- Due to the lack of regulations and codes the implementation of earth based constructions is restrained.



(a) superadobe/hyperadobe



(b) PET-a-pique



(c) rammed earth



(d) cob + cordwood (J. Dias, 2017)

Figure 2.8: Earth based building techniques in Brazil (edited by H. Heller)

- Some building methods that construct on site, such as cob with cordwood, are challenging to construct straight walls.
- Constructing a wall and layering glass bottles horizontal, also has its challenges. It is time consuming, hard to construct straight walls and one needs to wait until under-laying layers are sufficiently dry in order to prevent collapse during construction.

Table 2.1: Overview of building techniques superadobe/hyperadobe and cob and cordwood

building technique	superadobe/ hyperadobe	cob and cordwood (cob + wood logs)
<i>tools needed</i>	pointed tip shovels, spades, pickaxes, wheelbarrows, trowels, 'rammer', concrete mixer, polypropilen plastic bags/ polyethylene raschel knit tubular mesh bag	cob optional: large mixing equipment cordwood: surform shaver straight drawknife log wizard wood moisture meter
<i>earth mixture</i>	30% binding materials (20% clay, 10% stabilizer) 70% sandy soil (35% gravel, 35% sand)	85% sand 15% clay 2:1:1 sand, clay, sawdust 16:1 soil:water + straw/rice husks to bind: manure /cactus sap
<i>foundation and drainage</i>	continuous shallow foundation stone + gravel + sand drainage pipes	strong foundation needed as cordwood is heavy
<i>construction method</i>	mix and fill the bags place and compact forming concentric cirkels with decreasing radius	mix with feet/machinery drop earth dough make holes with fingers for attachment cordwood: add wood logs prevent insect infestation: lime
<i>finishing</i>	inner wall: goretex outer wall: 3 layers plaster 1)4:1 sand:lime, t=1-5mm 2)4:1 sand:lime, t=15-20mm 3)pure lime, t=5-8mm	lime/ earthen plaster/ whitewash
<i>esthetic</i>	egg-like /dome	more design freedom wood is visible in the walls
<i>pro's and cons</i>	- labor intensive - limited design freedom - use of plastic + easy to construct	- protect from rain - strong foundation - labor intensive - low insulation value of cob - difficult to make straight walls + stable interior humidity + no use of moulds + good earthquake perf.

Table 2.2: Overview of building techniques rammed earth and earthen stucco with PET

<i>building technique</i>	rammed earth	earthen stucco with PET (PET-a-pique)
<i>tools needed</i>	formwork rammer/tamper mixing equipment leveling tools shovels, wheelbarrows, spades	very limited needed: hawk, trowel, mixing equipment ...
<i>earth mixture</i>	30-40% clay 60-70% sand/gravel optional: water repellent additives	raw earth blend reinforced stucco: earth + 10% cement/lime chicken frame
<i>foundation and drainage</i>	can also be used as foundation	no specific requirements
<i>construction method</i>	fill the timber forms with soil and tamp it move the forms up	frames attached to columns between it is filled with: raw earth blend, optional PET bottles
<i>finishing</i>	none/ coloured/ sealed with stucco	earth/ plasters/ paint
<i>esthetic</i>	can be coloured	only earth is visible
<i>pro's and cons</i>	+ strong + multistorey + good earthquake perf. + high thermal mass + good sound insulation + good fire resistance - porous - good moisture resist. - need for professionals	when using PET bottles: + thermal insulation + acoustic insulation + very inexpensive - protect from rain

3

Glass Pollution & Resource Constraints

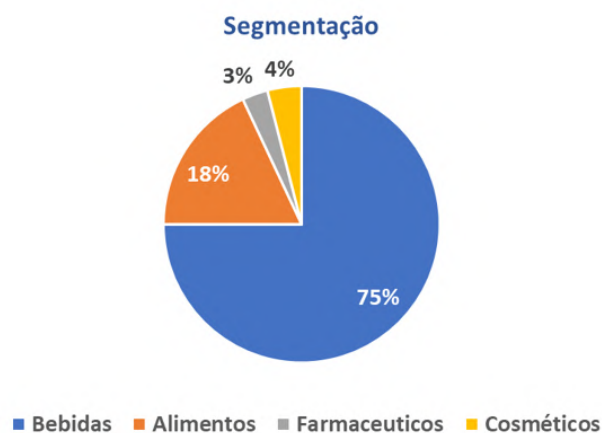
This chapter delves into a comprehensive exploration of the container glass market in Brazil. Its aim is to provide detailed insights into areas of highest glass consumption and susceptibility to glass pollution issues. Through this analysis, potential locations suitable for the implementation of glass bottle walls can be identified. Various topics will be covered, including production and consumption of hollow container glass in Brazil. Furthermore, the chapter will examine quantitative targets for glass waste recycling rates across different regions, as well as the potential impact of re-purposing glass bottles on the waste management system and its influence on informal actors in glass waste management.

3.1. Hollow Glass Market of Brazil

3.1.1. Production of glass packaging

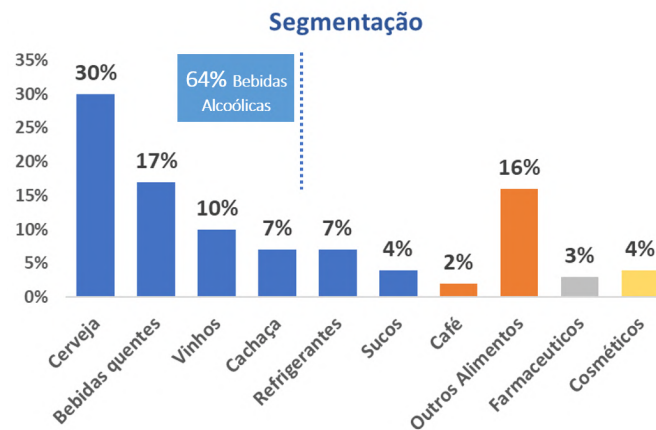
An estimation of the bottle market in Brazil is made by MASSFIX [53] and is around 1.6 million tons/year and the Total Hollow Glass Market is 2.1 million tons/year. It is also estimated that the beverage segment represents 75% of the Total Hollow Glass Market, which is illustrated in pie chart 3.1. From the entire bottle market, 64% are beverages including alcohol. Whereas the largest share is represented by beer which is 30%, as illustrated in bar chart 3.2. With some quick math one can conclude that an estimation of 480 000 tons/year of beer bottles are produced. Another estimation is made by Mauro

Figure 3.1: Hollow Glass Market in Brazil: Pie chart of production segments by MASSFIX of respectively: beverages, food, pharmaceuticals, cosmetics. [53]



Akerman, who estimates the total production of glass packaging is 2,328,700 tons/year which is close

Figure 3.2: Hollow Glass Market in Brazil: Bar chart of production subdivisions by MASSFIX of respectively: beer, liquor, wine, cachaça, sodas, juices, coffee, other food, pharmaceuticals, cosmetics.[53]



to the estimation of MASSFIX of 2.1 million tons/year. He also mentioned that some manufacturers are planning on increasing their capacity. The manufacturer Vidroporto located in Porto Ferreira is planning on expanding their capacity with an additional 300 tons/day. Additionally in the manufacturers in the city's Jacutinga, Juiz de Fora and Ponta Grossa are planning on increasing their capacity with an extra 350 tons/day.

Although there is no formal source stating it, after discussion with professionals in the glass industry it is stated that the long neck beer bottle is sold the most. Which can be validated by the estimation made by MASSFIX. The minimum regional and national recycling index percentages are regional relative low, but the government has incentives in increasing these until 40 % by 2032.

3.1.2. Glass consumption and discard

According to the Brazilian government, it is estimated that approximately 1 billion glass bottles are discarded in the country each year [10]. Unfortunately, a significant portion of these bottles is improperly disposed of in various locations, such as beaches, rivers, vacant lots, and landfills. Additionally, some of these bottles end up in sanitary landfills. While sanitary landfills are considered acceptable waste management structures, the disposal of glass bottles in this manner is deemed inappropriate because the bottles can be reused and recycled. This improper disposal contributes to the growing size of landfills and ultimately shortens their lifespan.

It is also mentioned by the government that this improper disposal also have significant implications for public health. As empty bottles in nature accumulate rainwater which result in a rapid multiplication of organisms which can carry diseases. An example is the *Aedes aegypti* mosquito which transmits dengue, chikungunya, Zika and urban yellow fever. [29]

An approximation of the national glass consumption in 2006 has been estimated by MASSFIX. And it showed that the main area's for consumption are in São Paulo (11.8%), Rio De Janeiro (5.4%) and Brasília (<5.4%). The geographic distribution is illustrated in Figure 3.3. On this map, the red and blue area present together 85% of all glass consumed. When assuming a positive relationship between consumption and discard, these are the most relevant area's.

3.2. Recycling and Reusing Glass Waste

3.2.1. Recycling of glass waste in Brazil

The quantitative targets for the recycling rate of disposable glass packaging concerning the mass quantity of single-use glass containers placed on the internal market in Brazil is currently around 30% [66].

Table 3.1: Estimation of glass production in Brazil by M. Akerman (2023)

State	City	Manufacturer	Furnaces	Capacity tons/day
<i>Pernambuco</i>	Recife	O-I	2	490
	Vitória de Sto Antão	O-I	2	220
<i>Sergipe</i>	Estância	Vidroporto		250
<i>Rio de Janeiro</i>	Rio	O-I	1	300
	Rio	Ambev	2	750
<i>São Paulo</i>	Porto Ferreira	Verallia	1	300
	Porto Ferreira	Vidroporto	3	900
	São Bernardo	Wheaton	4	100
	São Paulo	O-I	3	1000
	Jacutinga	Verallia	2	700
	São Paulo	Anchieta	1	70
<i>Minas</i>	Juiz de Fora	Ardagh	1	350
<i>Parana</i>	Ponta Grossa	Ambev	1	350
<i>Rio G do Sul</i>	Campo Bom	Verallia	1	600
Total tons/day				6,380
Total tons/year				2,328,700

The minimum regional and national percentages are established according to the National Solid Waste Plan, approved by Decree No. 11,043, of 2022 are illustrated in Table 3.2 and 3.3. From this data can be derived that over a period of nine years, the goal is to increase recycling by 46.8%.

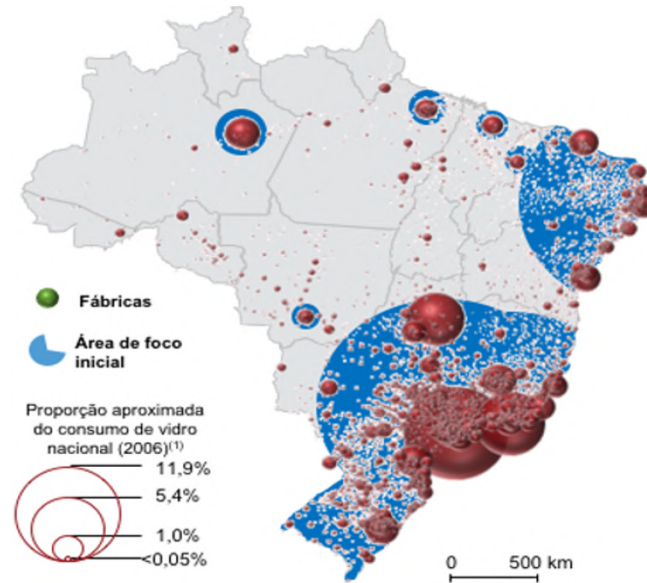
The challenge of a country with continental complexity such as Brazil is predominantly the size of the country and the internal distances of the glass industry. As the glass industry's are located at the east side of the country, glass should travel large distances to be consumed and to be recycled when going to the west-side of the country. The glass industry is primarily situated in the eastern part of the country, marked by the blue zone on the map (refer to Figure 3.3). This placement is logical, as approximately 85% of all glass consumption occurs in these areas. However, in the case of glass located outside of these zones, the glass has to cover an extremely long distance to reach the glass industry. To provide an example, the distance from Manaus to Recife is 3,300 kilometers. This could lead us to suspect that these regions are less appealing for recycling investments, which is also reflected in the recycling rate data that the Government of Brazil aims to achieve. These rates remain quite low fluctuating around 3 to 5% for the Northern and Center regions (see Table 3.2 and 3.3).

Table 3.2: Minimum regional and national percentages for the recycling index 2023-2027 [66]

Region	2023	2024	2025	2026	2027
<i>North</i>	2.64 %	3.00%	3.35 %	3.50 %	3.75%
<i>North-East</i>	4.39%	5.00%	5.00 %	5.00 %	5.00 %
<i>Center-East</i>	4.39%	5.00%	5.00 %	5.00%	5.00%
<i>South-East</i>	10.55%	12.00%	12.50%	13.00 %	13.50 %
<i>South</i>	5.27%	6.00%	6.25%	6.50%	6.75%
<i>Brazil</i>	27.25%	30.00%	32.00 %	33.00%	34.00%

Table 3.3: Minimum regional and national percentages for the recycling index 2028-2032 [66]

Region	2028	2029	2030	2031	2032
<i>North</i>	4.00 %	4.00%	4.00 %	4.00 %	4.00 %
<i>North-East</i>	5.00 %	5.25%	5.50 %	5.75 %	6.00 %
<i>Center-East</i>	5.00%	5.25%	5.50 %	5.75%	6.00%
<i>South-East</i>	14.00%	14.50%	15.00%	15.50 %	16.00 %
<i>South</i>	7.00%	7.25%	7.50%	7.75%	8.00%
<i>Brazil</i>	35.00%	36.25%	37.50 %	38.75%	40.00%

Figure 3.3: Hollow Glass Market in Brazil: Map of glass consumption within Brazil [53]

3.2.2. Influencing factors of recycling glass waste

The actual recycling rate of glass waste in each country and continent depends on several complex factors. A study conducted in 2020 examined the effect of socioeconomic characteristics on materials recycling and circularity in the EU [45]. Results of this study show that economic wealth, fertility rate, the level of environmental taxes and R&D expenditures have a positive effect on recycling and circularity rates. One can feed back this information looking at Europe. In 2020, in the EU27 + UK, on average 79% of all the produced glass bottles and jars were collected and recycled into new glass packaging solutions [23]. The collection of glass waste does not always guarantee the glass is recycled as it can be contaminated with other materials, or as different colored glass mixed together increases recycling difficulties. Noteworthy is that some European countries have a considerably low recycling rate compared to the European average, so has Turkey the lowest waste glass collection rate of 14% followed by Hungary, Greece and Cyprus [24].

Additionally the policy chamber plays an important role in encouraging recycling and sustainable waste management. The EU has taken several measures to promote glass packaging recycling, a target is set to recycle 75% by 2030 [23]. A good working infrastructure is also beneficially for waste collection and thus recyclability. According to the earlier mentioned study in 2020, the correlation between urbanization and materials recycling follows a nonlinear, inverse U-shape [45]. From which follows that urbanization shows a positive association with recyclability due to economics of scale until a certain threshold.

To conclude, these listed factors differ greatly both nationwide and continental, as well as the recycling rate of glass packaging waste. The average estimated recycling percentages of glass packaging in Europe 76% (2018) [23] is high in comparison to the rest of the world. An estimation of recycling rates in some other parts of the world are: Asia 56.3% (2021) [5], U.S 25% (2018) [22], China 20% and South Africa 41% [34].

3.2.3. The role of informal actors in glass waste management

Especially in developing countries, informal waste pickers contribute significantly to waste management by resourcing, collecting and trading waste to generate an income. The informal sector can be defined as a sector that works unregistered and unregulated which includes private and individual enterprises. The informal sector approaches waste as a resource with the benefits of reducing waste, saving public expenditures for waste management and a creation of jobs. As a result of a study about the role of the

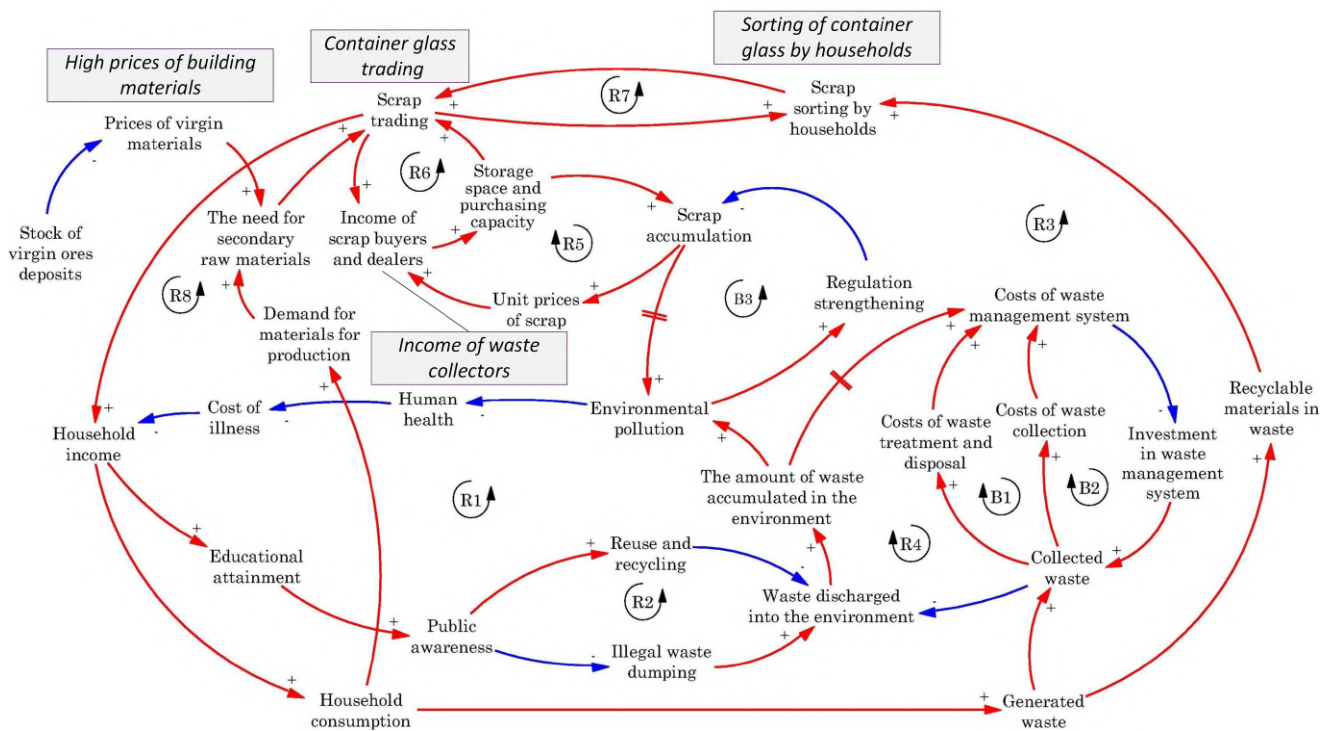


Figure 3.4: Casual loop diagram for stakeholders within the waste management system. Note: The red arrow with a plus symbol denotes a positive cause-and-effect relation, in which two variables change in the same direction; The blue arrow with a minus symbol shows the negative causal influence, in which two variables change in the opposite direction. Double bar (//) indicate lag time between two variables.

[76]

informal sector and its impact on the recycling system, a flow diagram (see Figure 3.4) is built which integrates the actors and activities of the informal sector in a wider solid waste management system [76].

Following categories can be distinguished in this sector: street pickers, landfill scavengers, collection crews, itinerant buyers, dealers, small-scale entrepreneurs and large-scale entrepreneurs. The interaction between the formal and the informal sector in waste management is rather complex and interlocked, as shown by a study about the role of formal and informal sectors in waste management [75]. But to simplify it comes down to the informal collectors (tricyclists, street scavengers, pick-up traders, collection crews, and landfill scavengers) who sell waste to dealers (formal and informal recycling firms) or directly from the firm to the manufactures. The contribution of the informal sector to waste management is significant. This can be endorsed by a study where the city Phitsanulok in Thailand has been surveyed to assess its efficiency concerning the relief of the local landfill [75]. This study shows that the informal sector contributes to the biggest part of recycling with 58,7%. It also shows that glass packaging is the most collected recyclable, and especially the landfill scavengers where 58% of the composition of recyclables are glass bottles.

To recap, the task of solid waste collection and disposal is far beyond the cost of some municipal governments. Where in this occasion the contribution of the informal sector in glass waste management is significant. Due to the increased prices of building materials, the need for alternative materials increase. Using glass bottles as an alternative building material causes a positive loop diagram within the waste management system, as shown by figure 3.4. From this it can be seen that several opportunities stand out, (e.g. waste discharges into the environment). Section 5.2.5 delves more into the opportunities created by reusing glass packaging as an alternative building material.

4

Characteristics of the Longneck Beer Bottle

In the exploration of glass bottle integration within walls, some properties must be evaluated. As established in Chapter 3, the longneck beer bottle emerges as the focal point of this thesis. This chapter focuses on this bottle type, including its physical and mechanical characteristics. The aim of re-purposing bottles involves utilizing those that have already been used, which inevitably impacts the strength of the bottles due to surface defects.

4.1. Physical Characteristics

4.1.1. Geometrical characteristics

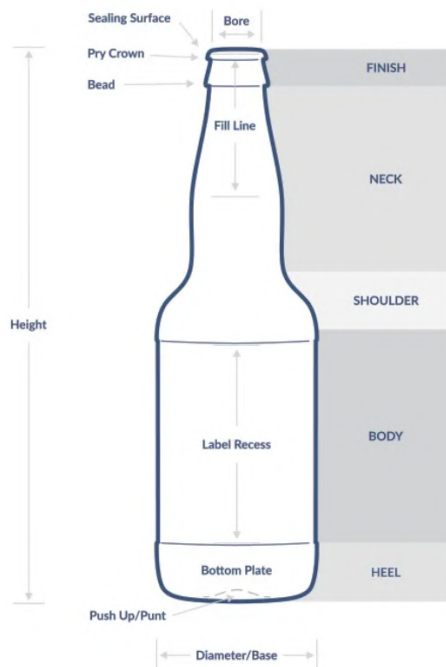


Figure 4.1: Bottle anatomy (Saxco, n.d.)

In this paper when referring to parts of the bottle, these are taken as in figure 4.1.

The finish is where the closure is applied to seal the bottle, for the longneck beer bottle this is sealed by a crown closure. This is why the finish is molded as a pry crown to receive this type of closure. The neck is starting below the finish and stops at the shoulder of the bottle. The transition from the neck to the body is called the shoulder of the bottle. Talking about the body, this is where the label is applied. In some bottles there is a label recess where the body is slightly indented to protect the label. However for this thesis no indent is assumed for the label.

Moving down towards the bottom of the bottle, at the bottom plate one can find the mold number and manufacturing markings. The push up, is required to minimize the amount of glass that comes into contact with the conveyors. At the base of the bottle there is a ring around the outside of the bottle on the location where the bottle rest, also called the bearing surface. This has a stippled finish in order to prevent the container from being weakened from concentrating abrasions. [70]

Table 4.1: Geometrical characteristics of longneck beer bottle, 33 cl, by Brouwland

Dimension	Value	Unit
<i>Height</i>	238	mm
<i>Diameter</i>	61 ± 1.3	mm
<i>Weight</i>	Ca. 300	gr
<i>Content</i>	33	cl

For more specific measurements of a longneck beer bottle, a technical drawing is added in Appendix A. A general overview of the Geometrical characteristics of the longneck beer bottle is given in Table 4.1

4.1.2. Coatings

Non-refillable glass containers are lighter and have a thinner thickness compared to refillable glass bottles. This requires that the outside surface of the bottle should be protected with both hot-end and cold-end coatings. These coatings provide both a protection against scratches to maintain the high glass strength and a smooth surface to enable an effortless transport of the bottles through the filling lines. [27]. According to a study conducted by Guin and Gueguen [30], a large difference between usable and intrinsic strength is due to the surface flaws glass bottles undergo during their lifecycle.

The most common type of cold-end coating within glass packaging is a slightly oxidised, low density form of polyethylene. The level of which this type of coating has covers the glass surface, is never completely. However this can be measured through the use of the contact angle degree. In this type of test, a 10 micro-litre droplet of de-ionised water is dropped onto the bottle surface when holding it in a horizontal position. The angle that the droplet makes with the glass surface is then measured. The thickness of this coating can be measured with coating meters [73]. A study conducted by Southwick et al. [74] found coefficients of friction of the surface depending on the presence and type of the coating. A glass bottle surface with only a hot-end coating has a coefficient of friction of 0.38, which was constant over 50 tests, whereas a glass bottle surface with both hot-end coating and cold-end coating had a coefficient of friction of 0.03.

Hot End Coating

Hot-end Coating is applied to increase the bond strength of the cold-end coating to the glass surface. Applied post-molding and before the annealing process, these coatings are pivotal for achieving optimal performance. The molecule mono-butyl tin tri-chloride (MBTC) serves as a precursor for the application of tin oxide SnO_2 onto the glass bottle surface using a technique known as chemical vapor deposition (CVD). The temperature during this process typically ranges between 400 and 500 degrees Celsius. [56]

However, challenges arise due to the breakdown of MBTC at high temperatures, potentially compromising the full coverage of the glass surface with the tin oxide layer [67]. The thickness of hot-end coatings varies significantly, with Nakawaga et al. [56] suggesting a typical thickness of 40 nm, Penlington [62] proposing a range between 2 and 10 nm, and Smay [47] specifying a conventional thickness of about 40 CTU (Coating Thickness Unit). For optimal properties such as bursting pressure, scratch resistance, and coefficient of friction, Bhargava et al. [9] recommend a thickness of approximately 50 CTU, where 1 CTU corresponds to about 0.25 nm [12].

They serve as a crucial preparatory layer, facilitating the application and adhesion of cold-end coatings. Described as a 'bond coat', the hot-end coating enhances the adhesion of the subsequent cold-end coating. [62] [46]. Tin oxide's hydrophobic nature compared to the general glass surface contributes

to its superior attraction to the cold-end coating, typically composed of organic compounds [26]. In essence, the hot-end coating functions as a 'primer' for the cold-end coating, as explained by Bhargava et al. [9].

Moreover, hot-end coatings play a protective role by minimizing surface damage between the molding and annealing processes [46]. This preventive measure ensures the longevity and quality of the glass bottle. As highlighted by Nakawaga et al. [56], the application of SnO_2 or TiO_2 coatings on one-way bottles has been a well-established practice for approximately two decades, offering an abrasion-resistant surface and garnering substantial documentation in the field.

Cold End Coating

This type of coating will protect the glass surface by decreasing its friction coefficient. Cold-end coatings play a vital role in enhancing the performance and durability of glass bottles, offering a diverse range of options such as polyethylene emulsions, waxes, and glycols [14]. The prevalent choice, particularly in conjunction with hot-end coatings like tin oxide, is polyethylene. The application of cold-end coatings typically occurs within the range of 90 to 150 degrees Celsius [46].

Unlike hot-end coatings that serve as primers, cold-end coatings primarily contribute to increased lubricity and a reduction in the coefficient of friction [9]. Glass inherently lacks lubricious properties, making this surface treatment essential for preserving strength [46]. The thickness of cold-end coatings is comparatively smaller, ranging from 1 to 2 nm [9].

The effectiveness of these coatings diminishes after three to five lifecycles for returnable bottles, leading to a decline in lubricity and resistance to abrasion [20].

4.2. Knurls

Knurl patterns, present on the bearing surface of glass containers, are typically available in four designs: bar, crescent, dot, or chain. While bar and crescent-shaped knurls are commonly seen on beverage containers, food jars typically feature bar, crescent, and dot patterns. Chain knurls, though less prevalent, can sometimes be found on liquor and still wine bottles. However, their usage is restricted due to their tendency to cause tiny cracks during the bottle molding process. Damage to the bearing surface of bottles usually occurs at the knurls' tips during regular handling. This damage weakens the glass surface but concentrates stress in regions with low stress levels, thus preventing breakage. [36]

The primary objective of knurling on glass containers is to focus the unavoidable damage in areas where tensile stresses are significantly diminished, thus preventing breakage. However, while variations in stress generation were observed among different knurl patterns, the selection of knurl type is typically influenced more by aesthetic and manufacturing considerations than by the need to reduce tensile stresses. [36]

Utilizing Finite Element Analysis (FEA) simulations, Dr. Wenke Hu, a PhD researcher affiliated with American Glass Research (AGR), investigated the influence of knurl height and spacing on stress levels experienced by glass bottles under conditions of internal pressure or heel impact [37]. His study showed that in terms of knurl height, stress between knurls increases as knurl height rises, while stress at the knurls' tips decreases. Similarly, increasing the number of knurls results in greater stress between them, with minimal variation between knurl patterns, and reduced stress at the tips of knurls under internal pressure. Regarding the number of knurls, while differences in stress generation were observed, the decision on the number of knurls is usually driven by manufacturing considerations during bottle design.

However, stress at the knurls' tips remains relatively stable during heel impact. Knurl height, on the other hand, can change over time due to factors such as physical wear, accumulation of mold release agent, and improper filling of knurls. Reduced knurl height can impact stress levels in the bearing surface region, leading to performance issues if not addressed. As knurl height decreases, stress between

knurls diminishes, but stress at the knurls' tips increases significantly, potentially causing damage during normal handling. [36] [37]

4.3. Mechanical Characteristics

4.3.1. Surface and Defects: Abraded Bottle Strength

As investigated by Y. Maachi's research [52], it was corroborated that imperfections and damage to coatings have a substantial impact on the mechanical strength of bottles after use. Specifically, his study involved manually abrading 330 ml Longneck beer bottles and subjecting them to simulated line conditions. Employing two distinct finite element models and a Weibull Analysis, the research revealed a characteristic tensile strength of abraded container glass at 20 MPa and for line-simulated bottles is 27 MPa. The difference between these two values can be explained by the different level of damage. The latter resemble glass bottles which have gone through the production line of a beverage factory. This finding underscores the importance of considering this abraded state when designing structures with reused glass bottles.

Engineering codes such as NEN2608 (2014) mention a characteristic tensile strength for float glass of 45 MPa. The difference between these values can be explained with the purposely induced damage on the bottles which damage the coatings and thus weakens the mechanical strength. Moreover, the production processes are different to one another, which could explain the change in characteristic strength.

Müller-Simon et al. [55] further assert that a container's strength isn't solely determined by stress distribution within it. Apart from coatings, imperfections, flaws, and homogeneity's play crucial roles in container glass strength. Their research indicates that each defect type has a unique distribution on a glass bottle. By testing the bursting pressure of beer bottles and plotting fracture stress in a Weibull plot, they observed that the slope of the distribution changes at the tail of the distribution. Showing that this difference in slope has to do with the different types of defect and showed that this distribution is a characteristic of a certain defect. Thus, container glass strength is not only influenced by defect presence but also by the type of defect.

Investigating which regions of a bottle certain defects might dominate becomes intriguing. Müller-Simon et al. [55] concluded that fractures due to seeds and bubbles predominantly occur in the side-wall, while fractures due to stones and metal inclusions are more common in the bottom of the bottle. Understanding potential defects in glass bottle manufacturing is crucial. Aldinger and de Haan [6] categorized defects into six subdivisions: melting, dimensional and flaws (forming defects), handling, ACL, and tubing. Under 'melting' and 'flaws,' the following defects are discussed: Cord (inclusion of glassy material, stress-increasing), Knots (glassy inclusions on the inside surface, usually stress-increasing), Seeds and Blisters (inclusions of gas inside the glass, strength-reducing or critical), Stone (solid inclusions, strength-reducing), and Poor Annealing (causing residual stresses, stress-increasing).

Manufacturers employ an annealing lehr to cool down bottles after the molding process and hot-end coating application. Without an annealing lehr, the outer surface cools faster than the inner surface, creating tensile stresses on the inner surface [33]. Poor annealing becomes problematic as it can lead to earlier bottle failures due to these added tensile stresses.

4.4. Stress Distribution of Glass Bottles under Loading

4.4.1. Glass bottle under vertical load

Kepple and Wasylyk [43] contribute insights into the mechanical behavior of glass bottles under vertical loads. According to their findings the outside surface experiences tension primarily in the heel and shoulder locations due to load-induced bending of the container wall. Besides, principal stress is directed circumferential, resulting from the vertical load's attempt to increase the diameter of the shoulder

and heel. Vertical load fractures typically originate on the outside surface from tensile stresses oriented in the circumferential direction. A phenomenon discussed by Southwick et al. [74], reveals that under vertical compressive loads, tensile stresses occur in and around the shoulder and heel regions in both longitudinal and circumferential directions.

Finite element models have been developed to explore the relationships between applied vertical loads and the stresses within a glass bottle. This endeavor aims to comprehend the mechanical behavior of the bottle and extract maximum principal stress values corresponding to failure loads. The maximum principal stresses (σ_1) exhibit a tensile nature in the shoulder region, propagating in the circumferential direction.

A study conducted by Y. Maachi [52] observed that the mentioned phenomena by Southwick et al. [74] and Kepple and Wasylyk [43] align with both the finite element model and actual bottle fractures.

5

Key Insights from the State of the Art and its Influence on the Research

5.1. Barriers to Repurpose Glass Bottles in Earth Based Buildings

5.1.1. Underdeveloped building techniques

The widespread adoption of earth-based constructions using glass bottles faces challenges due to a shortage of skilled builders and limited educational resources dedicated to these methods. Structural vulnerabilities, like leaning walls and moisture infiltration, are exacerbated by underdeveloped building codes for earth building techniques. The literature study reveals various methods for stacking bottles, each presenting its own advantages and challenges. Challenges include difficulties in constructing straight walls due to the bottles' asymmetric and round shapes. The round and complex shape also complicates mortar connections, leading to gaps and a lack of a uniform building technique.

Earth building techniques has seen limited innovation, and underdeveloped building codes make it susceptible to vulnerabilities, especially in poorly constructed structures. Factors like clay type significantly influence the material's behavior during wetting and drying cycles, making it prone to cracks. Moisture sensitivity necessitates precautions to avoid direct rain exposure. Protective measures are implemented to enhance the resilience of earth-based constructions. These measures include qualitative finishes, large eaves, predominant plaster for external walls, and a natural coating of cactus sap and flour for internal walls. The objective is to address vulnerabilities, protect against insect infestation, and ensure the durability of the structures.

For a building technique with limited codes and skilled labours these measurements are not always applied, or not in a qualitative way. This resulting in construction pathology's, and a negative connotation with these techniques.

5.1.2. Underdeveloped and limited building codes

As can be concluded from Chapter 2, there is a limited availability of knowledge and educational resources dedicated to these specific building methods. Building codes for these techniques are underdeveloped and often lacking comprehensive testing for performance evaluation. These factors significantly contribute to the vulnerability of these construction methods to structural issues and other construction-related challenges.

In Brazil there is a standard about building with earth, however, only assessing cement stabilized rammed earth *NBR 13551 (1996)*. Despite the notable gap in codes and standards compared to other building materials, the existing codes do provide a valuable starting point for developing an earth-based wall in combination with glass bottles. However, building standards have been developed in some countries (19 in total) over the past decades, addressing soil classification, earth building materials

and construction systems. Nonetheless, an universally agreed-upon and internationally recognized terminology for earth building materials doesn't exist [71]. An overview of Building Codes concerning building with earth and their scope, are given in Table 5.1 and 5.2.

Table 5.1: Overview of Building Codes about earth based buildings and scope: Africa, Australia, Brazil, Columbia and Germany [72]

Document		Scope			
Country/ Continent	Name	Type	Building Material	Constr. Method	Geogr. Level
<i>Africa</i>	ARS 671-683 (1996)	S	EB	EBM	R
<i>Australia</i>	CSIRO Bulletin 5, 4th ed. (1995)	ND	EB, CSEB, EMM	RE, EBM	N
<i>Australia</i>	E BAA (2004)	ND	EB, EMM	EBM,RE	N
<i>Brazil</i>	NBR 8491-2, 10832-6, 12023-5, 13554-5 (1984-96)	S	CSEB		N
<i>Brazil</i>	NBR 13553 (1996)	S		CSRE	N
<i>Columbia</i>	NTC 5324 (2004)	S	CSEB		N
<i>France</i>	AFNOR XP.P13-901 (2001)	S	EB		N
<i>Germany</i>	Lehmbau Regeln (2009)	S	C, LC, EB, EM, CP	RE, C, EBM, EP, EI, WL	N
<i>Germany</i>	RL 0803 (2004)	ND	EP		N
<i>Germany</i>	TM 01 (2008)	ND	EP		N
<i>Germany</i>	TM 02 (2011)	Dd	EB		N
<i>Germany</i>	TM 03 (2011)	Dd	EMM		N
<i>Germany</i>	TM 04 (2011)	Dd	EP		N
<i>Germany</i>	TM 05 (2011)	ND			N

Table 5.2: Overview of Building Codes about earth based buildings and scope: India, Kenya, Kyrgyzstan, Nigeria, Peru, Spain, Sri Lanka, Switzerland, Tunisia, Turkey, USA, Zimbabwe [72]

Ref.	Document		Scope			
	Country/ Continent	Name	Type	Building Material	Constr. Method	Geogr. Level
	<i>India</i>	IS: 2110 (1998)	S		RE	N
	<i>India</i>	IS: 13827 (1998)	S	EB	EBM, REa	N
	<i>India</i>	IS 1725 (2011)	Dd	CSEB		N
	<i>Kenya</i>	KS02-1070 (1999)	S	CSEB		N
	<i>Kyrgyzstan</i>	PCH-2-87 (1988)	S		RE	N
	<i>New Zealand</i>	NZS 4297-9 (1998)	S	E, EB	RE, EBM, EP	N
	<i>Nigeria</i>	NIS 369 (1997)	S	CSEB		N
	<i>Nigeria</i>	NBC 10.23 (2006)	BC		EBM,RE	N
	<i>Peru</i>	NTE E.080 (2000)	S	EB	EBM	N
	<i>Spain</i>	MOPT Tapial (1992)	ND		RE	N
	<i>Spain</i>	UNE 41410 (2008)	S	CEB		N
	<i>Sri Lanka</i>	Specification for CSEB, SLS 1382 part 1–3 (2009)	S	CSEB	EBM	N
	<i>Switzerland</i>	Regeln zum Bauen mit Lehm (1994)	ND	EB, LE, EM	EBM, RE, EI, WL	N
	<i>Tunisia</i>	NT 21.33, 21.35 (1998)	S	CEB		N
	<i>Turkey</i>	TS 537, 2514, 2515 (1985–97)	S	CSEB		N
	<i>USA</i>	UBC, Sec. 2405 (1982)	BC		EBM	L
	<i>USA</i>	14.7.4 NMAC (2006)c	BC	EB, EMM	EBM, RE	L
	<i>USA</i>	ASTM E2392/E2392M (2010)	S	EB, EM,	C, EBM, RE, EM, WL	N
	<i>Zimbabwe</i>	SAZS 724 (2001)	S		RE	N

5.1.3. Challenges and knowledge gap

Load-Bearing capacity

Limited research exists on the structural integrity of buildings constructed with glass bottles. Understanding how well these structures can bear loads and withstand environmental factors is crucial. The load-bearing capacity of glass bottles as a primary construction material remains a significant knowledge gap. Questions about the material's resistance to weathering, UV radiation, and other environmental stresses over time need more exploration.

Connecting methods

The literature indicates challenges in connecting glass bottles securely. A knowledge gap exists regarding effective methods for connecting bottles to form stable and durable structures, especially considering the irregular and round shape of bottles.

Contamination

Glass bottles can contain contaminants as labels, caps, residues from the content. So they need to be processed and cleaned before it can be used in structures. Contamination could affect the quality and durability in the final construction.

Weight

Bottles of glass have a relative high self-weight in comparison to other structures. This can be structurally challenging and will also increase transportation costs.

Fragility

Glass behaves very brittle and thus is prone to breakage. So after usage there could be scratches and other imperfections that may influence the mechanical behaviour of the bottles, see Chapter 4. So when designing a structure with glass, special attention should be paid for safety. As the material doesn't yield, there is no clear sign when glass is close to its breaking point. Additionally, the scattering of glass shards poses a safety hazard. Consider implementing safety protocols such that in the event of breakage, the damaged bottle can be easily replaced.

Variety in size and shape

Glass waste bottles contain different sizes and shapes which makes it challenging to use in constructions. Different bottles may have different mechanical properties. Depending on the location, there is a different availability of glass waste, which can make it challenging to apply on a larger scale.

Building physical aspects

Overall, glass is not an effective barrier for acoustics which could be challenging in some environments. Besides, glass can be a poor conductor of heat and result in an uncomfortable indoor climate and increased energy costs. It is unclear what long-term exposure to UV radiation effects the bottles.

Collection of glass bottles

In some cases it was mentioned that the collection of glass bottles was a time consuming process. Mainly informal waste pickers contribute to the waste management in Brazil. The task of solid waste collection and disposal is far beyond the cost of some municipal governments, especially in a such an enormous widespread country such as Brazil. As this waste collection is quite low, it could be more challenging to acquire glass bottles in an efficient way.

Knowledge gap as a building material

There is very limited knowledge about reu-purposing glass bottles as a construction material. It is unknown how stresses occur in the bottles under certain loading conditions and especially bounded by mortar. It is unknown how safety and structural integrity can be assured.

5.2. Opportunities For Innovation when Repurposing Glass Bottles In Earth Based Buildings

Based on the findings from the literature study, numerous challenges and drawbacks currently impede the effective re-purpose of glass bottles in earth-based constructions. As a student in the Department of Building Engineering, the focus of this thesis is on improving these building techniques and addressing the challenges faced by builders.

A major obstacle lies in the current method of connecting glass bottles using mortar which can be cement or earth-based, a time-consuming process exacerbated by the round and irregular shape of the bottles. To streamline construction time and enhance quality, an innovative approach involves pouring and casting the (earth) mortar between the bottles instead of manually applying it. This not only accelerates the construction process but also addresses the issue of the bottles' unconventional shape, making it more suitable for working with concrete.

Furthermore, this innovation serves as a bridge between the unconventional method of building with glass bottles and the more widely known and accepted technique of using concrete. Incorporating glass bottles directly into bricks enables easy stacking, offering benefits such as faster execution, reduced construction pathologies, and increased production flexibility. Prefabricating these blocks in a controlled environment further adds to the efficiency.

The shift towards techniques like concrete and masonry blocks also addresses the shortage of skilled professionals in the current earth-based building methods. Since working with concrete is a well-established practice, this transition eliminates the barrier associated with a lack of experienced personnel, providing a more accessible and widely recognized alternative for builders.

Moreover, local earth buildings can still utilize native soil, with the added benefit of manipulating the earth to exhibit concrete-like properties. This involves creating molds with pre-placed glass bottles, allowing Earth-Based mortar to be poured between them for connection. This method aligns with the trend in earth-based building methods, emphasizing easy manual handling, as highlighted in the literature study. Looking ahead, as technology advances, there is potential to explore large-scale applications, such as prefabricating entire monolithic walls while pouring earth-based mortar between glass bottles.

5.2.1. Poured earth: self-compacting earth-based mortar

Earth is one of the oldest and most widely used construction materials, with estimates suggesting its utilization in over 150 countries, providing shelter for more than 2 billion people [19][41][17]. Building with earth-based materials is a deeply rooted tradition, with knowledge predominantly transmitted orally from one generation to the next. In contrast to many other building materials, earth-based materials have not witnessed significant innovation, rendering them less competitive in comparison to alternative construction materials. A relative new technique is in development which is known as 'poured earth', 'liquid earth' or 'clay concrete'. In Nevada (US) around 1990, the first experiments with this technique is conducted where 15% of gypsum is added in order to solidify the earth [25]. Also in Grenoble (France) the architectural company Characol started using liquid earth in their projects. Local earth is used where then 2%-4% of portland cement is added to improve its mechanical properties and demoulding process.

As these techniques still add a percentage of cement, which clashes with the motivation to built earth-based, new researches are conducted with using a biosourced polymer instead of portland cement. A recent study showed that gelified alginates can be used as an alternative for cement [60].

Self-Compacting Earth-Based Mortar (SCEBM) is an innovative mortar that combines the environmentally friendly qualities of earth-based materials with the conveniences of a self compacting mortar. This material has the potential to innovate traditional and contemporary earth based building practices. There are several important motivators towards working with self-compacting mortar. Being improved

working conditions, by eliminating the necessity for manual compaction during installation or the use of heavy machinery for compaction. This not only leads to reduced noise pollution — eliminating the need for loud machinery — but also translates into lower labor costs, potential energy savings, and a reduced demand for skilled labor. Additionally, studies has shown that thanks to this fluidization, compaction of the earth increases and thus the mechanical strength increases [54]. When using local earth, the need for transportation and packaging is reduced, lowering the carbon footprint of construction projects. The mix is primarily composed of natural materials present in soil such as clay, silt, sand and gravel. Small amounts of cement, lime and superplasticizer are added to the mix.

Already some research efforts were made to give earth-based materials properties similar to concrete, with the aim of enabling casting and enhancing their competitiveness in relation to other construction materials. [1] [50] [59] [15] [51] [48] [58]. This approach also contributes to the wider acceptance of earth as a viable construction material, given the familiarity with concrete in construction practices. Some researchers have employed superplasticizers commonly utilized in cement-based materials, such as polycarboxylate ethers, to formulate earth materials that can be cast. Typically, these earth materials are fortified with hydraulic binders, such as lime (comprising 10–15% of the total mass of soil), Portland cement (up to 5–8% of the total mass of soil), calcium sulfoaluminate cement, or blended mixtures. These additives serve to render the fresh earth composite more fluid, facilitate quicker setting times, and enhance mechanical and durability performance. Even better, some researchers are taking it even a step further by investigating if one can achieve solidification by bio-sourced polymers [15]. A study conducted in 2017 used sodium alginate to induce a liquid-solid transition [60]. *BIØN*, a network of organisations active in low impact building techniques, mention the use of citric acid as a natural biopolymer.

Influence of clay present in natural soil

Numerous studies have demonstrated the significant influence of clay type and content in soil on water ingress as well as the swelling and shrinking behavior of earth-based construction materials, as cited in references [59][15][58][40]. When an earthen structure undergoes cycles of wetting and drying, resulting in alternating expansion and contraction, it is susceptible to developing cracks. Natural soil contains a diverse range of clay minerals, with the most prevalent ones being kaolinite, illite, and montmorillonite. These clay types exhibit distinct characteristics that are highly dependent on soil moisture content, thereby affecting soil properties.

Clay minerals exhibit a tendency to absorb substantial amounts of water, transitioning from a hardened state in dry conditions to a softened state when they absorb water. The presence of clay significantly contributes to various soil attributes, including plasticity, cohesion, swelling, shrinkage, permeability, compressibility, strength, and more. To identify specific clay minerals, researchers often employ techniques such as X-ray Diffraction analysis or the Blue-methylene test. [65]

Natural fibers as reinforcement

Natural fibers play a crucial role in enhancing the cohesion and stability of concrete-earth mixtures. They offer a significant advantage by reducing, and preventing crack formation caused by plastic shrinkage. Numerous research studies have been conducted to examine the physical and mechanical properties of soil reinforcement [68] [44] [57] [8] and concrete reinforcement [2] [69] using natural fibers.

One particular study [44] explored the application of locally abundant fibers in Brazil, such as coconut and sisal fibers, in conjunction with three types of locally suitable soil to produce composite soil blocks. The findings were promising, demonstrating that with the inclusion of 4% by weight of fibers, visible cracks were completely eliminated, and the blocks exhibited high ductility. Key factors influencing the strength of the earth composite were the tensile strength of the fibers, their water absorption properties, and their bonding capabilities with the soil. Notably, sisal fibers exhibited higher water absorption compared to coconut fibers.

Another study [57] investigated the impact of the percentage and length of flax fibers on the fracture behavior of earth concrete, yielding promising results. The addition of flax fibers enhanced the ductility of the earth mixture, increased tensile strength, and improved deflection at the peak load.

However, a research involving the stabilization of soil with wheat straw fiber and cement showed that the addition of the fiber doesn't show increased strength properties, results stayed somewhat the same [8]. Instead, it led to higher weight loss and capillary absorption. Research efforts have also explored the incorporation of natural fibers, such as oil palm and sisal fibers, into concrete [2] [69]. These studies demonstrated that the addition of natural fibers substantially improved the mechanical properties of concrete, including increased flexural toughness and ductility, albeit with a decrease in workability.

When adding natural fibers to earth mixtures, new challenges emerge. Firstly, the interaction between natural fibers and drying soil can create voids around the fibers due to their expansion and shrinkage with moisture content, potentially compromising the bond between the earth and the fibers [44]. A solution could be to make the fibers water-repellent. Secondly, the addition of natural fibers tends to decrease the workability of concrete proportionally [2]. Lastly, several factors strongly influence the mechanical properties of fibers, including growing conditions, climate, harvest timing, fiber separation processes, storage conditions, and variations in length and diameter, among others [44].

Due to time constraints in this research, the addition of natural fibers will not be thoroughly investigated. However, previous research indicates promising results, making it highly recommended for further exploration and study.

Alternative mixture designs with gypsum as a binder

The primary challenge in formulating a mixture for this project lies in the absence of established guidelines and codes. The knowledge of this construction method is typically transmitted through generational knowledge, often lacking a structured engineering approach. Consequently, a substantial amount of information is disseminated through blogs and media channels such as YouTube resulting that these mix designs are very different from each other and are often inadequately documented.

It's worth mentioning that some of these mixtures utilize calcined gypsum as a binding agent. However, due to the time constraints of this research, an in-depth investigation into the use of calcined gypsum as a binder was not conducted. Given that it is a naturally occurring product, exploring its viability as an alternative to cement could be interesting to enhance the sustainability of the material. Furthermore, the existing mix designs are not inherently self-compacting, but investigating the possibility of achieving self-compaction with calcined gypsum could be a valuable research endeavor.

Architect M. Frerking started the construction of his first earth cast home in 1996 in Arizona [18]. The main difference between other earth building techniques is the use of calcined gypsum as a binder. As gypsum is compatible with clay, cast earth often shows a better strength than rammed earth, adobe and pise. According to M. Frerking, the soil used for cast earth can contain up to 20% of clay without a reduction in strength, making more soil types compatible for this mixture. According to his research a mixture with a 20% clay mixture can lead to a compressive strength over 6890 kPa.

A study by B. Y. Pekmezci et al. also investigating gypsum as a binder [7] suggest that first the lime and soil should be added together and mixed with water. Subsequently stirring the gypsum in a separate container and then adding it to the lime-soil-water mixture. The setting time of earth + lime + gypsum is estimated to be up to 20 - 25 minutes. The mixture is complete to be poured inside a mould. When the setting time of the gypsum is completed, the mould can be removed and prepared for the next sample.

In a series of videos from BION Design, the mix preparation for poured earth is illustrated also adding gypsum to the mix. The first step is to dissolve 17 grams of citric acid in one bucket of water. Next, this mixture is added in a concrete mixer together with two buckets of gypsum. Subsequently, 2,5 buckets of the soil mixture is also added in the concrete mixer. Also adding 7,5 buckets of gravels with a diameter between 0-20 mm. It is important to add water slowly and a maximum of 24 Liters. When the mixture is ready, a field test with the Abraham cone is conducted where a slump height of around 150 mm is recommended. Finally the soil is poured in the mould and vibrated. Whenever the mix is dry, formwork is removed.

Advantages of glass bottle earth bricks with poured earth

- increase in mechanical strength in comparison to traditional earthen building techniques (better interlocking of particles when drying)
- faster execution
- less labor intensive than other earth based construction techniques
- increased production flexibility: prefab is possible
- one can prefabricate the earth blocks in a controlled environment
- uses the same widely known production technique as concrete (as traditional building techniques often showed a lack of professional experienced people)

5.2.2. Reflection on case studies

Based on these reference projects, it can be concluded that container glass waste is repurposed due to their environmentally friendly nature, unique aesthetics, and affordability as a building material. Most of these applications are on a small scale, possibly because traditional building methods tend to be labor-intensive with a lack of building codes. Additionally, a trend is observed where owners with creative and practical backgrounds conceive and construct these projects themselves, without the assistance of experts. This is partly because the construction process does not require complex and expensive machinery and may also be due to a lack of available experts.

Horizontal orientation of bottles in walls is predominantly used, as it facilitates structural stability and allows light to pass through. In some cases, bottles are utilized in their entirety, while in others, the neck area is removed and the remaining pieces are connected. According to Younes' thesis [52], the latter approach leads to imperfections and a decrease in mechanical properties. Furthermore, this method adds to the labor-intensive nature of the construction process. Therefore, in this thesis, we focus solely on the use of intact bottles.

It is worth noting that the bottles are typically used without caps. Occasionally, individuals prefer to orient the openings outwardly to enjoy the sound produced when wind passes through the bottles, and they may also have concerns about insects and dust accumulating inside. Cement is the most common material used to connect the bottles together, although in the case of the Beer Bottle House in India, a mixture of local soil and cement is utilized. Besides, some mention to remove the labels as it could lead to the shrinkage of the labels and embedding them in the mortar. But in other case studies the labels weren't removed, and complications were not mentioned.

There are several reasons why raw earth buildings are so attractive. The possibility to build a sustainable house which is considerably cheaper than an average building, thermally comfortable and unique looking are the main appealing reasons. Most of the buildings are constructed by its owner which is due to the practical and legal barriers this construction method is still facing in Brazil. This contributes to the prevalence of these houses primarily in rural areas rather than urban centers. Furthermore, the scarcity of skilled builders and construction experts specialized in earth buildings can be attributed to the limited dissemination of knowledge and education on this particular construction technique, resulting in its low prevalence in the industry. There is another problem that precludes raw earth buildings from being used on a larger scale in Brazil: the presence of an insect named *Triatoma infestans*. This insect causes the *Chagas Disease* which is often associated with earth constructions. This reputation was formed in the past as some buildings were made in poor conditions and containing holes, which led to an ideal habitat for insect proliferation. Some extra ingredients can be added to the earth mix to prevent insect manifestation, such as lime and cement. [63] [13]

5.2.3. Sustainable building material

The reuse of glass packaging helps to reduce the amount of waste in landfills. The amount of bottles that go to landfill every year depends on the country and region. However, estimated globally by *recycle across america*, more than 28 billion glass bottles and jars end up in landfills every year [64]. Using these bottles in constructions instead of traditionally buildings materials, prevents the needs to extract new raw material and use new energy to produce these. This helps to conserve natural resources and

reduces the carbon footprint. By encouraging the reuse of glass bottles, people can be encouraged to think creatively about re-purposing other waste materials.

Re-using glass bottles which are in certain regions discarded and illegally dumped due to the lack of a proper waste collection and infrastructure (see Chapter 3), embraces a sustainable structure. The concept aims to elongate the lifespan of materials, diverting waste from landfills and promoting a more environmentally conscious approach to construction. This not only reduces the demand for traditional construction materials but also minimizes the environmental impact associated with resource extraction and manufacturing.

While re-using glass bottles contribute to sustainability by repurposing waste, it's important to note that the product cycle of the bottle isn't completely closed. Glass bottles have initially served a different purpose, and while they find new life in construction, they may not be endlessly recyclable or biodegradable. As a result, the concept raises questions about the ultimate environmental impact and the need for comprehensive waste management strategies.

Despite these considerations, it is emphasizing resourcefulness and reducing reliance on conventional building materials. This concept challenges traditional notions of construction and advocates for a more circular and regenerative approach to building, emphasizing not just the use but the reuse of materials in the pursuit of a more sustainable future. Additionally, building with earth is classified to be more sustainable when comparing the embodied energy to concrete. From literature research a list which summarizes the energy needed to produce different building materials is presented in table 5.3.

Table 5.3: Embodied energy

material	embodied energy	source
<i>rammed earth</i>	0.7 [Mj/kg]	[49]
<i>mud brick</i>	0.7 [Mj/kg]	[49]
<i>clay brick</i>	2.5 [Mj/kg]	[49]
<i>lightweight aerated concrete block</i>	3.6 [Mj/kg]	[49]

5.2.4. Indoor performance

Many literature studies mention that housing made out of earth have good thermal insulation properties and is a good protection in terms of extreme climate [65]. Additionally, earth-based buildings often incorporate features such as breathable walls, which help maintain optimal humidity levels, ensuring a healthier and more pleasant indoor atmosphere.

5.2.5. Indirect opportunities

Housing deficit and Resource Constraints

In regions facing geographical obstacles, widespread locations, or resource constraints, obtaining traditional building materials like cement and bricks can pose significant challenges, especially in developing countries. A consequence can be a shortage of available housing. Developing countries also have a low recyclable rate of glass packaging, and thus glass bottles are widely available and can be obtained for a low cost. By re-purposing glass bottles in constructions, cheap and environmental friendly houses can be constructed.

While working on this thesis, I've heard from fellow students and researchers who sometimes conduct research in fairly remote areas, they've come across buildings made from glass bottles in these locations. For instance, they've witnessed a school with walls constructed from glass bottles, as well as fences and houses. This is often because these places are quite secluded and have limited resources

available. Additionally, I was informed that people in these areas often make their own building materials.

Improving brand image

As people are getting more aware about the environment, companies that prioritize sustainability and environmental responsibilities can be more appealing to some customers. By using an environmental conscious construction material they can improve their brand image. Structural elements made from glass bottles stand out, have a specific aesthetic and are great to make a statement.

Job creation

Since constructing using glass bottles requires a significant amount of manual labour, the reuse of glass bottles in constructions can create several job opportunities. The bottles need to be collected, cleaned, inspected and prepared for use. Furthermore, it can create job opportunities for educators who can teach people about the benefits and techniques of re-using glass bottles in the construction industry. Also people with artistic design skills can be employed creating unique and visually appealing structures, playing with different patterns and colors.

5.3. Glass Bottle Earth Brick: The Concept

5.3.1. List of requirements

From the findings of previous chapters, a list of requirements is made for when re-purposing glass bottles in earthen wall structures. This list will highlight certain design choices and reinforce why certain building methods are chosen.

- The glass bottles should be visible. The visual aesthetically pleasing aspect is a main motivator for people to re-purpose glass bottles. The bottles are placed horizontally, ensuring light to pass through the bottom, with the additional benefit of being easily stack-able.
- In some case studies not removing the labels resulted in some issues when sticking to the mortar. So the labels should be removed from the bottles.
- It should be possible to construct the wall without expensive machinery. The prefab components produced, should have a certain dimension and weight which makes it easy to handle them with only body strength.
- The wall should fulfill serviceability and ultimate limit state requirements.
- The wall should have the options to prefab construct components to increase its flexibility in space and time. Also that it can be constructed in a controlled environment, to avoid delays and errors caused by the weather.



Figure 5.1: Precast bottle embedded panel by Mud Hands for a residence in Bangalore



Figure 5.2: Construction process in a mould by Mud Hands

As it should be possible to construct the wall with increased flexibility in time and space, blocks are constructed where the glass bottles are incorporated. This has the benefit of making prefab possible with numerous advantages. Such as working in a controlled environment which avoids delays and errors caused by the weather but also provides a more comfortable working environment for the constructors as they can be sheltered from the sun.

The pre-cast glass bottle panels by Mud Hands form an inspiration for the concept, which can be seen in Figure 5.1 and 5.2. For the construction of this panel, bottles are placed inside a mould and then concrete is cast around them. Subsequently, the bottles then are chopped off, only remaining the bottom part of the bottle.

The difference in this application will be the use of an earthen mixture instead of concrete. Besides, the bottles will be used as a whole and not chopped off and different bottle patterns will be investigated. Also, the panel will have a dimension and weight which allows it to handle it easily without the use of expensive machinery.

5.3.2. Manual handling

Injuries resulting from poor manual handling is one of the most common causes of workplace accidents. It is therefore important that the building component has a safe manual handling weight. The *HSE's lifting and lowering risk filter* outlines general safe lifting capacities for men and women, these will be taken as a reference for the weight of a component. The chart shows that a safe upper limit for an average man and woman are respectfully 25 kg and 16 kg, this when handling a weight at knuckle height. However when constructing a wall, the weight will pass different heights relative to the body. In this case, the lower band values are chosen of 5 kg and 3 kg for an average man and woman. When frequency is involved in lifting, according to *HSE's Manual Handling Assessment Charts*, when lifting 60 times an hour, a weight of 14 kg is considered to have no risks.

For this research, a weight between 3-5 kg for the component is aimed to provide safe handling. When having access to machinery or strong constructors, a larger scale could be investigated.

Here an overview of expected weight:

-
- Long neck beer bottle of 330 ml: 200-300 grams
 - Long neck beer bottle used in this research from Brouwland: 300 grams
 - Earth mixture: $\pm approx. 1540 [kg/m^3]$

Experimental Investigations

6

Self-Compacting Earth-Based Mortar

6.1. Introduction

This research has the objective to create a self-compacting earth-based composite from local earth which will be utilised to construct a brick where the glass bottles will be casted in. Already some research efforts were made to give earth-based materials properties similar to concrete, with the aim of enabling casting and enhancing their competitiveness in relation to other construction materials. [1] [50] [59] [15] [51] [48] [58]. This approach also contributes to the wider acceptance of earth as a viable construction material, given the familiarity with concrete in construction practices. See Section 5.2.1 about constructing with liquid earth.

Firstly different mixture designs are made, which can be read in section 6.3.2. The soil is stabilised with Portland cement and a polycarboxylate ether superplasticiser is added for improving workability. An artificial soil is created by adding red clay powder to a mixture of sand. Also a natural soil is utilised typically used to create rammed earth bricks, provided by *Oskam v/f* originating from Emmen in the Netherlands. The following aspects are important for the mixture:

- The mixture shouldn't show any segregation
- The flow diameter is aimed to be between 200 and 300 mm to ensure it can self-compact and easily flow between the bottles
- The mixture should be demouldable at least 24h after casting
- The failure pattern should be a similar satisfactory failure pattern as for concrete
- Early signs for excessive shrinking (crack forming) is not favorable

Afterwards the mixes are assessed on fluidity and mechanical performances. Then the optimal mix will be selected and used further during this research to construct the bricks with Longneck beer bottles.

6.2. Materials

6.2.1. Materials list

A comprehensive overview of all the materials utilized, along with additional information, can be read in Table 6.1. Technical properties of the superplasticizer used can be read in table 6.2. Since the research is being conducted at Delft University of Technology, located in the Netherlands, obtaining Brazilian soil was not feasible. Guidance was sought from Normando Perazzo Barbosa, a Brazilian professor specializing in earth construction and sustainability. He emphasized that it's unnecessary to replicate Brazilian soils, as long as the soil maintains the correct proportions of clay, silt, and sand.

Furthermore, this issue is also discussed with Dr. Yask Kulshreshtha, an expert in bio-based mud/earthen

Table 6.1: Material list

Material	Product Name	Supplier
<i>Earth</i>	Leemstuc	OSKAM V/F
<i>Clay powder</i>	GR - T	Sibelco
<i>Superplasticizer</i>	MasterGlenium 51 con. 35%	Mast. Build. Sol. NL B.V.
<i>Cement</i>	CEM I 52.5R	
<i>Limestone Filler</i>		

Table 6.2: Properties Superplasticizer

Properties MasterGlenium 51 con. 35%	
<i>Chloride Content in %m</i>	max. 0.1
<i>Total Chloride Content in %m</i>	max. 0.1
<i>Natriumoxide-eq. in %m</i>	max. 2.0%
<i>Volumetric density in kg/l</i>	1075
<i>Dry matter content EN480-8</i>	35
<i>pH</i>	5.0-8.0

constructions with a geotechnical background. Dr. Kulshreshtha noted that if Dutch soil is used, which is suitable for earth-based constructions, as the starting point, it will facilitate the transition to studying Brazilian soils in the future. Both experts emphasized that soils exhibit significant diversity, even within geographically close regions.

To address these considerations, an artificial soil mixture is initially created by incorporating clay powder to understand the impact of clay addition. Additionally, a natural Dutch soil, well-suited for earth-based construction is used.

6.2.2. Soil

Retrieved from the literature study, an optimum clay content is between 8% and 14% by mass. Clay and silt together should be between 20% and 35% of the mass. Additionally, the percentage of sand should be between 50% and 75% of the mass [40]. Professor Normando Perazzo Barbosa recommends a sand content between 65% and a maximum of 70% of the mass. The appropriate granulometry according to different sources can be seen in Graph 6.1 together with the granulometry of the local soil used for this research. This granulometry is retrieved from sieve analysis as described in Subsection 6.2.2.

Upon examining the various granulometries presented in Graph 6.1, it becomes evident that the local soil deviates from the recommended composition found in the literature study. While an option exists to blend this soil with a different type to alter its composition, this research has chosen to maintain the original composition. This decision is grounded in the belief that different earth applications may have specific preferences for particular soils.

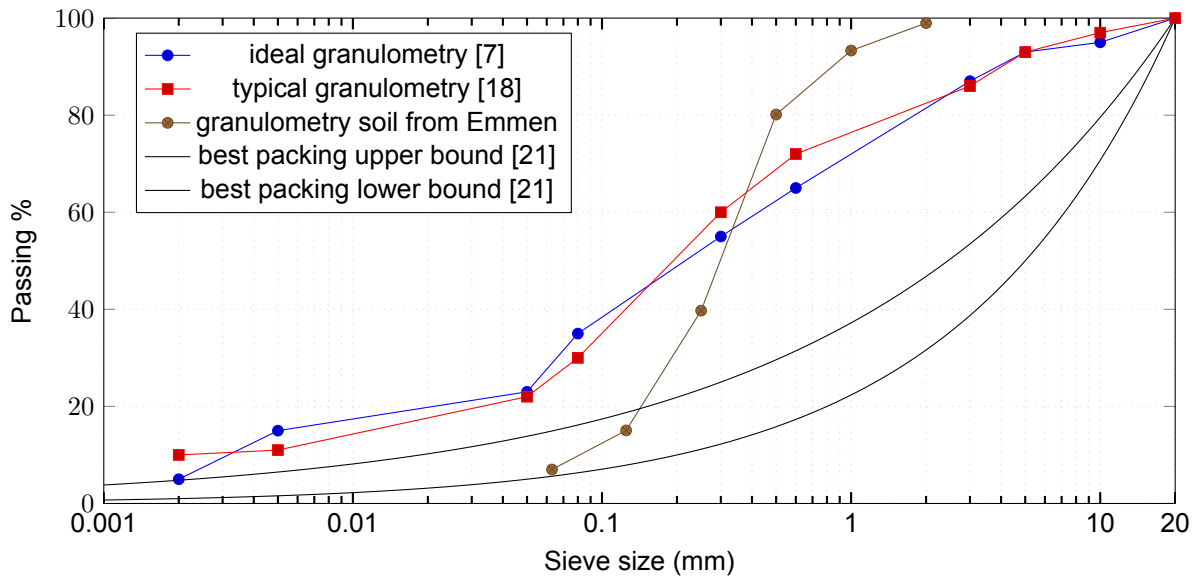


Figure 6.1: Granulometry

However, it's important to note that a self-compacting earth-based mortar represents a novel application, and as of now, no research has been conducted to provide a definitive conclusion regarding the ideal soil composition for this specific application.

In order to select the appropriate soil for the test, according to NZS 4298:1998 *Materials and workmanship for earth buildings* [32], it is recommended that the soil should fulfill following conditions:

1. The soil shouldn't contain any organic material as this can rot and disintegrate the wall.
2. Whenever large aggregates are present, the soil must be screened
3. Soils that contain surface cracks when dried should be avoided as over time the surface will flake off
4. The soil must succeed the wet/dry appraisal test
5. Gravels and stones present in the soil should not exceed a diameter of 25 mm.
6. Clay lumps present in the soil should not exceed a diameter of 25 mm

A sieve analysis is conducted to understand the granulometry of the soil and to remove large clay lumps, gravels and stones. This test is elaborated in following subsection.

Sieve analysis of local soil from Emmen, the Netherlands

The Dutch soil originates from Emmen, a place in the North of the Netherlands. The clay is extracted from road construction and construction pits by *OSKAM V/F*. This is then processed, but without heating such that the clay quality is retained in the products. Therefore the clay is known to promote a healthy indoor climate. The soil is mixed and large clumps are removed or crushed.

The earth sample is prepared by drying it in the oven at $60^{\circ}\text{C} \pm 5^{\circ}\text{C}$ for one hour. After the sample is cooled down, it is placed in sieves with sizes 2 mm, 1 mm, 0.5 mm, 0.25 mm, 0.125 mm and 0.063 mm. Then the sieves are vibrated for 30 minutes on setting fine aggregates. An image of the test set-up can be seen in figure 6.2, and a result of the sieve analysis can be seen in graph 6.1.

The particle size distribution of the soil is illustrated in Figure 6.2. One can retrieve from the analysis that the soil comprises 7% clay, 8% silt and 85% sand. According to some literature [18] [7] [21], this soil composition is not recommended for use in earth-based structures.

However, contrasting information can be found in other literature, suggesting that a sand loam soil is highly suitable for cement or cement and lime stabilization [65]. Notably, there is limited research



Figure 6.2: Sieve analysis Dutch soil originating from Emmen

available on self-compacting earth-based mortars, making it challenging to determine the ideal composition for this type of application. Furthermore, it's important to recognize that the preferred soil composition may vary for different types of earth-based applications.

It is essential to clarify that this research does not aim to identify the perfect earth composition for self-compacting earth-based mortar, partly due to the time constraints of this research. Instead, the existing soil composition without alteration is utilized. The results obtained from this study will hold value for future research endeavors.

Soil density of local soil from Emmen, the Netherlands

The density of the soil is measured with the pycnometer method. The earth sample is prepared by drying it in the oven at $60^{\circ}\text{C} \pm 5^{\circ}\text{C}$ for one hour. Next, the pycnometer is cleaned and dried thoroughly and weighed before use to ensure accurate measurements. Afterward, the pycnometer is filled with tap water, and its mass is recorded once more. This process is repeated for the weight of the pycnometer containing dry soil and water, as well as for the pycnometer holding only the dry soil. The density of the soil is calculated using following formula:

$$\text{soil density} = \frac{D-A}{B-A} * \text{density of water}$$

1. A = mass of empty pycnometer
2. B = mass of pycnometer filled with water
3. C = mass of wet soil sample
4. D = mass of pycnometer with soil and water

Results of the pycnometer method can be read in table 6.3. Images of the test can be seen in figure 6.3. Note that after one hour the fine particles are settled and you can clearly see the different grain sizes in the soil, with the finest one on top. The soil has a Specific Gravity of 2.48 or 2480 kg/m^3

6.2.3. Binders

The soil is stabilised by adding a blended type of cement CEM I 52.5R, and limestone filler in some mixes. A polycarboxylate ether (PCE) based plasticizer is used with a specific gravity of 1075 kg/l , see table 6.2 for the chemical and physical properties of the superplasticizer. As the mix will focus mainly on achieving a good flow-ability, metakaolin (MTK) is not chosen as a binder. This because MTK mainly consists out of angular plate-like shape particles which decreases the workability of the mortar [1].

Table 6.3: Specific gravity using Pycnometer

Specific Gravity Pycnometer	Mass (grams)
<i>Empty Pycnometer</i>	702.98
<i>Pycnometer + dry soil</i>	1102.73
<i>Pycnometer + dry soil + water</i>	2270.33
<i>Pycnometer + water</i>	2031.45
<i>Specific Gravity Soil</i>	2.48



(a) Test set-up Pycnometer



(b) Soil after one hour

Figure 6.3: Pycnometer test with soil from Emmen, the Netherlands

6.2.4. Clay

The soil utilized in this research project, sourced from Emmen, has a reddish to dark brown color. Red earth predominantly contains kaolinite-type clay, which is characterized by its relatively low expansiveness. The swelling and shrinking behavior of this type of clay mineral is considerably less pronounced, particularly when compared to soil types such as black cotton soil containing predominately morillonite, which exhibits a dark brown to black coloration. Black cotton soil can experience volumetric shrinkage ranging from 200-300% during drying, making it challenging to stabilize and therefore not ideal for this research endeavor. [65]

In order to better understand the influence of clay, an artificial soil is composed by adding red kaolinite clay powder to the mix. This is a red earthenware body for casting mainly used for ceramics, provided by Sibelco. Technical data is retrieved from the Sibelco website [28]. The chemical composition is depicted in Table 6.4. The full Technical Data sheet can be read in Appendix 6.4.

6.2.5. Cement

The soil has been stabilized using cement type CEM I 52.5R. There are various methods to stabilize soil, but for this research, cement was selected as it is the most commonly employed and widely utilized approach. Cement stabilization offers several advantages, primarily aimed at enhancing the strength of the stabilized soil product and increasing its resistance to erosion caused by rain. The strength of the cement-stabilized soil experiences augmentation with an increase in cement content, density and time. However, these improvements are strongly influenced by factors such as soil composition, the

Table 6.4: Chemical Analysis of GR-T, red clay powder by Sibelco [28]

Chemical Analysis of GR-T	%
<i>SiO₂</i>	66.6%
<i>TiO₂</i>	1.20%
<i>Al₂O₃</i>	19.0%
<i>Fe₂O₃</i>	4.00%
<i>CaO</i>	5.80%
<i>MgO</i>	0.5%
<i>K₂O</i>	2.60%
<i>Na₂O</i>	0.30%

percentage of cement used, the degree of compaction, as well as the duration, temperature and humidity of the curing process. [65]

A study conducted by Herzog and Mitchel in 1963 [35], investigating the reactions involved in the stabilization of clay minerals with cement, revealed the occurrence of a pozzolanic reaction during the hydrolysis and hydration of Portland cement with clay minerals. This particular reaction results in additional strength of the stabilized soil product and is not present in conventional concrete due to the absence of clay.

6.2.6. Limestone filler

Limestone filler is added as a binder. Lime is often used to stabilise compressed earth blocks and is essential to control the swell-shrink characteristics of clay [65]. OSKAM V/F mention they stabilise their soil with about 10% lime to weight. As mentioned in the book about compressed earth blocks [65], the optimum lime content is about 0.8 times of the clay content with kaolinite clay mineral. For a soil with montmorillonite clay, the optimum lime content ranges between 1.0-1.3 times the clay content. This can be substantiated by the fact that expansive clay minerals can absorb more lime. However, limestone filler also has an influence on the flow-ability and mechanical strength of the mix. To better understand its influence, mixes with and without limestone filler will be made.

6.2.7. Silt

When using a local soil, the soil isn't washed and processed which means silt will be present. Silt has a particle size smaller than 0.063 mm and larger than 0.002 mm and will be unfavorable for adhesion.

6.2.8. Organic materials

In a natural soil contaminants of natural origin are present. This is typically in the form of wood residues, decaying plant matter, and humus. They compromise the strength development. The raw soil is sieved, crushed and dried in the oven at $60^{\circ}\text{C} \pm 5^{\circ}\text{C}$ for one hour.

Table 6.5: Experimental program

Property	Slump Flow test	Flexural Bending	Compressive Test
<i>Standard</i>	NEN-EN 12350-8		NEN-EN 1015-11
<i>Curing</i>		T = 20°C ± 2 °C and HR = 95 ± 5	
		T = 20°C ± 2°C and HR = 50 ± 5	
<i>Testing Age</i>		7 days	7 and 24 days
<i>Number of Samples</i>	1	3	6
<i>Sample Geometry</i>	prisma 40 x 40 x 160 mm ³		

6.3. Experimental Methods

6.3.1. Experimental program

A summary of the experimental program is provided in Table 6.5. This table offers an overview of the various tests that are conducted, encompassing standards, testing duration, curing procedures, specimen quantities, and their respective dimensions. Different mixtures were prepared (subsection 6.3.2) using an artificial soil and evaluated for their work-ability and mechanical strength. Subsequently, a mixture was prepared using natural soil and subjected to similar assessments. Following these evaluations, an optimal mixture was chosen for measuring water capillary absorption and erosion. The research will then proceed with the selected mixture to assess the bottle brick.

As for the curing, initially the samples were cured in a room with a high relative humidity of 95±5 and in a room with a relative humidity of 50±5. However, when noticing the samples wouldn't harden that well in the room with the high humidity, it is chosen to not harden the samples in the humid casting room.

6.3.2. Mixture design

An experimental study was carried out by creating five different types of earth - based mortar mixtures incorporating different compositions. For the first three mixtures (A1,A2,A3) an artificial soil is composed as depicted in Table 6.7. For the latter two (N1, N2) the natural soil is used. A summary of the different mixture designs can be found in Table 6.6. Additionally, the ratio of the different compounds is depicted in the last five rows. The selection of mixture proportions was informed by a comprehensive review of the existing literature, as documented in references [1], [50], [59], [15], [51], [48], and [58]. Additionally, valuable insights were retrieved from discussions with experts in the fields of earth-based materials and self-compacting concrete and my experienced lab supervisor.

The Earth-based mixtures were made in batches of 1.20 L, using a mixer of Hobart Type N-50. Firstly, all the dry components (soil and cement) are added together and mixed for one minute on the slowest speed. Then, the mix is hand mixed as I noticed that the bottom of the bowl isn't mixed thoroughly. The dry mix is then placed again in the mixer for one minute on the slowest speed. The next step is to add water slowly while the Hobart is still mixing. Let it mix for two minutes. After two minutes, the sides and the bottom of the bowl is scraped to ensure good mixing. Repeat this process. For the last step, about 75% of the superplasticizer is added to the mix. This is added slowly while the Hobart is still mixing. Let it mix for two minutes on the slowest speed and then scrape the sides and the bottom of the bowl again. Lastly, add the last part of superplasticizer while the Hobart is mixing again for two minutes.

Table 6.6: Mixture proportions of Earth-Based Mortar

Mix ID	A1	A2	A3	N1	N2
<i>Constituent materials</i> [kg/m^3]					
<i>Cement</i>	168.2	168.2	168.2	114.286	194.4
<i>Limestone filler</i>	67.28	67.28	0	0	0
<i>Soil (Artificial/Natural)</i>	1585.45	1585.45	1585.45	1142.857	1550
<i>Superplasticizer</i>	10.8518	13.02	13.02	16	16
<i>Water</i>	274	274	274	500	349
<i>main ratios</i>					
<i>binder/soil</i>	0.149	0.149	0.106	0.152	0.12
<i>cement/soil</i>	0.106	0.106	0.106	0.1	0.12
<i>sp/fines (%)</i>	2.481	2.978	3.512	4.513	5.622
<i>water/cement</i>	1.807	1.807	1.807	4.375	1.795
<i>water/soil</i>	0.192	0.192	0.192	0.438	0.215

Table 6.7: Composition of Artificial Soil of $1585.45 kg/m^3$ as used in Table 6.6

Constituent materials	Vol. Mass [kg/m^3]	Quantity [kg/m^3]
<i>Sand 1-2 mm</i>	2640	542.5
<i>Sand 1 - 0.5 mm</i>	2640	271.25
<i>Sand 0.5 - 0.25 mm</i>	2640	271.25
<i>Sand 0.25 - 0.125 mm</i>	2640	298.375
<i>Clay powder</i>	2600	201.81

6.3.3. Characteristics of fresh mortar: mini cone test

Due to the high fluidity during the plastic phase of self-compacting mortar, intricate form-work and molds can be filled without entrapping air. Due to the highly variable and complex shape of glass bottles, using a self-compacting mortar is a suitable application without the use of compacting machinery. Additionally, when incorporating natural fibers, a good encapsulation of dense fiber reinforcement with mortar poses fewer issues.

Producing mortar with high fluidity without experiencing segregation during mixing requires a different approach than conventional mortar. Fine fillers and special additives ensure the production of a stable and highly fluid mortar. The mini flow test is conducted to assess the self-compacting behavior, right after the production of the mix as described in subsection 6.3.2. The mini cone is filled with the fresh made mix, and then the top of the cone is taken off. The cone is then lifted in a smooth movement. When the fresh mix stops flowing, two perpendicular diameters are measured as can be seen in Figure 6.4. The average value of the two measured diameters is taken as the flow diameter D_{flow} in mm.

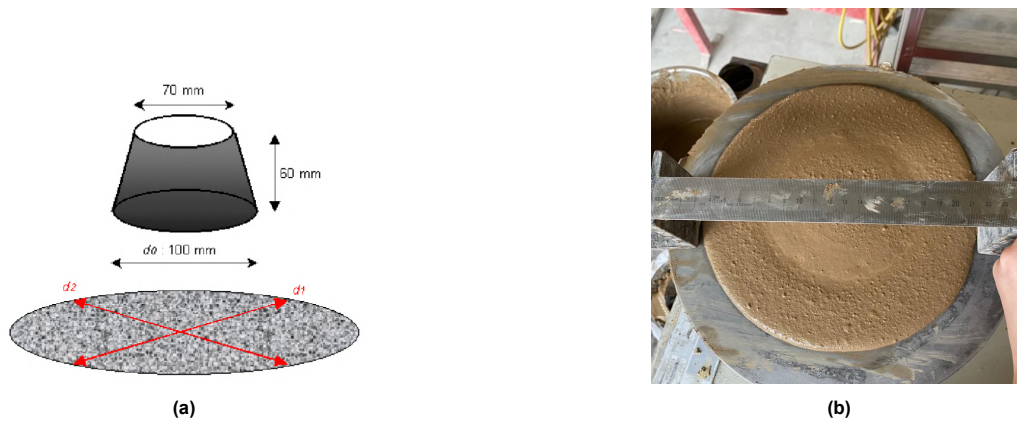


Figure 6.4: Mini slump flow test (a) and measurement of the flow diameter (b)

6.3.4. Flexural bending test

The specimen will be tested on flexural strength after seven days of curing according to NEN-EN 1015-11. This strength is determined by three point loading of three specimen of each 40x40x160 cm until failure. The apparatus has a loading rate of 0.1 kN/sec with a start load of 0.1 N. The area is taken to be 426.667 mm^3 .

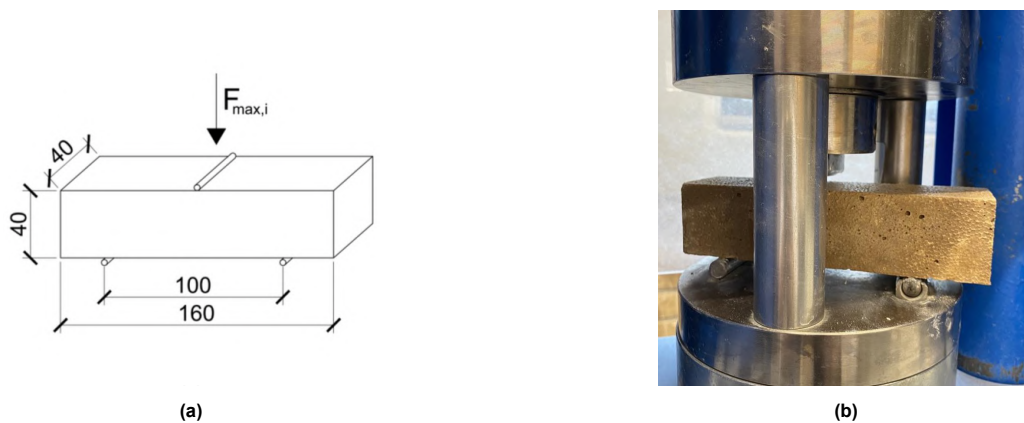


Figure 6.5: Determination of tensile strength: (a) static scheme, loading, and geometry of tested specimens; (b) the view of the specimen ready to test.

6.3.5. Compressive strength test

The compressive strength depends on several factors such as the composition of the materials, mix design and quality control during the production. The compressive strength of the mortar is determined by using the remaining halves after the compression test to compress a cube of 1600 mm^2 . The specimen are tested after 7 and 28 days of curing, with each three samples. The rate of compression is taken to be 0.5 kN/s with a start load of 1 kN .



Figure 6.6: Determination of compression strength: (a) static scheme, loading, and geometry of tested specimens; (b) the view of the specimen ready to test.

6.4. Results of Earth Based Mortar (EBM)

6.4.1. Self-compactability

After production of the different mixes, the mini slump flow test is conducted. Results of the mixes after the mini slump flow test can be seen in Figure 6.8. The average flow diameters of the mixtures are depicted in Graph 6.9. For the Artificial Mixtures A1, A2 and A3, the water/cement and water/soil ratio was kept constant. One can derive a positive relationship between the increase of sp/fines(%) and the flow diameter which is illustrated in Graph 6.7. As mix A2 has an increased amount of superplasticizer with respect to mixture A1. Besides, mixture A2 has less amount of fines with respect to mixture A3.

To conclude, increasing the superplasticizer content can enhance fluidity, while elevating the fines content may adversely impact fluidity and, consequently, self-compactation. With this conclusion, additional fines such as limestone filler are excluded from the mix using the natural soil.

6.4.2. Mechanical Performance

Flexural Tensile Strength

After seven days of curing, the specimen are subjected to a flexural bending test. The average flexural strength of the different mixes is depicted as in Graph 6.10. Table 6.8 displays the results of the flexural tensile strength test of all the samples. When comparing mixture A1 with A2, it seems that the addition of superplasticizer has a negative effect on the average flexural tensile strength, although the compaction is higher with more plasticizer. When comparing mixture A2 with A3, it looks like decreasing the fines may have a positive impact on the flexural strength. With this observation, it is decided to remove limestone filler in the final mix with natural soil.

Compressive strength

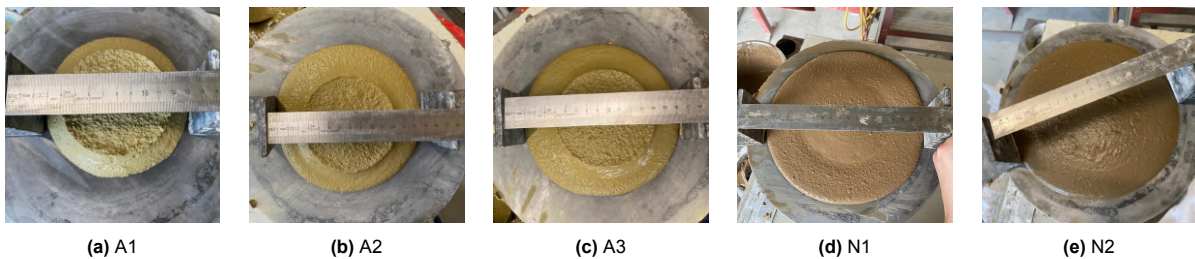
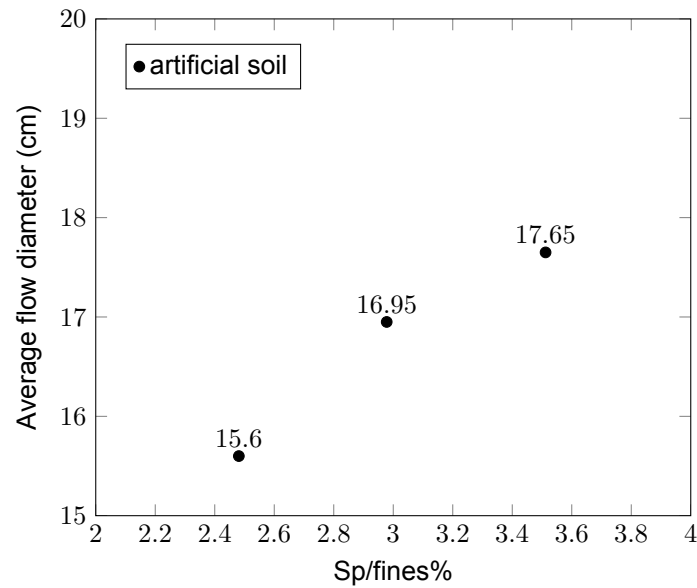
After seven and 28 days of curing, the samples are subjected to a compressive strength test. The average compressive strength of the different mixtures is depicted as in Graph 6.11. Table 6.9 displays the results of the compressive strength test of all the samples.

Table 6.8: Flexural Tensile Strength Test Results

Mix ID		A1	A2	A3	N1	N2
	Sample 1	2.559	2.082	2.458	0.810	3.745
<i>Flexural strength (MPa)</i>	Sample 2	2.415	2.053	2.342	0.839	3.485
	Sample 3		2.039	2.386	0.781	3.745
	Average	2.49	2.06	2.40	0.81	3.67
<i>Standard used</i>	NEN-EN 1015-11					
<i>Test location</i>	Stevinlaboratory TU Delft					
<i>Tested by</i>	H. Heller					

Table 6.9: Compressive Strength Test Results after 7 and 28 days of curing

Mix ID		A1	A2	A3	N1	N2
	Sample 1	5.066	5.024	5.178	1.18	8.032
<i>Compressive strength (MPa): 7 days</i>	Sample 2	4.685	4.82	5.436	1.037	8.245
	Sample 3	6.359	4.607	5.598	1.261	9.070
	Average	5.37	4.817	5.404	1.159	8.449
	Standard deviation	0.716	0.612	0.173	0.093	0.448
	Sample 1		5.980	6.038	1.535	11.837
<i>Compressive strength (MPa): 28 days</i>	Sample 2		5.988	6.754	1.403	12.158
	Sample 3		5.325	7.164	1.573	12.286
	Average		5.764	6.652	1.504	12.094
	Standard deviation		0.311	0.465	0.073	0.189
<i>Standard used</i>	NEN-EN 1015-11					
<i>Test location</i>	Stevinlaboratory TU Delft					
<i>Tested by</i>	H. Heller					

Figure 6.7: PCE superplasticizer effect on flow diameter**Figure 6.8:** Slumps of the mini slump flow test

Modulus of elasticity of earth

According to NZS 4297:1998 [31], an average estimation of the elastic modulus for a certain soil type can be expected to be in the following range:

1. Silty - sandy clays: 120 kPa - 3 GPa
2. Poorly graded sands: 3 GPa - 7 GPa
3. Silty sands: 7 GPa
4. Gravelly soils 7 GPa - 20 GPa

The earth used for this experiment can be classified as silty - sandy clays and can expect an elastic modulus of in the range of 120 kPa - 3 GPa according to [31]. However, this estimation is based on compressed earth bricks and not in the case of a self compacting earth based mortar using cement. However, as the mixture shows many similarities with a low strength concrete it could be that the elastic modulus is more in this range. For a concrete C8/10 an elastic modulus of 25000 N/mm^2 can be expected. This is used as an upper bound to estimate the elastic modulus of the earth based mortar.

Failure pattern

All the samples show a failure pattern very similar to a satisfactory failure pattern for concrete according to NEN-EN 12390-3:2019. This can be seen in Figure 6.12. One can see a clear hourglass shape and a good distribution of the aggregates within the mix.

Characteristic Compressive Strength

The characteristic strength, is the strength below which 5% is expected to fail during the compressive test. A Weibull strength distribution graph is prepared to define the characteristic compressive strength

Figure 6.9: Average flow diameter of Mix ID's A1,A2,A3,N1,N2

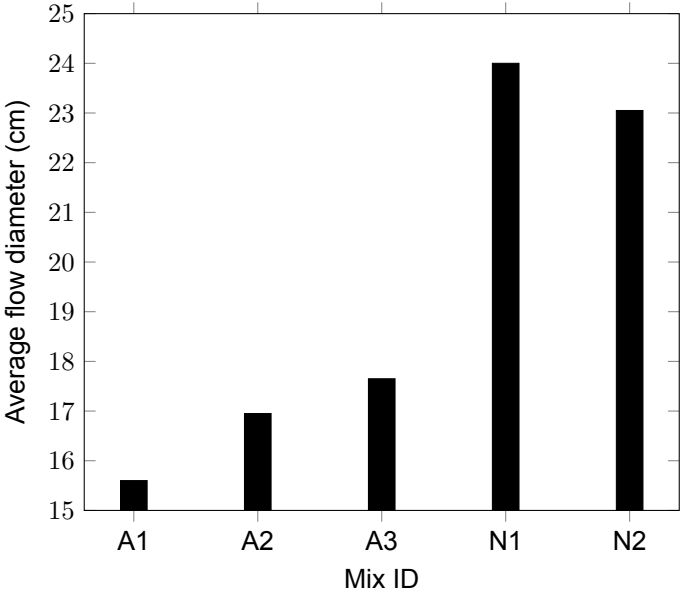


Figure 6.10: Average Flexural Strength after seven days of Mix ID's A1,A2,A3,N1,N2

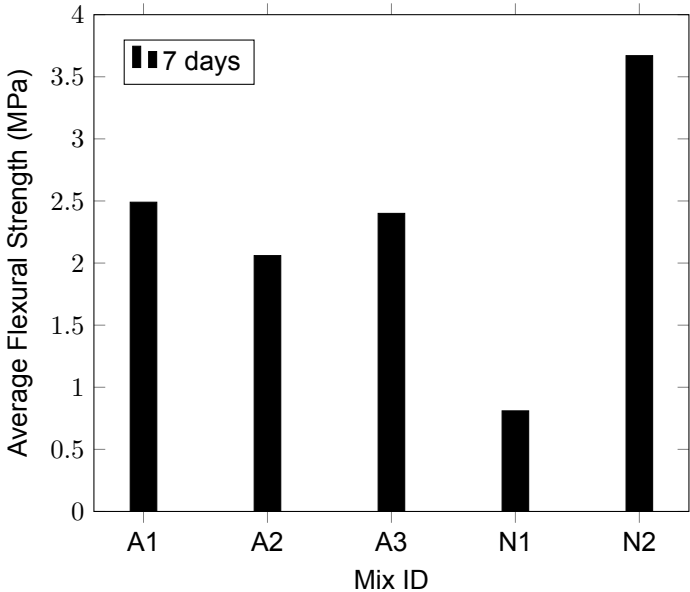
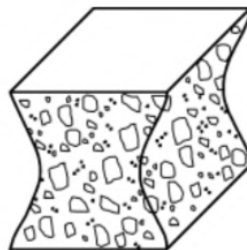
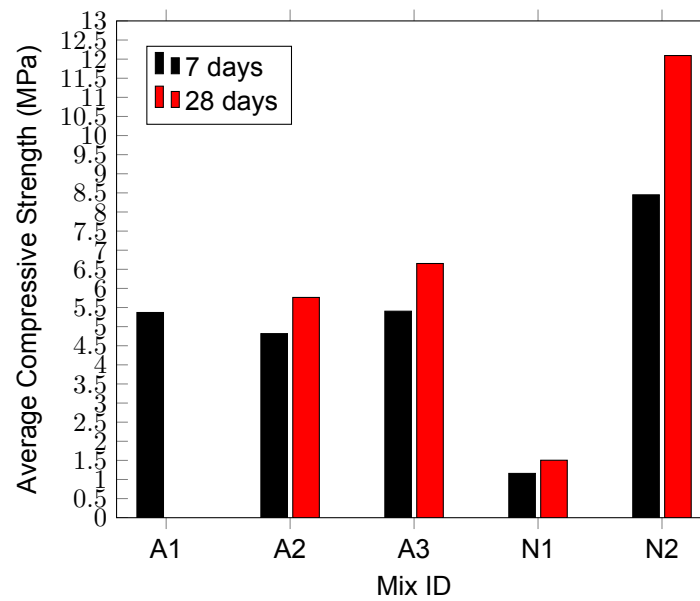


Figure 6.11: Average Compressive Strength of Mix ID's A1,A2,A3,N1,N2**Explosive failure**

(a) Satisfactory failure NEN-EN
12390-3:2019

**(b) Artificial soil****(c) Natural soil****Figure 6.12:** Failure mechanisms earth based mortar

as can be seen in Graph 6.13. A line is fitted through the data using a linear regression analysis. The first step is to order the data retrieved from the compressive test from lowest to highest strength. Subsequently the natural logarithms of these stresses are calculated and depicted in the third column of Table 6.10. The cumulative probability of failure represented by P_f , is estimated for each value which represents the y-axis of the Weibull plot. A commonly used estimator for linear regression analyses is $p_f=(i-0.5)/n$, which has a low bias.

The characteristic compressive strength is interpreted as for a compressive strength of 11.77 MPa, 5% of all failed specimen are weaker and 95% will be stronger. However, note that the sample size is small and accuracy can be improved by improving sample size.

The linear regression for the compressive strength of Earth Based Mortar (EBM) retrieved from the Weibull analysis using linear regression is depicted as in Equation 6.1:

$$y_{fck,c} = 192.5x - 654.23 \quad (6.1)$$

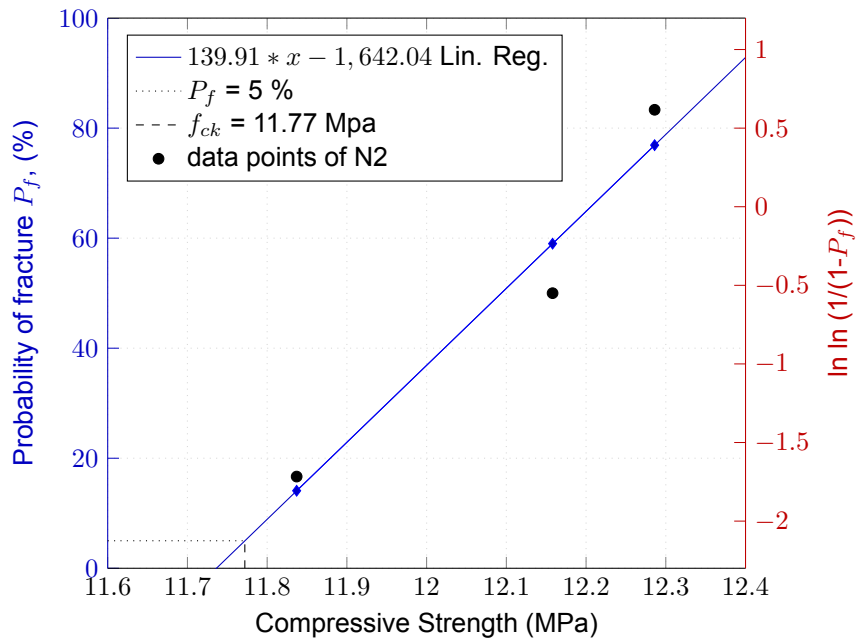


Figure 6.13: Weibull graph of the Compressive Strength of N2 with the linear regression estimator

Characteristic tensile strength

The characteristic tensile strength, is the strength below which 5% is expected to fail. A Weibull strength distribution graph is prepared to define the characteristic tensile strength as can be seen in Figure 6.14. A line is fitted through the data using a linear regression analysis, with calculation steps showed in Table 6.10. The cumulative probability of failure represented by P_f , is estimated for each value which represents the y-axis of the Weibull plot. A commonly used estimator for linear regression analyses is $pf = (i-0.5)/n$, which has a low bias.

The characteristic tensile strength is interpreted as for a tensile strength of 3.42 MPa, 5% of all failed specimen are weaker and 95% will be stronger. However, note that the sample size is small and accuracy can be improved by improving sample size.

The linear regression for the Tensile Strength of Earth Based Mortar (EBM) retrieved from the Weibull analysis using linear regression is depicted as in Equation 6.2:

$$y_{fck,t} = 139.91x - 1642.04 \quad (6.2)$$

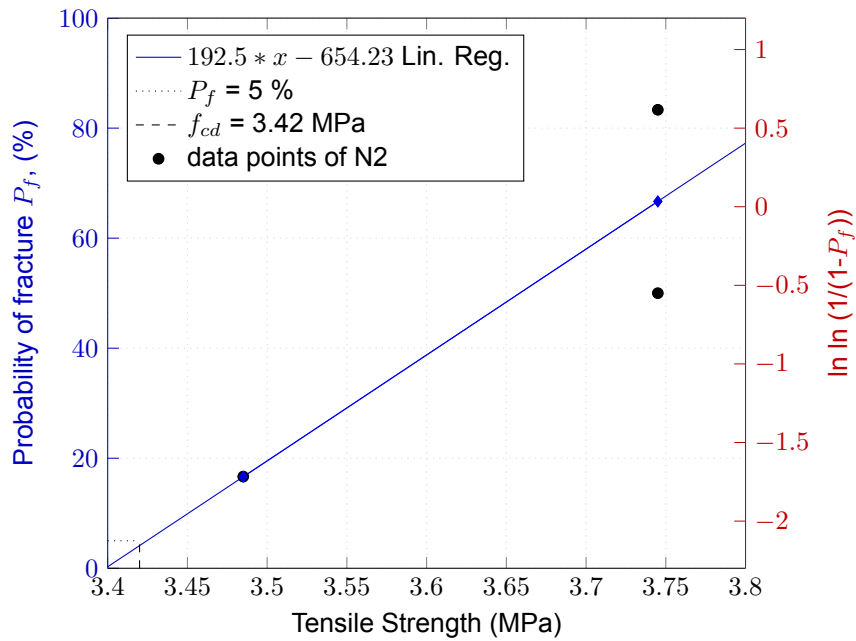


Figure 6.14: Weibull graph of the Tensile Strength of N2 with the linear regression estimator

An overview of the calculation steps for the linear regression for both characteristic compressive and tensile strength is listed in Table 6.10.

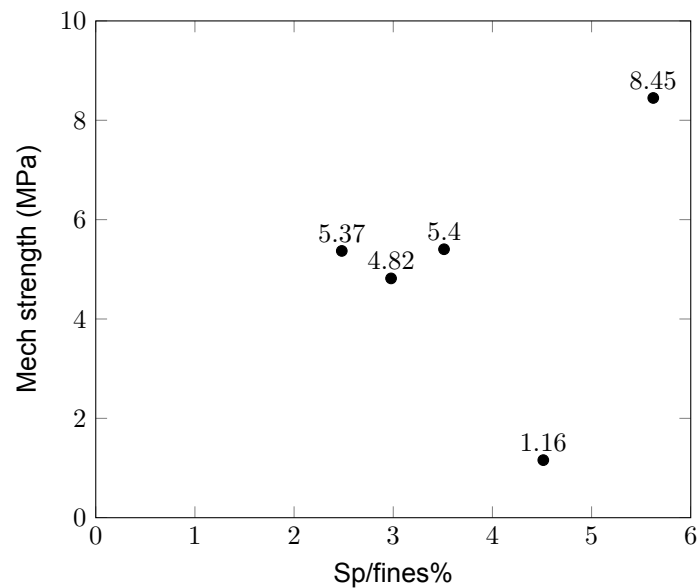
Table 6.10: characteristic compressive and tensile strength of EBM, calculation steps linear regression

i	Strength (MPa)	X = ln(strength)	$P_f = (i-0.5)/n$	Y = ln ln [1/(1-P _f)]
<i>Compressive</i>				
1	11.837	2.471	0.167	-1.702
2	12.158	2.499	0.5	-0.367
3	12.286	2.508	0.833	0.583
<i>Tensile</i>				
1	3.485	1.248	0.167	-1.702
2	3.745	1.320	0.5	-0.367
3	3.745	1.320	0.833	0.583

6.5. Discussion

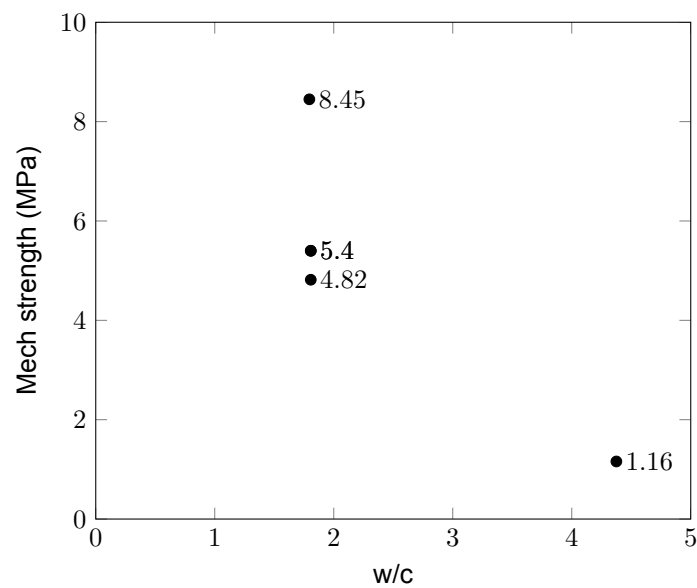
6.5.1. Mixture design and self-compactability

As can be perceived as in Figure 6.15, there is no clear trend can be derived from the amount of Sp/fines% and the flow diameter. In no mixtures, segregation was observed. At first glance, after the tensile strength tests, the cross sections appeared to have a homogeneous distribution of the aggregates.

Figure 6.15: Sp/fines% effect on mechanical strength

6.5.2. Mixture design and mechanical performance

In Figure 6.16, the water/cement ratio in relationship with the mechanical strength is plotted. When looking at the Mixture proportions, one can conclude that increasing the w/c ratio is not beneficial for the strength. For the three mixtures maintaining the w/c ratio constant, a strength increase result when the amount of superplasticizer/fines increase.

Figure 6.16: w/c effect on mechanical strength

6.5.3. Compatibility with existing standard (NZS)

In order to see if the New Zealand code for earth buildings NZS 4297:1998 also applies for a self compacting earth based mortar, a comparison is made with the expected flexural tensile strength according to the code and the actual flexural tensile strength in Table 6.11. As one can see is that the flexural tensile strength according to code NZS 4297:1998 highly underestimates the flexural tensile strength of the EBM. The flexural tensile strength can be approached as in equation 6.3.

$$f_{et} = 0.10 * f_e \quad (6.3)$$

A comparison of the tensile strength from the laboratory experiments and the tensile strength derived from the compressive strength according to the New Zealand Standard is depicted in Table 6.11.

Table 6.11: Comparison Flexural tensile strength according to building code and tests

Mix ID	Avg. fct (Mpa)	fct (Mpa) NZS 4298
<i>A1</i>	2.49	0.537
<i>A2</i>	2.06	0.482
<i>A3</i>	2.40	0.540
<i>N1</i>	0.81	0.116
<i>N2</i>	3.67	0.845

7

Longneck Beer Bottle Casted in Earth Based Mortar

7.1. Introduction

The focus of this chapter is to investigate how the glass bottle and the earth-based mortar behave together. Three bricks are made where one glass bottle is casted and bounded by the mortar created in Chapter 6. By subjecting the bricks to rigorous compression tests, we seek to understand their mechanical behavior and evaluate their potential as a reliable and safe construction material. Additionally, a simple assessment is made on how comfortable constructions with the bricks would be on a warm day.

7.2. Materials

To produce the brick, a mold is crafted using multiplex, as depicted in Figure 7.1 (a). To facilitate an effortless demolding process, a thin layer of oil is uniformly applied to the interior of the multiplex mold. The Longneck beer bottle is then positioned vertically at the center of the mold, as schematically represented by Figure 7.1 (b). Following this, the earth-based mortar, as detailed in Chapter 6, is prepared and poured into the mold. A weight is placed on top of the bottle, to prevent the bottle from floating up. The brick undergoes a curing process at ambient temperature and is subsequently demolded after a 24-hour duration. When removing the mold, a smooth surface is revealed as can be seen in Figure 7.1 (c).

Three bricks are manufactured, with exact geometric specifications outlined in Table 7.1. The glass bottle utilized in this experimental setup is retrieved from Brouwland, with specific details provided in Appendix A.

Table 7.1: Sample Geometry of Brick with Longneck Beer Bottle

Sample	Width	Height	Depth
<i>Sample 1</i>	197 mm	199 mm	210 mm
<i>Sample 2</i>	197 mm	199 mm	209 mm
<i>Sample 3</i>	197 mm	199 mm	231 mm

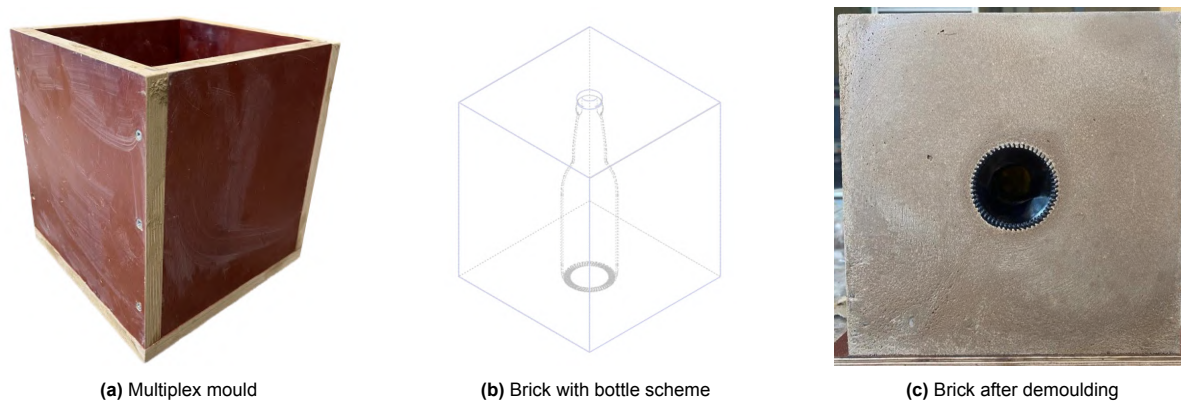


Figure 7.1: Longneck Beer Bottle Brick Making

7.3. Compressive Strength Test

Upon delving into the characteristics of container glass and Earth Based Mortar (EBM), a notable gap in understanding emerges regarding how these two components interact. To bridge this knowledge void, a compressive strength test is undertaken, aiming to uncover the complexities of their behavior, identify the point of material failure, and potentially draw insightful conclusions from the observed failure patterns. This experimentation also provides a foundation for correlating these findings with the numerical investigations discussed in *Numerical Investigations*. By coupling back the findings from these tests into the numerical study, the aim is to enhance our understanding of how these materials interact, providing valuable contributions to structural analysis and design.

7.3.1. Experimental program

A compressive strength test is conducted on each specimen after 28 days of curing with three samples. The rate of compression is taken to be 6 kN/s. The test set-up can be seen as in Figure 7.2. The test will automatically stop when no strength increment is measured. The exact geometry of each sample is depicted in Table 7.1.

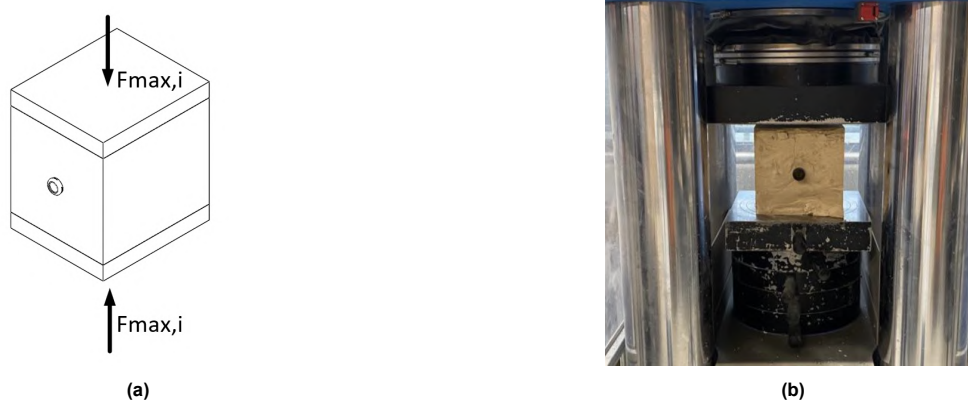


Figure 7.2: Determination of failure and compression strength: (a) static scheme, loading and geometry of tested specimens; (b) specimen ready to test

7.3.2. Results

The three samples exhibited similar behaviors and failure patterns following the compression test. Firstly, all samples displayed circumferential failures at the heel region, causing the bottom of the bottle to 'fall out' during the test, as depicted in Figure 7.3. Notably, clean cuts circled in red indicate the path where tension travels at these locations. Secondly, each sample exhibited fractures along

the side of the bottle on the inner glass surface, as shown in Figure 7.4. These fractures result from tensile stresses in the orthotropic direction on the inside of the bottle. The third common failure pattern, particularly noticeable under flash photography, revealed cracks on the outer surface of the bottle, aligning with the direction of cracks on the inner bottle but along the horizontal line of the cross-section, as illustrated in Figure 7.5. Additionally, vertical cracks were visible at the shoulder-to-neck transition, as depicted in Figure 7.5.

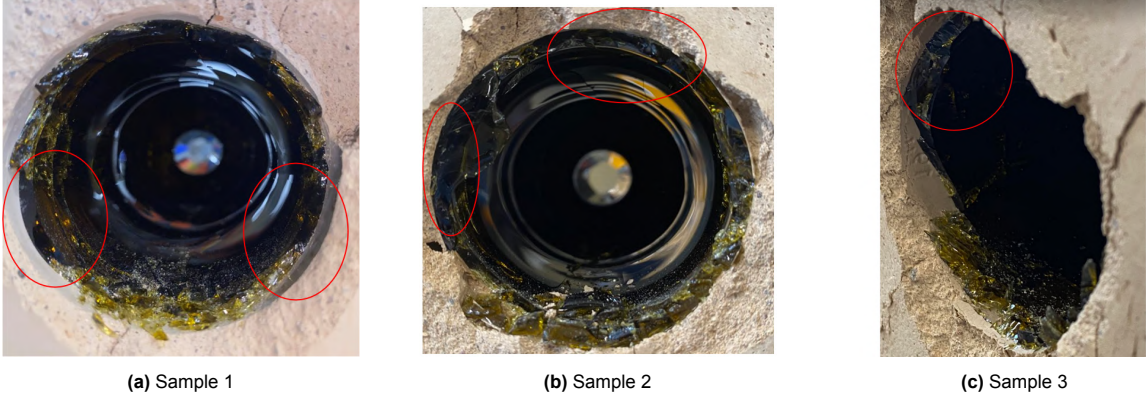


Figure 7.3: Images of Failure Around the Heel of the Bottle, Clean Cuts Circled in Red

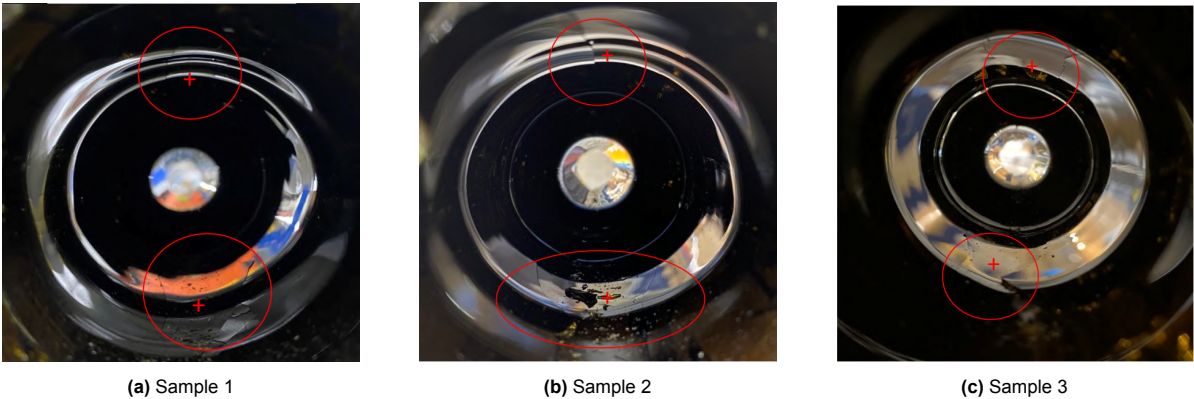


Figure 7.4: Images of Failure Along the Height of the Bottle on the Inside

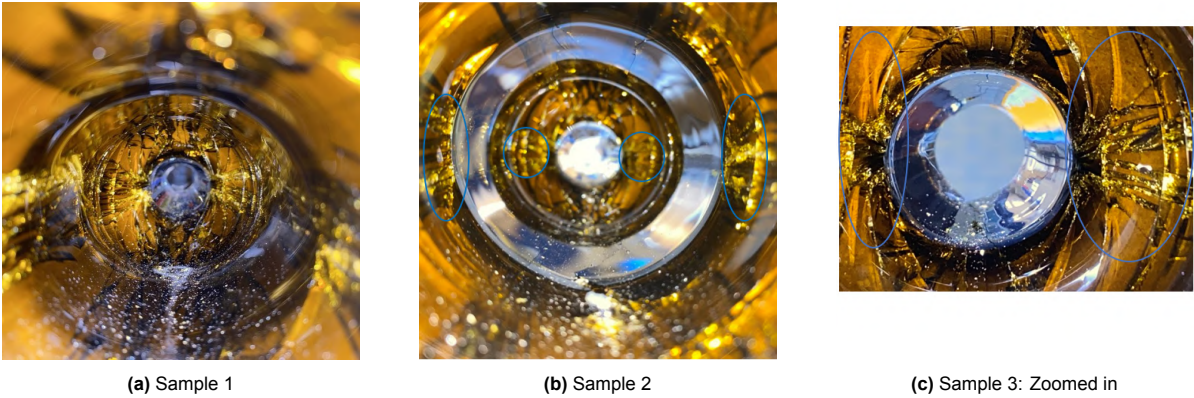


Figure 7.5: Images of Failure Outside Surface Bottle: Cross-Like Pattern

7.3.3. Conclusion and discussion

In all the samples, the glass bottle exhibited visible cracks and failed first. Initial observations of the crack pattern suggest the presence of tensile stresses on the vertical axis inside the bottle travelling along side the height, stemming from opposing tensile stresses. Which means that stresses in this direction should also be expected in the numerical model. Additionally, cracks run along the height of the bottle on the outside surface, and circumferential cracks are occurring at the transition between the neck and shoulder. While these images provide a general understanding of where tensile stresses are likely to occur and how stresses manifest in the bottles, the specific origin and cause of the initial crack, as well as the stress level leading to glass failure, remain unclear. To address these uncertainties, fragments of the glass are collected for a fracture analysis.

7.4. Fracture Analysis

Fracture analysis techniques were used to evaluate the fracture patterns, identify the fracture propagation directions, and locate the fracture origin (the point where the breakage started). In order for breakage to occur, a load must be applied to the bottle, and a flaw must be present to act as the origin of the fracture. Fracture analysis evaluates the load type, the flaw, and the breaking strength at which the witnessed breakage occurred.

7.4.1. Experimental program

An optical microscope was utilized at magnifications up to 60X to determine the origin location, origin orientation, and mirror dimensions. A calibrated Vernier caliper was used to determine the thickness at the origin.

Examination with a scanning electron microscope (JEOL JSM-IT510LV) equipped with X-ray spectroscopy capabilities was performed to image the fracture origins at higher magnifications and to identify any residues on the glass surface.

The experiment is conducted by *AGR American Glass Research*

7.4.2. Results

In both samples, the fracture originated at a cleavage scratch. In Sample 2, the fracture origin was located at the lowermost heel region of the bottle, which is just above the bottom/bearing surface. The location of the fracture of Sample 2 is indicated with red arrows in Figure 7.6. In Sample 3, the fracture origin was located at a knurl on the bearing surface. The location of the fracture of Sample 3 is indicated with red arrows in Figure 7.7.



Figure 7.6: Location of fracture origin indicated with arrows: Sample 2

For both samples the mirror origin has been found, which enables to calculate the stress at failure.

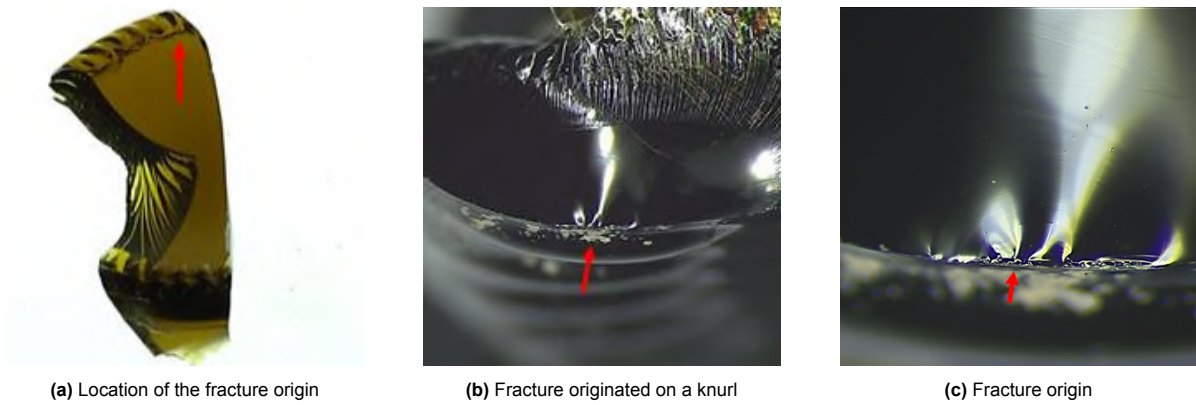


Figure 7.7: Location of fracture origin indicated with arrows: Sample 3

The stress at failure (kg/cm^2) can be related to the dimensions of the fracture mirror using the Equation 7.1. Where r is the radius of the fracture mirror in cm as illustrated in Figure 7.8. The stresses at failure for Samples 2 and 3 were approximately $608 kg/cm^2$ (59.62 MPa) and $431 kg/cm^2$ (42.27 MPa), respectively.

$$S = \frac{190}{\sqrt{r}} \quad (7.1)$$

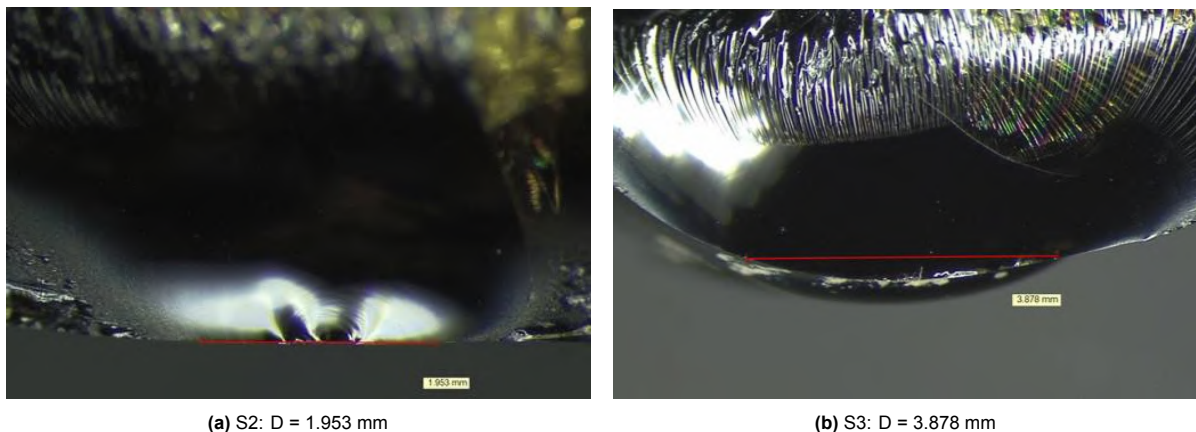


Figure 7.8: Mirror Measurement - Mirror Diameter of S2 and S3

In both samples, the fracture origin was located in a region previously covered with the earth-mixture. This part is removed with acetone to facilitate the fracture analysis. After the analysis with the optical microscope, the samples are subjected to an analysis with a scanning electron microscope with energy dispersive X-ray spectroscopy (SEM/EDS) to check if there was any metal residue at the fracture origin that could suggest a possible cause for the cleavage scratches.

7.4.3. Conclusion and discussion

Cleavage scratches result from the translation of a hard and sharp object across the glass surface under an increased normal load. The results from the analysis performed with the SEM-EDS indicated that, in both samples, there was metal residue composed of increased amounts of iron (Fe) and aluminium (Al) at the fracture origin, as shown below. The other elements there, like Ca, Na, Mg, and Si, is expected at typical container glass compositions.

Metal residue found at the fracture origins might initially suggest the use of metallic tools during bottle fabrication. However, upon examining the composition of the earth mixture, a striking similarity to that of the fracture origin emerges, implying that the earth mixture itself caused damage to the bottle surface.

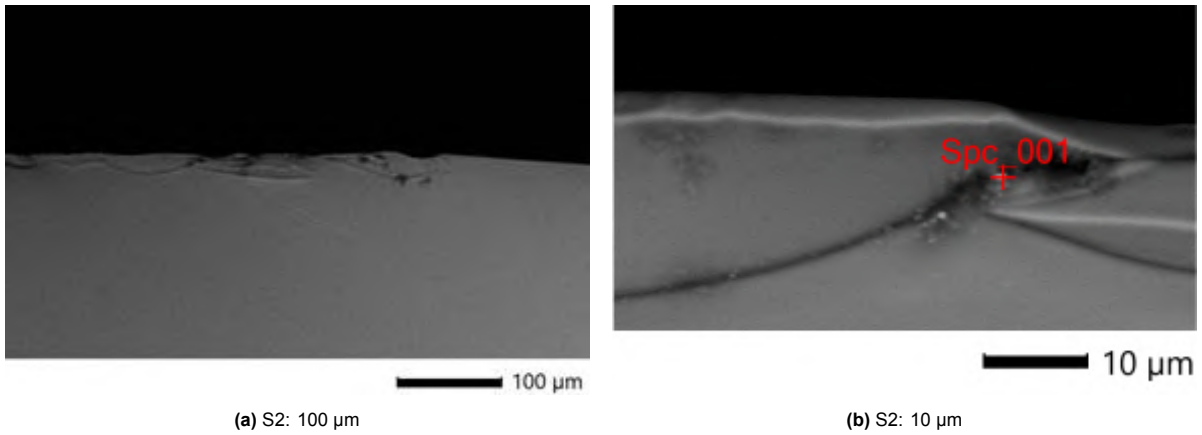


Figure 7.9: Sample 2 - Cleavage Scratch under High Magnification

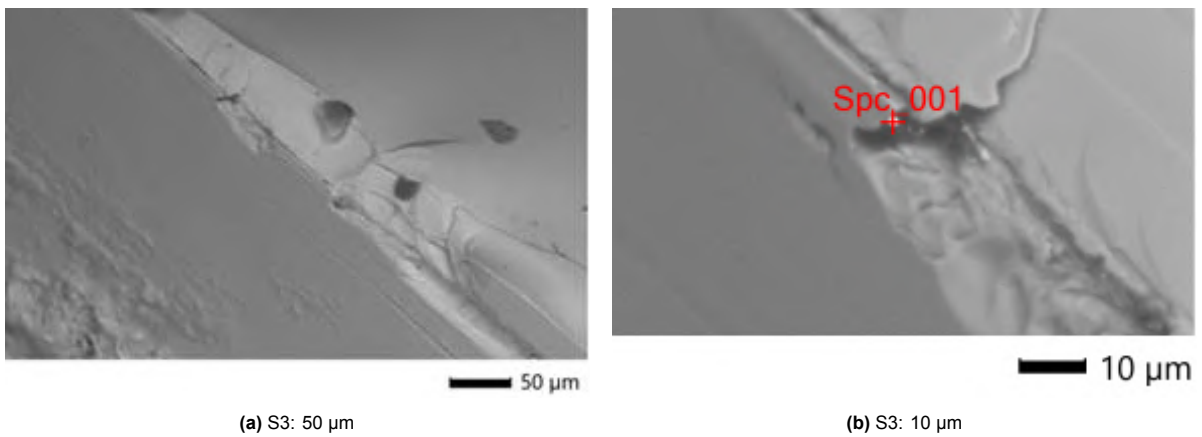


Figure 7.10: Sample 3 - Cleavage Scratch under High Magnification

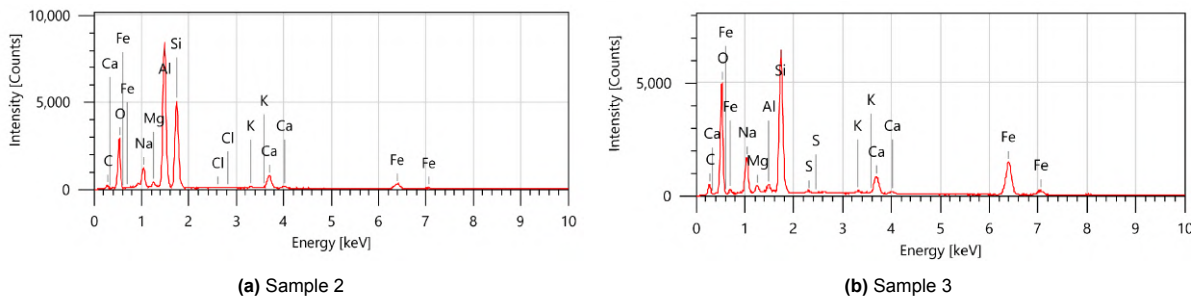


Figure 7.11: SEM-EDS Results: Table with iron (Fe) and aluminium (Al) at fracture origin

Element	Line	Mass%	Atom%
C	K	4.59±0.06	8.79±0.12
O	K	26.88±0.15	38.65±0.22
Na	K	4.39±0.05	4.39±0.05
Mg	K	0.75±0.03	0.71±0.02
Al	K	26.23±0.12	22.36±0.10
Si	K	21.18±0.12	17.35±0.10
Cl	K	0.20±0.02	0.13±0.01
K	K	0.47±0.03	0.28±0.02
Ca	K	6.32±0.08	3.63±0.05
Fe	K	8.98±0.14	3.70±0.06
Total		100.00	100.00

Spc_001 Fitting ratio 0.0114

(a) Sample 2

Element	Line	Mass%	Atom%
C	K	6.17±0.05	12.67±0.10
O	K	29.27±0.12	45.11±0.19
Na	K	6.37±0.06	6.83±0.07
Mg	K	0.96±0.03	0.98±0.03
Al	K	0.80±0.03	0.73±0.02
Si	K	17.75±0.09	15.58±0.08
S	K	0.30±0.02	0.23±0.01
K	K	0.48±0.03	0.30±0.02
Ca	K	4.76±0.06	2.93±0.04
Fe	K	33.14±0.23	14.64±0.10
Total		100.00	100.00

Spc_001 Fitting ratio 0.0080

(b) Sample 3

Figure 7.12: SEM-EDS Results: Graph with iron (Fe) and aluminium (Al) at fracture origin

Figure 7.13 displays results from the SEM-EDS analysis for both the hardened and raw earth. Detailed SEM-EDS analyses of the compositions at fracture origins, adjacent locations, and earth samples are provided in Appendix C.

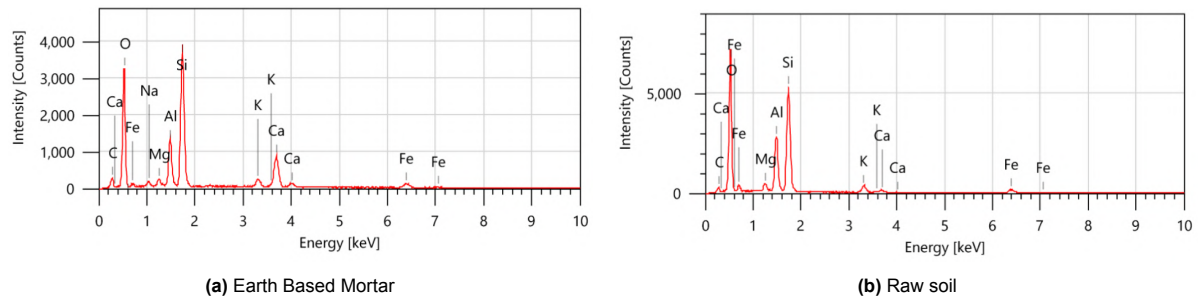


Figure 7.13: SEM-EDS Analysis Results: earth based mortar (left), raw soil (right)

In Appendix D, an overview of the approximate tensile breaking stresses of soda lime glass are given under different load duration's and surface conditions is given. For this test unused bottles, comparable to the surface condition "mild abrasions" are used. As one can see in the chart, the damage introduced during the use of bottles (rows "mild and moderate abrasion OW" and "mod sev abrasion RT") decreases their strength further than the scratches which were likely introduced during the manufacturing of the bricks. Additionally, the exact load duration is unknown, but it is at a maximum of one minute as for this time clear glass breakage was observed during the compressive test. So for a load duration of one minute, the approximate tensile breaking stress of soda lime glass is 703 kg/cm^2 for mild abrasions - bottle just fabricated. For mild and moderate abrasion OW this is respectively 352 and 281 kg/cm^2 . As for a severe abrasion one can expect an approximate tensile breaking stress of 176 kg/cm^2 after 1 min loading. The stresses at failure for Samples 2 and 3 were approximately 608 kg/cm^2 and 431 kg/cm^2 , respectively.

the goal of this research is to reuse bottles in a construction. So the bottle will have more abrasions and a longer load duration which will decrease the approximate tensile breaking stress of the bottle. It is possible to mimic the damage introduced in used bottles using abrasive paper (150-grit to 600-grit, the grain size depends on whether the bottle is returnable or not). Also a load duration factor has to be included as we can see from the stresses in the table and also because glass is susceptible to static failure.

7.5. Thermodynamics of the Brick as a Result of Sunlight Exposure

This experiment aims to assess the temperature rise experienced by both the earth mortar and the container glass when subjected to sunlight exposure. It serves as an initial evaluation to understand the thermal behavior of the bricks under solar influence, exploring the potential contribution to thermal comfort. This experiment is twice conducted, once when the brick was freshly made, after 6 days, still containing a lot of moisture. The other experiment is performed after 54 days of production, where the brick is more in a dry state.

7.5.1. Experimental program

Two Philips PAR38 infrared reflector light sources, exhibiting a combined power output of 350 watts, were placed at a distance of 60 centimeters from the brick and at a height of 10 centimeters. The infrared light sources were directed horizontally towards the brick. The set-up is shown in Figure 7.14. To measure the temperatures involved, three PT100 thermocouples were used. The thermocouples were placed on the brick and the bottom of bottle was exposed to the heat source and on the side not exposed to the heat source. The thermocouples were connected to three digital readout units, as illustrated in Figure 7.14 (b). During the entire experiment, the readout of the three PT100 thermocouples were recorded on video. The experiment progressed until the expected asymptotic temperature level was reached for the outside and inside of the brick.



Figure 7.14: Test set-up: Sunlight Exposure

7.5.2. Results

The temperature gradient of Earth Based Mortar (EBM) over time is illustrated in Graph 7.15. The experiment continues until reaching the asymptotic temperature level. The graph depicts two scenarios: in the first scenario, the brick is 6 days old, indicating a high moisture content, which is relevant in a wet, rainy climate represented by EBM_X_6. The experiment is then repeated on the same brick after 54 days of drying and curing, where the moisture content is expected to be lower, reflecting conditions on a dry, hot day. This data is represented by EBM_X_54. Thermocouples are strategically placed on the side exposed to the lamps of the Earth Based Mortar, representing the outside of the wall exposed to solar heat EBM_E_X. A sensor is also placed on the earth not exposed to the lamps, representing the inside of the wall. This data is represented by EBM_NE_X.

The temperature gradient of the glass bottle over time is illustrated in Graph 7.16. The experiment continues until reaching the asymptotic temperature level. Thermocouples are strategically placed on the bottle base, which is exposed to the lamps. This side represents the outside of the wall exposed to solar heat *Glass_E*. A sensor is also placed on glass finish exposed to the lamps, representing the inside of the wall. This data is represented by *Glass_NE*. The ambient temperature is represented by *T_ambient*.

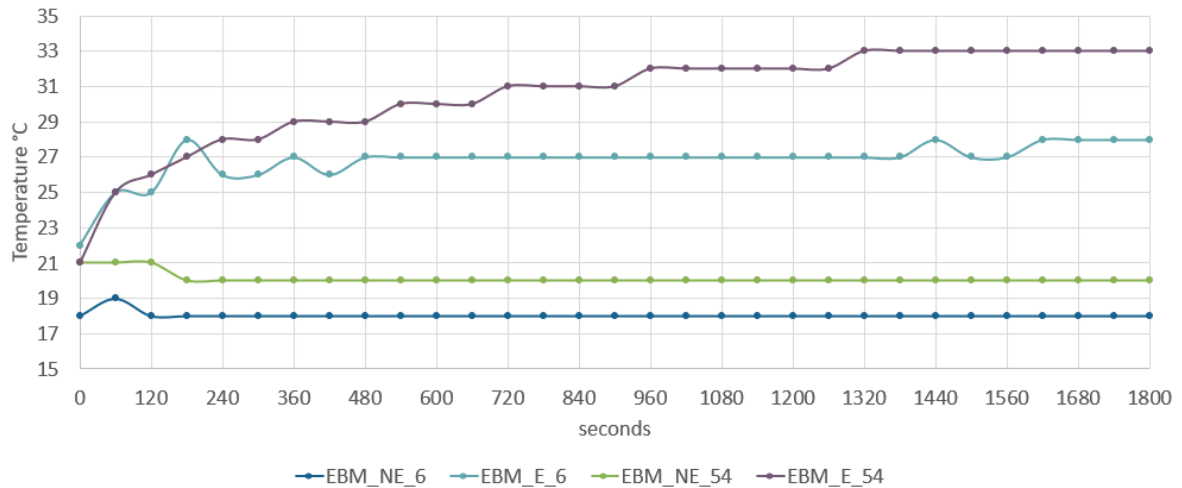


Figure 7.15: Graph Exposed Surface Temperature (outside) EBM_E vs. Not Exposed Surface Temperature (inside) EBM_{NE} , where 6 and 54 represents the age of the brick (days)

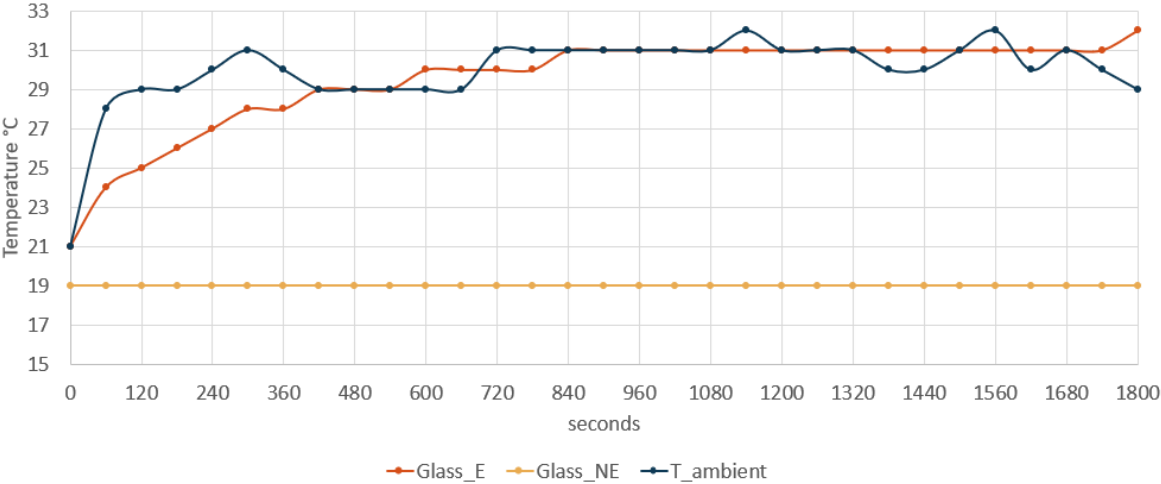


Figure 7.16: Graph Exposed Surface Temperature (outside) Bottom Bottle ($Glass_E$) vs. Not Exposed Surface Temperature (inside) Top Bottle ($Glass_{NE}$)

7.5.3. Discussion and conclusion

The Earth-based mortar functions as a heat sink, absorbing heat effectively. As anticipated, the moisture content plays a role in determining the asymptotic temperature, with higher moisture resulting in a lower temperature. Moreover, no temperature increase is observed on the unexposed side of the brick, representing the interior, for both the Earth-based mortar and the bottle. In conclusion, the brick can contribute to maintaining a comfortable indoor environment.

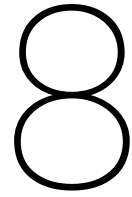


Figure 7.17: Crack Pattern Sample 1

Table 7.2: Results of Compressive Test of Earth Bottle Brick Samples

Compressive test Earth Bottle Brick		Area of Loading <i>mm</i> ²	kN	Mpa
	Sample 1	41370	358.4	9.14
<i>Sample ID</i>	Sample 2	41173	338.0	8.21
	Sample 3	45507	519.0	11.40
	Average	42683.3	405.1	9.58
	Standard deviation	1412.98	57.24	0.94
<i>Test location</i>	Stevinlaboratory TU Delft			
<i>Tested by</i>	H. Heller			

Numerical Investigations



Investigations on Stress Concentration of a Longneck Beer Bottle(s) Casted in Earth-Based Mortar

8.1. Introduction

To delve deeper into the propagation and behavior of stresses within glass bottle earth bricks (GBEBs), this chapter employs Finite Element Method (FEM) for numerical investigations. The aim is to simulate stress concentrations in GBEBs under compression, providing valuable insights into potential failure modes, the impact of bottle orientation on stress concentrations, and how varying internal distances between the bottles affect these stresses. Since some material properties of the earth-based mortar remain uncertain or can vary due to factors like moisture content and mixture composition, the effects will be explored of variations in elastic modulus and Poisson's ratio. Additionally, defining the boundary between the glass bottle and earth mixture will be investigated, including how friction at the interface influences results.

Subsequently, FEM simulations are set up using two different software packages: SolidWorks 2023 and DIANA FEA 10.7. At first, a Finite Element Method (FEM) model is created to replicate the laboratory compressive test described in Chapter 8. In this simulation, the GBEB undergoes a uniform downward deformation applied on top of the brick. A simplified 2D model is utilized to better understand stresses in a simplified context. Following this, a 3D FEM model is generated to enhance understanding of the influence of bottle patterns and their internal distances. A comprehensive comparison is made between the physical and FEM models, taking into account the influence of assumptions and mesh quality.

Furthermore, the FEM models undergo validation through mesh quality analysis and sensitivity studies. The obtained results and assumptions will be correlated with the experimental studies detailed in Chapter 6.

8.2. Material Properties

This section delves into the selected materials and its properties, which present several challenges, primarily due to the limited understanding of earth-based mortar and the intricate nature of glass strength.

8.2.1. Material properties of earth-based mortar

Given the novelty of Earth-Based Mortar, assumptions have been necessitated in the absence of comprehensive knowledge. To bridge this knowledge gap, these assumptions are systematically compared with existing data on rammed earth and low-strength concrete. In the subsequent Finite Element Method (FEM) analysis, the assumed material properties undergo scrutiny through sensitivity analyses within reasonable constraints. An overview of the material properties of Earth Based Mortar (EBM) as set in the FEM simulation are depicted in Table 8.1.

The Earth-Based Mortar fabricated in Chapter 6, exhibits similarities with low-strength concrete e.g. C8/10, manifesting comparable preferred failure patterns. Based on this knowledge The Youngs modulus is assumed to be 25000 MPa and the Poissons ratio 0.2. The compressive and tensile ultimate strength, is based on a small sample size of only three specimen which is defined by a Weibull plot representing the stress level at a 5% probability of failure, see Chapter 8. For the density, the average weight of the mortar prisms after 7 days is taken.

Sensitivity analyses will involve variations in the Young's modulus and the Poisson's ratio. A study conducted by Q. B. Bui et al. [61] measured the Poisson's ratio of rammed earth samples with different water contents. The results indicate a Poisson's ratio ranging from 0.22 to 0.4. Elastic modulus values for stabilized earth bricks typically exhibit considerable variation, with the sensitivity study encompassing a range from 2000 to 25000 (MPa).

Table 8.1: Material properties of Earth Based Mortar (EBM) as set in FEM Simulation

Material Property	Value	Unit
<i>Young's Modulus</i>	25000*	MPa
<i>Sensitivity Analysis Range</i>	2000 - 25000	MPa
<i>Poisson's Ratio</i>	0.2*	
<i>Sensitivity Analysis Range</i>	0.2 - 0.4	
<i>Tensile Ultimate Strength</i>	12.2	MPa
<i>Compressive Ultimate Strength</i>	3.7	MPa
<i>Density</i>	1.54e-06	kg/mm ³

* Assumptions based on similarities of behaviour with low strength concrete C8/10

8.2.2. Material properties of soda-lime container glass

The mechanical properties of soda-lime glass, crucial for longneck beer bottles, are influenced by several factors such as coatings, scratches, scratch interactions, and manufacturing methods. To assess these properties, a comparative analysis is performed using various standards that typically estimate the design tensile strength of soda-lime glass, primarily intended for flat glass applications. However, to ensure relevance to container glass, additional data from AGR's experiments is included in the comparison. The material properties, tailored specifically for the context of longneck beer bottle usage, are summarized in Table 8.6 for reference in the Finite Element Method (FEM) analysis.

Standards *NEN 2608*, *EN 16612*, *ASTM E1300*, and data provided by *AGR: American Glass Research* are compared to evaluate their methods for assessing the design tensile strength and load duration.

NEN 2608

According to the Dutch code *NEN 2608* design tensile strength ($f_{mt;u;d}$) can be calculated as in Equation 8.1.

$$f_{mt;u;d} = \frac{k_a * k_e * k_{mod} * k_{sp} * f_{g;k}}{\gamma_{m;A}} \quad (8.1)$$

Where,

k_a is the area factor

k_e is the edge factor

k_{mod} is the load duration factor

k_{sp} is the surface factor

$\gamma_{m;A} = 1.6$ which is the material factor for float glass

The load duration factor (k_{mod}) according to *NEN 2608*, is formulated by Equation 8.2.

$$k_{mod} = \left(\frac{t_0}{t}\right)^{\frac{1}{c}} \quad (8.2)$$

Where,

c is the corrosion constant, taken as 16

t is the load duration in seconds

t_0 is the reference duration, which is taken as 5 seconds

Following Equation 8.2, the load duration factor for a design load of 50 years is determined as followed:

$$k_{mod,NEN2608} = \left(\frac{5}{1577880000}\right)^{\frac{1}{16}} = 0.29$$

EN 16612

According to Eurocode *EN 16612* design value of bending strength for annealed glass material ($f_{g;d}$) can be calculated as in Equation 8.3.

$$f_{g;d} = \frac{k_e * k_{mod} * k_{sp} * f_{g;k}}{\gamma_{m;A}} \quad (8.3)$$

Where,

k_e is the edge factor

k_{mod} is the load duration factor

k_{sp} is the surface factor

$\gamma_{m;A} = 1.6$ which is the material factor for float glass

The load duration factor (k_{mod}) according to *EN 16612* is formulated by Equation 8.4.

$$k_{mod,EN16612} = 0.663 * t^{-\frac{1}{16}} \quad (8.4)$$

Where,

t is the load duration in hours

Following Equation 8.4, the load duration factor for a design load of 50 years is determined as followed:

$$k_{mod,EN16612} = 0.663 * 438290^{-\frac{1}{16}} = 0.29$$

ASTM E1300

The load duration factor (k_{mod}) according to *ASTM E1300*, is listed as in Table 8.2. The load factor for a design load of 50 years, referred to as 'beyond 1 year', is taken as followed:

$$k_{mod,ASTME1300} = 0.31$$

AGR: American Glass Research

An overview of the approximate tensile breaking stresses of container soda-lime glass in relation with surface conditions and load duration is listed in Appendix D.

The load duration factor (k_{mod}) according to data from *AGR: American Glass Research* and their appropriate test methods, is listed in Table 8.3. The load factor for a design load of 50 years, referred to as 'long/warehouse', is taken as followed:

$$k_{mod,AGR} = 0.6$$

Table 8.2: Load duration factors according to ASTM E1300, calculated to 8/1000 lites probability of breakage

Duration	Duration in seconds (s)	Factor
3 s	3	1.00
10 s	10	0.93
60 s	60	0.83
10 min	600	0.72
60 min	3600	0.64
12 h	43200	0.55
24 h	86400	0.53
1 week	604800	0.47
1 month (30 days)	2419200	0.43
1 year	31557600	0.36
beyond 1 year		0.31

Table 8.3: Load duration factors according to the data provided by AGR:American Glass Research, see Appendix D

Duration	Duration in seconds (s)	Factor
<i>Impact Test</i>		
0.001 s	0.001	2.00
<i>Crowning</i>		
1 s	1	1.34
2 s	2	1.27
<i>Thermal Test</i>		
3 s	3	1.23
4 s	4	1.18
10 s	10	1.12
15 s	15	1.09
20 s	20	1.07
30 s	30	1.04
<i>Pressure testing</i>		
1 min	60	1
5 min	300	0.91
<i>Pasteurizer</i>		
20 min	1200	0.85
30 min	1800	0.83
1 hour	3600	0.80
12 hours	43200	0.71
1 day	86400	0.69
3 days	259200	0.67
1 week	604800	0.64
long (warehouse)		0.6

Comparison of load duration factors

As depicted in Figure 8.1, the load duration factor k_{mod} exhibits a nearly identical behavior across various standards. In Table 8.5, the load duration factor for a design load of 50 years according to the different standards are listed.

The notable variance in the load duration factor k_{mod} observed in the AGR data can be attributed to the testing being conducted on container glass rather than flat glass. Despite both being soda-lime glass, differences in production methods and coatings exist. Furthermore, the fact that container glass typically undergoes storage in a warehouse for a maximum load duration of one month could also contribute to this noticeable deviation.

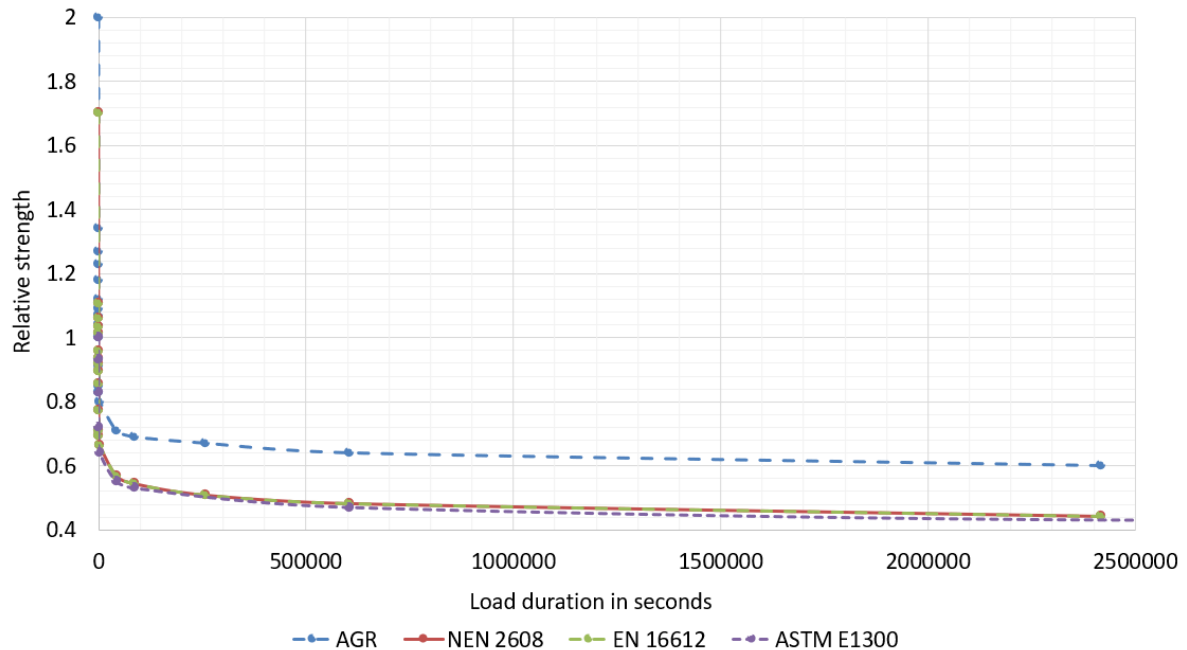


Figure 8.1: comparison of relative strength of soda-lime glass in relationship with load duration: AGR, NEN 2608, EN 16612 and ASTM E1300

Table 8.4: Comparison of load duration factors for a design load of 50 years: NEN 2608, EN 16612, ASTM E1300 and data by AGR: American Glass Research

Standard	k_{mod}	Load Duration
<i>NEN 2608</i>	0.29	50 years
<i>EN 16612</i>	0.29	50 years
<i>ASTM E1300</i>	0.31	'beyond 1 year'
<i>AGR: American Glass Research</i>	0.6	'long/warehouse'

Comparison of tensile strength of soda-lime glass according to different standards

A summarized comparison of the various standards is presented in Table 8.5. It's notable that when comparing the tensile design strength from AGR, which is based on container glass, it aligns closely with the design tensile strength defined by standards EN 16612 and NEN 2608. The surface condition 'severe abrasions' will be relevant when re-purposing glass bottles. For this research, a design tensile strength of 6.5 MPa for a load duration of 50 years will be adopted. This value is derived from tests conducted on container glass, which is more applicable to this context compared to standards based on flat glass. Additionally, the value of 6.5 MPa closely aligns with the minimum value defined by NEN 2608, which is 6.52 MPa.

Table 8.5: Comparison of tensile strength of soda-lime glass for a design load of 50 years according to different standards: EN 16612, NEN 2608 and data by AGR

Standard	k_a	k_e	k_{mod}	k_{sp}	$f_{t,ck}$ [MPa]	γ_M	$f_{t,d}$ [MPa]
EN 16612	1	1	0.29	1	13.05	1.8	7.25
NEN 2608	1	0.8	0.29	1	10.43	1.6	6.52
AGR: Severe Abrasions			0.6		11.7	1.8	6.5
						1.6	7.31
AGR: Mild Abrasions			0.6		41.4	1.8	23
						1.6	25.88

Table 8.6: Material Properties of an abraded Longneck Beer Bottle (severe abrasions) as set in FEM Simulation

Material Property	Value	Unit
Young's Modulus ¹	69930	MPa
Poisson's Ratio ¹	0.2149	
Shear Modulus ¹	28780	MPa
Long-term Characteristic Tensile Strength ²	11.7	MPa
Density ¹	2.465e-06	kg/mm ³

¹ Data of Soda-Lime Glass compiled by the Granta Design Team at ANSYS, incorporating various sources including JAHM and MagWeb

² Data of AGR: American Glass Research, see Appendix D: approximate tensile strength of soda-lime glass with load duration 'long' for 'severe abraded' surface condition

8.3. Finite Element Model (FEM)

Finite Element Method (FEM) models are created in DIANA FEA and SolidWorks, each offering their own advantages. DIANA FEA stands out as a more sophisticated software which excels in complex structural analysis, often applied for large-scale projects. However, SolidWorks has a more user-friendly design tool, integrating CAD modeling capabilities with finite element analysis. This makes it particularly well-suited for product design, catering to smaller-scale projects such as a glass bottle.

8.3.1. FEM: SolidWorks 2023

In SolidWorks, a Finite Element Method (FEM) model is established. This model replicates the compressive test conducted on the Glass Bottle Earth Brick (GBEB), as outlined in the experimental study (refer to Section 8). Material properties for both the earth mortar and the glass bottle are selected based on the specifications detailed in Section 8.2. Boundary conditions are specified, the model is constructed, and its precision is confirmed to offer valuable insights.

Modelling methodology

The geometry involves inserting an empty longneck beer bottle of 330 ml into a beam, as illustrated in Figure 8.2. This 'beam' represents the earth based mortar which bounds the bottle. The dimensions of the brick in the FEM model will give a WxDxH of 200 mm x 200 mm x 230 mm.

Regarding boundary conditions, the bottom surface is vertically restrained, while a uniform downward displacement is applied on the top. On one side of the brick, the vertices are constrained perpendicular to the face, mirroring the same restraint on the opposite side of the brick.

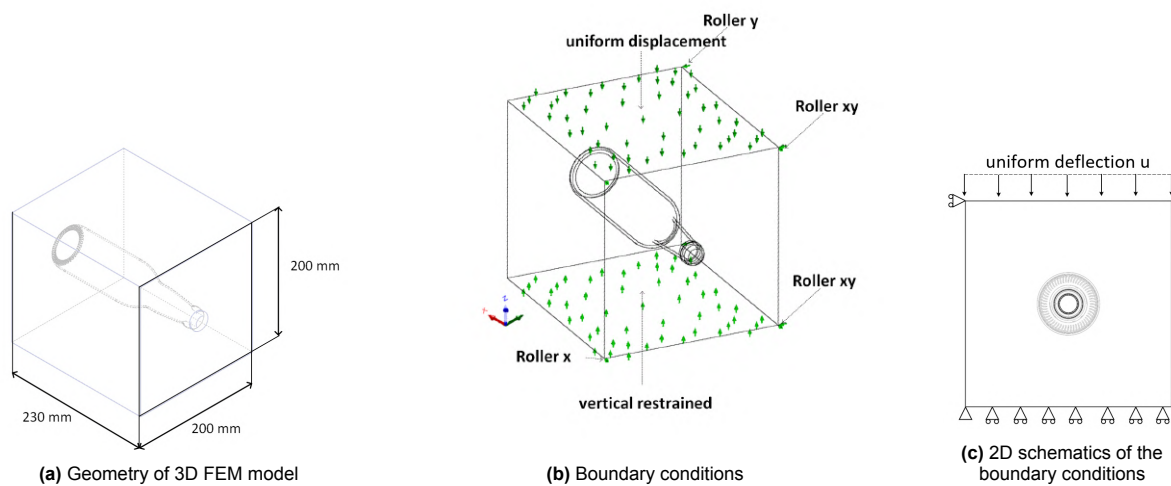


Figure 8.2: Finite Element Method (FEM) SolidWorks: geometry and boundary conditions

Meshing

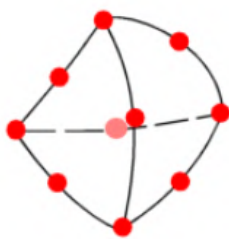


Figure 8.3: Parabolic solid element

For the 3D model of high quality, parabolic tetrahedral solid elements are generated. This meshing type is chosen as they are more accurate representation of curved boundaries, which is definitely the case around the bottle. Additionally, they produce better mathematical approximations than a linear solid element. A tetrahedral element with parabolic characteristics is characterized by four corner nodes, six mid-side nodes, and six edges. The accompanying illustration 8.3 depicts a schematic representations of a parabolic tetrahedral solid elements.

A blended curvature based mesh is applied which generates parabolic tetrahedral solid elements. This type of mesh automatically adapts the element size to the local curvature of the geometry to create a smooth mesh pattern.

A minimum element size is calculated based on the minimum radius of curvature from the geometry. This calculation relies on the number of elements in a circle which is set to 8. The minimum element size is then computed as the radius of the curvature times 45 degrees.

In the FEM model, mesh refinement is implemented, followed by the application of a uniform downward displacement. Subsequently, for each level of refinement, the maximum tensile and compressive stresses of the model are determined, consistently occurring at the same location. Additionally, a mesh

quality check is performed for each refinement, assessing the aspect ratio. A visual representation of the mesh refinement is presented in Figure 8.4.

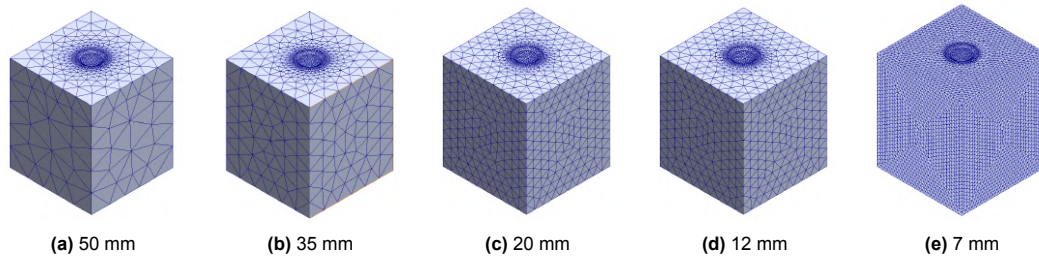


Figure 8.4: Mesh refinement of SolidWorks model: from coarse to fine meshes, with each labeled according to their maximum mesh size

As the quality of the mesh plays an important role in the accuracy of the results, the quality will be checked using the Aspect Ratio and the Jacobian Ratio. Various factors such as small edges and curved geometries contribute to the creation of elements with significantly disparate edge lengths. This discrepancy in edge lengths diminishes the mesh quality and thus the accuracy of the results obtained. The aspect ratio of an element is determined by the ratio between its longest edge and the shortest perpendicular distance from a vertex to the opposite face, standardized with respect to a perfect tetrahedron. In a perfect tetrahedral element, the aspect ratio is defined as 1.0, assuming straight edges connecting the four corner nodes. The software employs this aspect ratio calculation as a quality check to assess the overall mesh quality, where a good-quality mesh can be considered with an aspect ratio less than 3 for at least 90% of all elements.

The Jacobian Ratio, assesses how far an element's form deviates from an ideally shaped one (characterized by straight edges with identical lengths). In a flawless tetrahedral element with linear edges, the Jacobian ratio equals 1.0. As the curvature of an element's edges increases to conform to a curved geometry, its Jacobian ratio rises. In the proximity of extremely sharp or curved boundaries, an element's edges may intersect, distorting the element and resulting in a self-intersecting geometry. Distorted elements exhibit a negative Jacobian ratio, yielding imprecise results. If the elements with the highest Aspect and Jacobian ratios (exceeding 10) are distant from critical analysis areas, refining the mesh in those zones may not be worthwhile. However, for simulation-critical areas, localized mesh refinement can diminish the Aspect and Jacobian ratios of subpar elements, enhancing simulation outcomes.

The Jacobian ratio sets the number of integration points to be used in checking the distortion level of the tetrahedral elements. The amount of Gaussian points is set to 16.

A mesh refinement is applied in the FEM model. A uniform downward displacement is applied. For this same displacement for each mesh refinement the maximum tensile and compressive stress of the model is calculated. These remain all in the same location. For each refinement a mesh quality check is conducted, calculating the aspect ratio.

8.3.2. FEM: DIANA FEA 10.7

DIANA FEA is utilized to create two distinct types of FEM models. Firstly, a simplified 2D model is employed to investigate the impact of varying the friction coefficient at the glass-earth interface, along with exploring the effects of changing material properties such as elastic modulus and Poisson's ratio on stress distribution. Secondly, a 3D model is constructed in DIANA FEA to analyze the differences in reaction forces when alternating bottles versus not alternating them. Due to its advanced capabilities, DIANA FEA is chosen over SolidWorks for this purpose. It's important to note that while DIANA excels in structural analysis, it typically demands higher calculation times and computer resources.

Modelling Methodology

2D Model

For the 2D model a simplification of the 3D model is made, which based on the compressive test

detailed in Chapter 6. To gain a comprehensive understanding of the bottle's impact within the brick, three different scenarios are simulated. The derivation of the 2D simplifications based on the 3D model are illustrated in Figure 8.5.

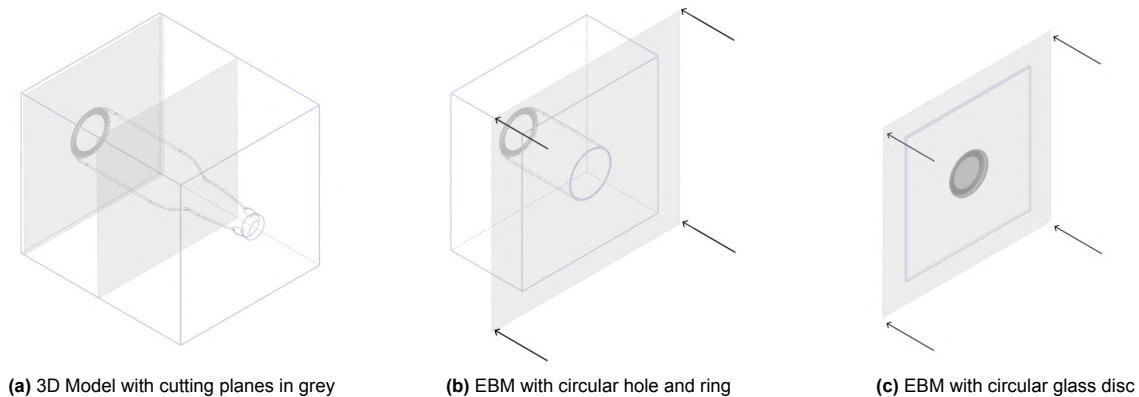


Figure 8.5: Derivation of 2D simplifications based on 3D model

The 2D models' geometry is depicted in Figure 8.6. The dimensions selected for the geometry prioritize the most influential factors. Considering production deviations in bottle manufacturing, a minimum thickness of 2.14 mm is anticipated, hence this glass thickness is adopted. Additionally, the largest feasible diameter for the glass bottle, accounting for manufacturing variations, is chosen at 62.3 mm. This maximum diameter selection aims to prioritize larger holes, as they result in higher stresses due to amplified stress concentrations around the hole edges and reduced cross-sectional area available to withstand applied loads.

Firstly, the model represents the brick with a circular hole, excluding the glass bottle. The results from this analysis can be compared to analytical formulas for a circular plate with a hole. Subsequently, the glass ring, symbolizing the bottle, is incorporated into the model as in Figure 8.6 (b). Finally, the bottom of the model is approached by completely filling the hole inside the earth brick with glass as in Figure 8.6 (c). The accuracy of these Finite Element Method (FEM) models will be validated through analytical calculations, meshing methods and sensitivity studies.

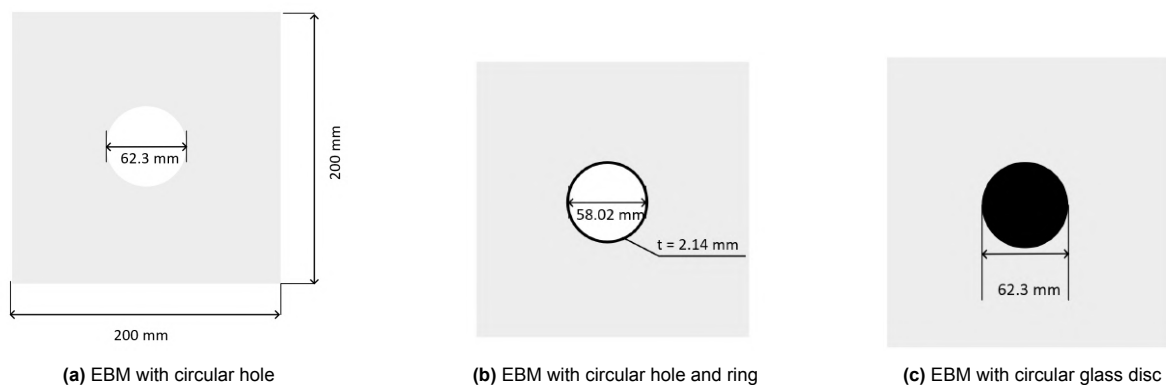


Figure 8.6: Geometric properties of 2D model

The boundary conditions applied for the 2D models in DIANA FEA 10.7 are illustrated as in Figure 8.7. Concerning the boundary conditions, the bottom of the brick is vertically restrained. On the left side of the brick, a horizontal restraint is added on the top and bottom vertex to assure stability of the model. On the top side of the brick an equal downward deformation is applied.

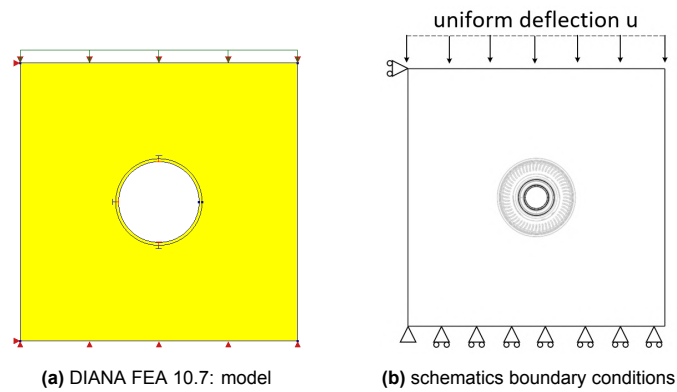


Figure 8.7: Geometric properties of 2D model

For the models with the ring and the disk, an interface condition is applied to take into account the connection of the glass bottle with the earth mortar. Mohr-Coulomb is chosen for the interface, this enables to apply a friction coefficient to take the surface condition of different gradients of abrasion of glass into account. Tension cut off is chosen zero as it is assumed to have no tension strength between the earth and the bottle at the interface. For the earth-based mortar and the soda-lime glass bottle, material properties are taken as in Section 8.2. A summary of the interface properties are listed as in Table 8.7.

Table 8.7: Interface properties between glass and earth based mortar: FEM DIANA FEA 10.7

Interface Property	Value	Unit
<i>Young's Modulus</i>	32677.57	N/mm^3
<i>Cohesion</i>	0	MPa
<i>Friction angle</i>	11.31*	°
<i>Sensitivity Analysis Range</i>	5.7 - 38.7	°
<i>Dilatancy angle</i>	0	°
<i>Tension cutoff</i>	0	MPa

* Assumptions based on similarities of behaviour with low strength concrete C8/10

3D Model

A 3D model has been constructed to analyze the distribution of reaction forces when alternating the bottles and when not alternating them. Two 3D models were created using DIANA FEA 10.7. Symmetry conditions, involving horizontal restraints, were implemented on the sides of the brick in both models. Similarly, a uniform downward displacement is applied to the top surface of each model, while the bottom surface was constrained vertically. Interface properties, as outlined in Table 8.7, were assigned to both models. A visualization of the FEM models are illustrated in Figure 8.8.

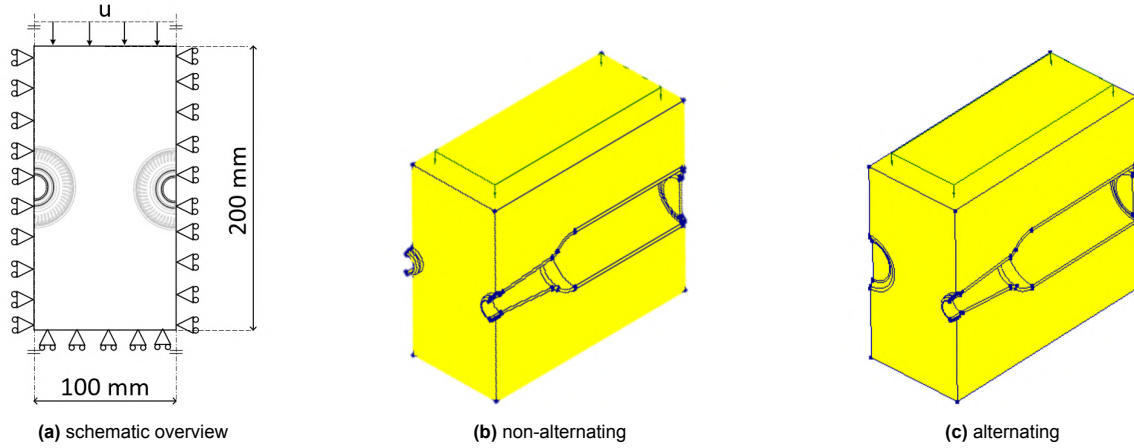


Figure 8.8: Modelling Methodology of Alternating vs. Non-Alternating Placement in Bricks using DIANA FEA 10.7

Meshing

Regarding meshing, two distinct mesh types — quadrilateral and triangular — are selected and subsequently compared. A predetermined element size is established; it's worth noting that this value serves as a target, with the mesher endeavoring to adjust accordingly to meet this criterion as closely as possible.

2D Model

Mesh refinement has been implemented for the aforementioned models. Model 1 represents the plane without the glass ring, while Model 2 depicts the plane with the glass ring, and Model 3 is filled with glass. The mesh refinement process involves applying a target mesh size of 40 mm, refining down to 1.5 mm. The results of the mesh refinement for Model 1 are presented in Table 8.8, those for Model 2 in Table 8.10, and for Model 3 in Table 8.11.

To gain confidence in the FEM models, results are compared to mathematical equations for calculating peak stresses around a hole under compression, are demonstrated in Equations 8.5 and 8.6. A study carried out in 2008 [38] delves into the investigation of the theoretical stress concentration factor for plates with finite width featuring centrally located circular openings. This study reveals that the accuracy of the analytical method hinges on the ratio of d/W (hole diameter/ width of the brick) and is deemed suitable for a ratio $d/W \leq 0.4$, a condition applicable to Model 1.

The stress concentration factor K_t is defined as the ratio of the highest stress in the part to the reference stress and is expressed in Equation 8.5. In the context of Model 1, the plate has a width (W) of 200 mm, and the hole has a diameter (d) of 62.3 mm. The highest peak stress is then calculated using Equation 8.6, where the applied compressive stress is denoted by σ_∞ . Finally the error percentage between the numerical values and FEM results will be calculated and also listed in Table 8.8.

$$K_t = 3 - 3.14 * \left(\frac{d}{W}\right) + 3.667 * \left(\frac{d}{W}\right)^2 - 1.527 * \left(\frac{d}{W}\right)^3 \quad (8.5)$$

$$\sigma_{max} = K_t * \frac{1}{1 - \frac{d}{W}} * \sigma_\infty \quad (8.6)$$

Where,

K_t is the stress concentration factor
 d (mm) is the diameter of the hole
 W (mm) is the width of the brick which is 200 mm
 σ_∞ (MPa) is the applied compressive stress
 σ_{max} (MPa) is the peak stress

Table 8.8: Meshing Properties DIANA FEA: Model 1 plane with circular hole

Mesh Type	Quadratical						Triangular					
	40	20	10	5	2.5	1.5	40	20	10	5	2.5	1.5
Element Size (mm)	40	20	10	5	2.5	1.5	40	20	10	5	2.5	1.5
Number Of Elements	38	94	356	1414	5702	15742	90	224	854	3399	14140	22268
Peak stress FEA (MPa)	27.02	25.25	29.95	30.73	31.01	31.21	22.43	23.71	28	30.26	30.90	31.05
Peak stress numerical (MPa)	33.3	33.21	32.65	32.46	32.42	32.41	34.03	33.65	32.82	32.51	32.43	32.41
error (%)	23.24	31.52	9.02	5.63	4.55	3.84	51.72	41.92	17.21	7.44	4.95	4.38

A comparison with DIANA FEA with SolidWorks is made in order to see if the same boundary conditions create similar results, the same 2D model of the plane without the hole is made in SolidWorks. The mesh type in this FEM model is a Voronoi-Delaunay Triangulation mesh. These results of the SolidWorks model are listed in Table 8.9.

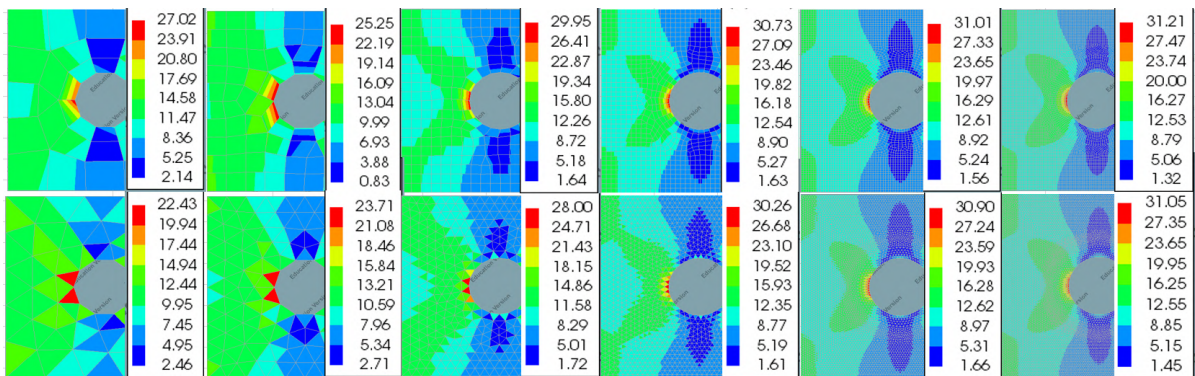


Figure 8.9: Mesh refinement Model 1 DIANA FEA: Quadratical (first row) and Triangular (second row)

Table 8.9: Meshing Properties Solidworks 2023: Model 1 plane with circular hole.

Mesh Type	Voronoi-Delaunay Triangulation					
	40	20	10	5	2.5	1.5
Element Size (mm)	40	20	10	5	2.5	1.5
Number Of Elements	68	190	740	2960	11835	32943
Number Of Nodes	164	430	1580	6120	24069	66553
Peak stress FEA (MPa)	23.97	29.04	31.05	32.67	33.21	33.27
error (%)	44.14	18.00	10.21	4.71	3.01	2.83

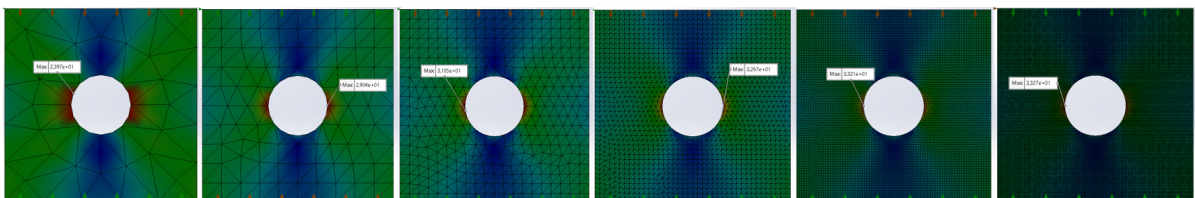


Figure 8.10: Mesh refinement Model 1 SolidWorks: Voronoi-Delaunay

The information from Table 8.8 and Table 8.9 is graphically represented to evaluate convergence and identify differences across the diverse FEM models. Figure 8.11 illustrates that the Voronoi-Delaunay mesh from the SolidWorks model achieves convergence more rapidly. Following closely in convergence speed is the Quadrilateral mesh. Additionally, the Voronoi-Delaunay model exhibits a quicker decrease in error percentage between numerical results and FEM results.

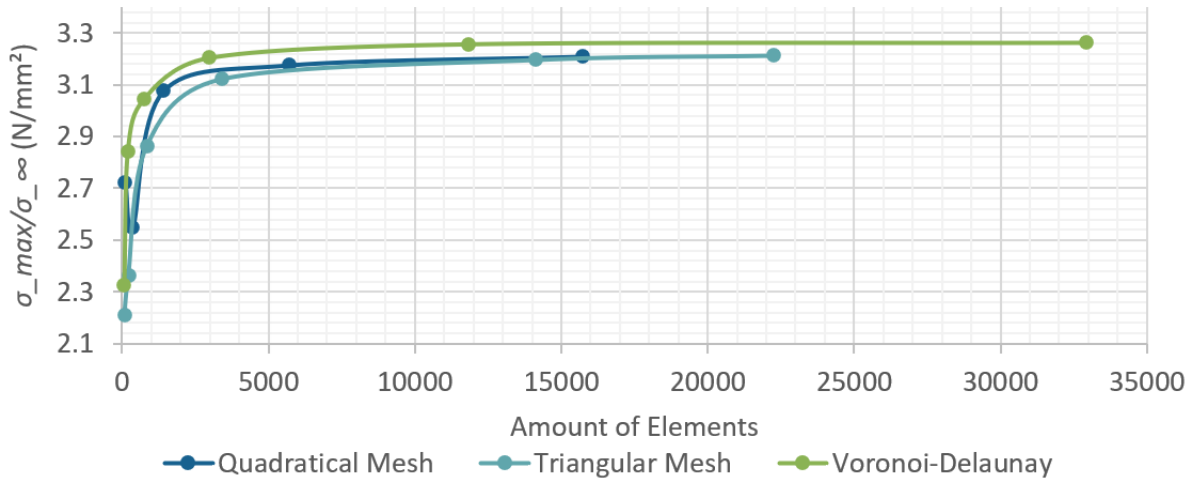


Figure 8.11: Graph Convergence Model 1: plane with circular hole

Now, mesh refinement is also conducted for Model 2. This model represents the plane with the ring. Result from the FEM analysis and the mesh refinement for the Quadratical and Triangular mesh can be seen as in Table 8.10.

Table 8.10: Meshing Properties DIANA FEA: Model 2 plane with circular hole and ring

Mesh Type	Quadratical				Triangular			
	2.4	1.2	0.6	0.3	2.4	1.2	0.6	0.3
Element Size (mm)	2.4	1.2	0.6	0.3	2.4	1.2	0.6	0.3
Number Of Elements Ring	82	323	1260	4432	158	619	2498	10036
Number Of Elements Plane	6137	24703	98740	395014	14320	56255	219268	873400
Total Number Of Elements	6219	25026	100000	399446	14478	56874	221766	883436
Peak stress (MPa)	75.83	76.29	76.43	76.59	74.82	76.13	76.5	76.63
Peak stress / Applied stress	6.994	7.039	7.057	7.079	6.900	7.023	7.064	7.082

To show convergence, the results from Table 8.10 for a Quadratical and Triangular mesh for Model 2 are plotted in Figure 8.13. One can see that Quadratical mesh show a faster convergence.

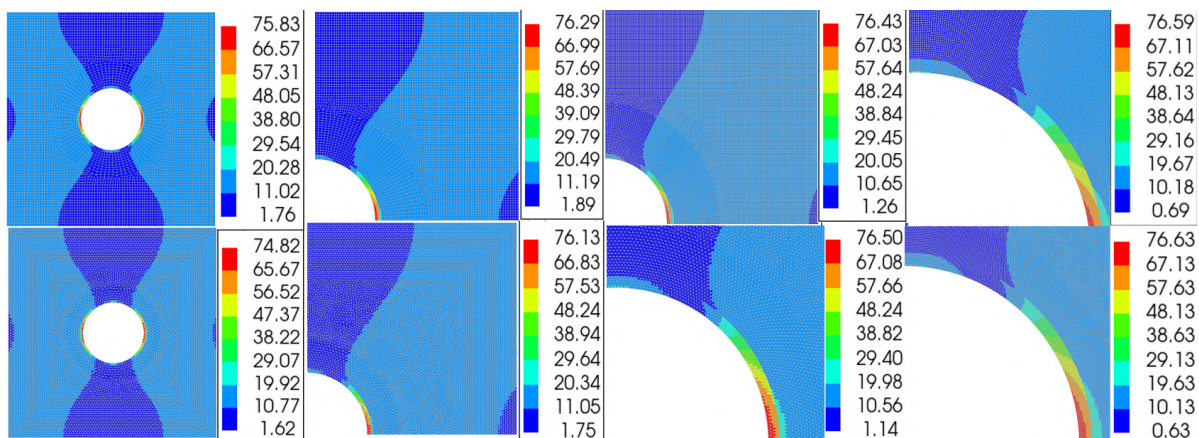


Figure 8.12: Mesh refinement Model 2 DIANA FEA: Quadratical (first row) and Triangular (second row)

To show convergence of Model 3, results from the FEM analysis of Table 8.11 are plotted as can be seen in Figure 8.14. The Quadratical mesh shows faster convergence.

Table 8.11: Meshing Properties DIANA FEA: Model 3 plane with disc

Mesh Type	Quadratical						Triangular					
	40	20	10	5	2.5	1.5	40	20	10	5	2.5	1.5
Element Size (mm)	40	20	10	5	2.5	1.5	40	20	10	5	2.5	1.5
Number Of Elements	44	98	397	1563	6199	17153	88	234	922	3598	14489	39484
Peak stress FEA (MPa)	26.62	26.96	30.95	32.55	32.81	32.96	23.75	25.56	29.67	31.81	32.67	32.94
$\sigma_{max}/\sigma_{\infty}$	2.49	2.57	3.02	3.19	3.22	3.24	2.21	2.42	2.88	3.11	3.21	3.23

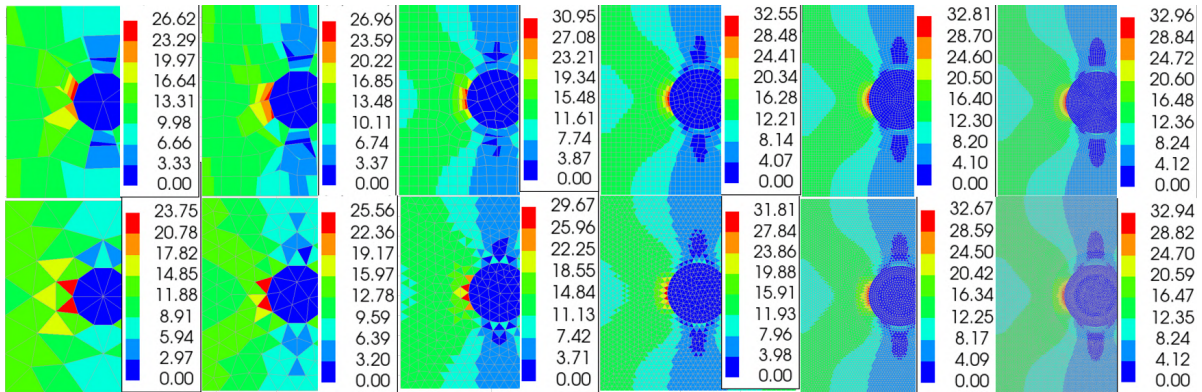


Figure 8.13: Mesh refinement Model 3 DIANA FEA: Quadratical (first row) and Triangular (second row)

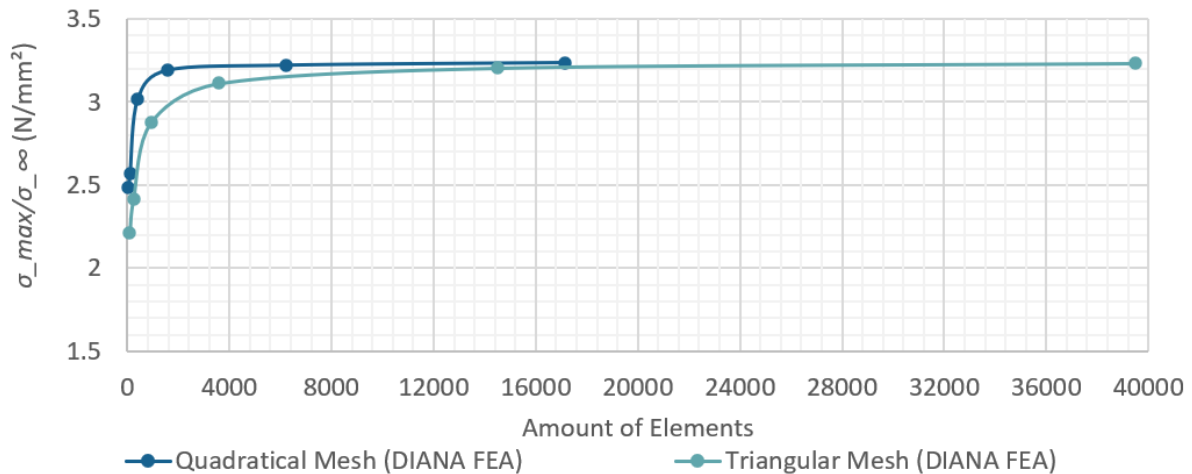


Figure 8.14: Graph Convergence Model 3: circular hole with disc

8.4. Sensitivity Studies

To construct the Finite Element Model, certain assumptions need to be made. For instance, the interface between the bottle and the earth, along with its internal friction, is unknown. Moreover, the fluctuating material properties of the earth, such as Poisson’s Ratio and elastic modulus in mortar, could also have significant effects. Therefore, we investigate the sensitivity and their influence on stress distribution of the model when these assumptions are varied within reasonable boundaries.

Poisson's ratio of the Earth Mortar

Various Finite Element Analyses (FEA) have been carried out on the 2D models, varying the Poisson’s ratio with 0.2, 0.25, 0.3, 0.35 and 0.4. Please refer to Subsection 8.2.1 *Material Properties of Earth-*

Based Mortar for a more detailed explanation. The analyses in DIANA FEA 10.7 pertain to 2D Model 2 and Model 3. Please refer to Subsection 8.3.2 *FEM: DIANA FEA 10.7* for a more detailed explanation of the set-up of these models.

For Model 2, where the cross section of the brick has a ring, one can see in Figure 8.15 (a) that there is almost a linear relationship between the Poisson's ratio and the peak stresses. Where increasing the Poisson's ratio, the peak stress is decreasing. The relationship between the Poisson's ratio and the peak stresses of Model 2, are illustrated in Figure 8.15 (b). Model 2 is the situation where the cross section contains a circular disc, which represents the bottom of the bottle. There is a non-linear relationship where the peak stresses increase when increasing the Poisson's ratio of the Earth Based Mortar. For both models an equal downward deformation of 0.1 mm is applied.

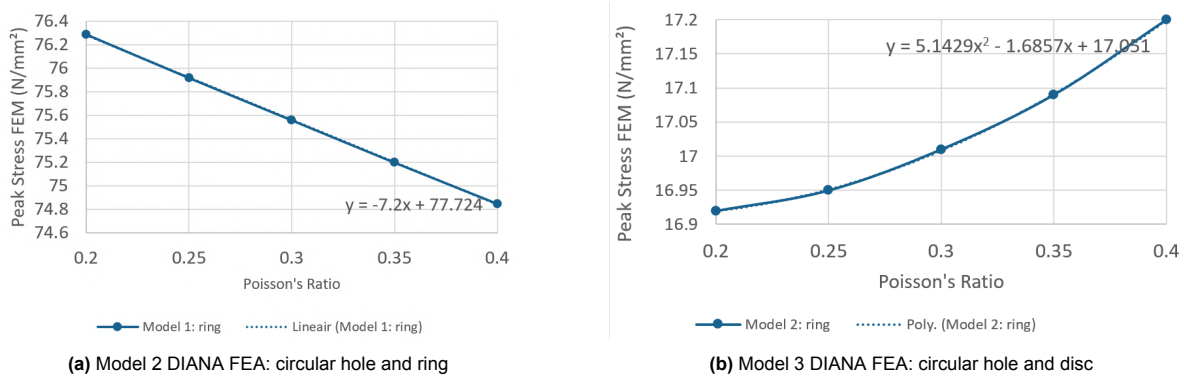


Figure 8.15: Sensitivity study: Poisson's ratio of the Earth Mortar

E-modulus of the earth mortar

Various Finite Element Analyses (FEA) have been carried out on the 2D models, varying the Young's modulus with 2000, 6000, 18000, 24000 and 30000 MPa. Please refer to Subsection 8.2.1 *Material Properties of Earth-Based Mortar* for a more detailed explanation. The analyses in DIANA FEA 10.7 pertain to 2D Model 2 and Model 3. Please refer to Subsection 8.3.2 *FEM: DIANA FEA 10.7* for a more detailed explanation of the set-up of these models.

Figure 8.16 illustrates the results of the sensitivity study for Model 2 and 3. Both models show that when increasing the Elastic Modulus of the earth, the peak stresses will increase. As for Model 1, a logarithmic trend can be seen where when increasing the E-modulus, the effect of it on the peak stresses weakens. Interesting to see is that for Model 2, representing the glass bottom, a somewhat linear relation is observed. For both models a deflection of 0.1 mm is applied downwards to the top.

The Young's modulus defines the correlation between stress (σ) and strain (ϵ), as depicted in Equation 8.7. This modulus is commonly associated with the material's 'stiffness.' As anticipated, Model 2 generally exhibits greater stiffness than Model 1. This is attributed to the presence of a glass disc filling the hole, in contrast to an empty hole with a glass ring.

$$E = \frac{\sigma}{\epsilon} \quad (8.7)$$

Referring back to the FEM analysis results, it is evident that Model 2 exhibits greater resistance to deformation, causing less variation in stress distribution compared to Model 1. This results in a more linear relationship and makes the changes in stress distribution less pronounced in the FEM analysis. Consequently, a lower peak stress is generally observed for Model 2 compared to Model 1, indicating its stiffer behavior. To visually demonstrate this, Figure 8.17 illustrates the alterations in stress distribution when modifying the Young's modulus (E-modulus) of Model 2. The less pronounced changes in stress distribution of Model 3, is illustrated in Figure 8.18.

Friction coefficient

The determination of the friction coefficient is complex and depends on various factors, such as the degree of glass abrasion, the type of earth used, and the distribution and particle size of aggregates

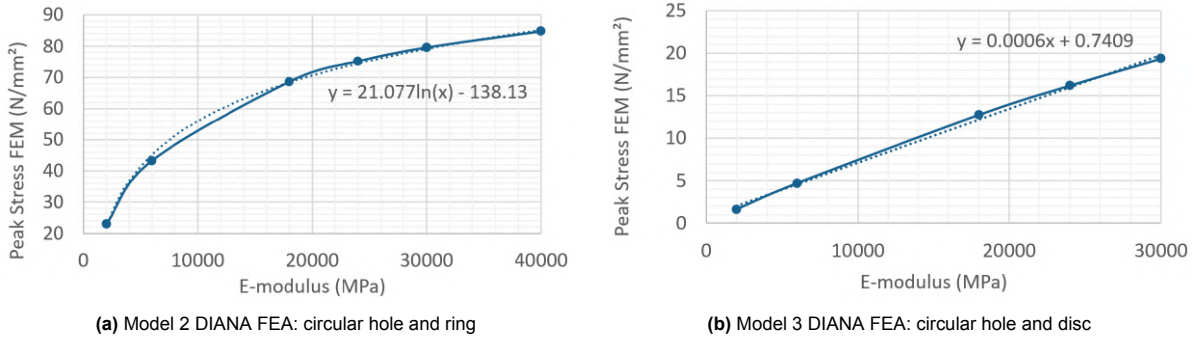


Figure 8.16: Sensitivity study: Young's Modulus of the Earth Mortar

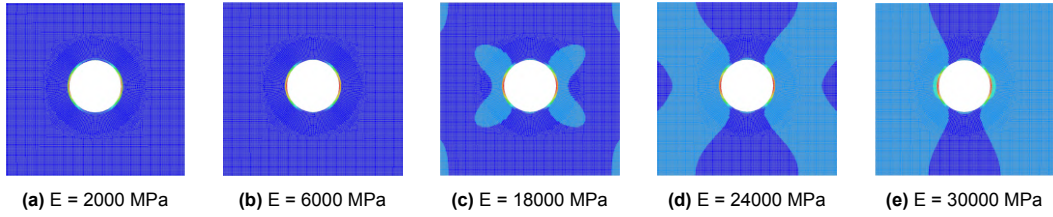


Figure 8.17: Sensitivity study Model 1: Young's modulus EBM stress distribution

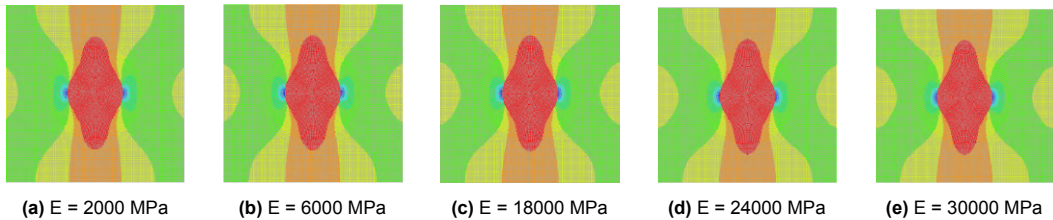


Figure 8.18: Sensitivity study Model 2: Young's modulus EBM stress distribution

in the earth. In this study, the friction coefficient (μ) exhibited a range from 0.1 to 0.8. To convert the friction coefficient into the friction angle, Equation 8.8 is employed. Literature indicates different friction coefficients for rammed earth ranging between 0.4 and 0.8, while for container glass, values are expected to be around 0.1 to 0.3. Distinct friction coefficients are assigned at the interface between the glass and the earth mortar.

$$\mu = \tan(\theta) \tag{8.8}$$

Maintaining all other parameters constant and altering the friction angle reveals no observable changes in peak stresses or stress distribution. Generally, based on the FEM analysis, it seems that the friction coefficient doesn't noticeably affect how stress is distributed. It is crucial to note, however, that factors such as increased glass abrasion, leading to higher friction, can result in the glass exhibiting weaker behavior due to the abrasions.

8.5. Effect of Knurls

To reduce the demand for computational resources and time, the knurls on the bottom of the bottle are excluded from the FEM analysis. Nevertheless, what impact does this simplification have on the stress results?

A study conducted by Dr. Wenke Hu [36], observed that stress at the tip of the knurl is less than the stress magnitude in the absence of knurling. This can be explained by the strain reduction resulting from the complex shape of the knurl. However, it is observed that in the area between the knurls an increase in stress occurs.

From the test results and the fracture pattern it can be concluded that the stress distribution shows similarities with an impact test. For different knurl shapes, the heel impact stress indices are listed in Table 8.12. Where the bearing surface without knurl is 0.21MPa/cps. In case for a longneck beer bottle, the knurl shape is a crescent knurl as seen in Figure 8.19.

The FEM model utilized in this thesis is simplified and does not include knurls. Currently, it remains uncertain whether stress concentration will occur between knurls in the case of an glass bottle earth brick (GBEB) under compression, and whether it will be significant.

Subsequently, two scenarios will be compared: a simplified model lacking knurls, assuming stress concentration is not significant, and the other incorporating an additional factor based on Dr. Wenke Hu's study. His research [36] demonstrates a 43% increase in stresses between the knurls. To accommodate potential variations, a safety margin of 50% is applied in the analysis. Consequently, a factor K_{knurls} is incorporated, set at 1.5, indicating a 50% stress increase between knurls when they are significant. Conversely, this factor is set at 1, assuming knurls are insignificant.

Table 8.12: Heel impact stress indices, W. Hu [36]

Knurl Shape	Stress Between Knurls	Stress at the tip
<i>Bar Knurl (45 degree)</i>	0.29	0.07
<i>Bar Knurl (straight)</i>	0.28	0.08
<i>Crescent Knurl</i>	0.30	0.10
<i>Dot Knurl</i>	0.29	0.05
<i>Chain Knurl (diamond)</i>	0.26	0.17
<i>Chain Knurl (round)</i>	0.25	0.14

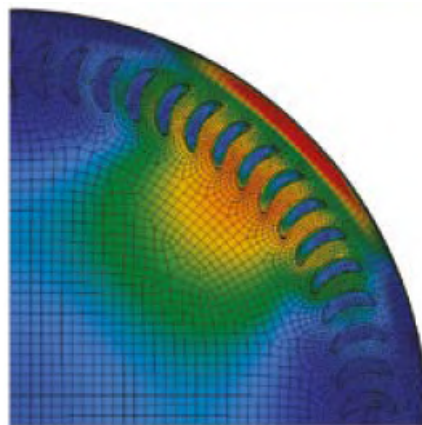


Figure 8.19: Heel impact stress distribution Crescent knurl, W. Hu [36]

8.6. Referring to True Response: FEM Analysis and Laboratory Performance of Bricks

In this section, the findings from the FEM analysis are utilized to establish a design strength and anticipate the performance of the tested brick in the laboratory. These values will then be compared. Detailed description of the laboratory experiments of the compressive test of the Glass Bottle Earth Brick (GBEB) can be reviewed in Section 8 *Longneck Beer Bottle Casted in Earth Based Mortar*. For the FEM model, the 3D model set up in Solidworks as detailed in Subsection 8.3.1 *FEM: SolidWorks 2023* with its corresponding material properties as detailed in Section 8.2 *Material Properties* is utilized.

In accordance with the Eurocode, at the ultimate limit state, the principle of design can be expressed as in Equation 8.9, where the design load should be equal or smaller than the design resistance. This principle is applied to the GBEB design and can be expressed as in equation 8.10 while including a factor incorporating knurl effect K_{knurl} .

$$F_d \leq R_d \quad (8.9)$$

Where,

F_d is the design load

R_d is the design resistance

$$\gamma * \sigma_{Fck,GBEB} \leq \frac{\sigma_{Rck,GBEB}}{\gamma_M} \quad (8.10)$$

Where,

γ is the safety factor for the load applied on the GBEB [-]

γ_M is the safety factor for the material [-]

$\sigma_{Fck,GBEB}$ is the characteristic value of the load on the GBEB [MPa]

$\sigma_{Rck,GBEB}$ is the characteristic value of the resistance to the load on the GBEB [MPa]

8.6.1. FEA: Resistance of the GBEB

The 3D model FEM model set up in Solidworks performs a linear elastic calculation is performed. Refer to *Subsection 8.3.1 FEM: SolidWorks 2023* for an elaborative explanation of the FEM model with its corresponding material properties as detailed in *Section 8.2 Material Properties*.

A downward displacement of 0.1 mm is uniformly applied to the top surface of the brick, which corresponds to the application of a load of 11.16 MPa on top of the brick. Figure 8.20 illustrates the distribution of principal stresses resulting from this deformation. The principle stresses are referred to as P1, P2 and P3. The calculation employs a linear elastic approach, with detailed results provided in Table 8.13. As depicted in the figure, the maximum tensile stress occurs at the bottom of the glass bottle. Although the tensile strength of the glass bottle exceeds that of the earth-based mortar, the tensile stress experienced by the glass is significantly higher, making it the governing factor according to the FEM model.

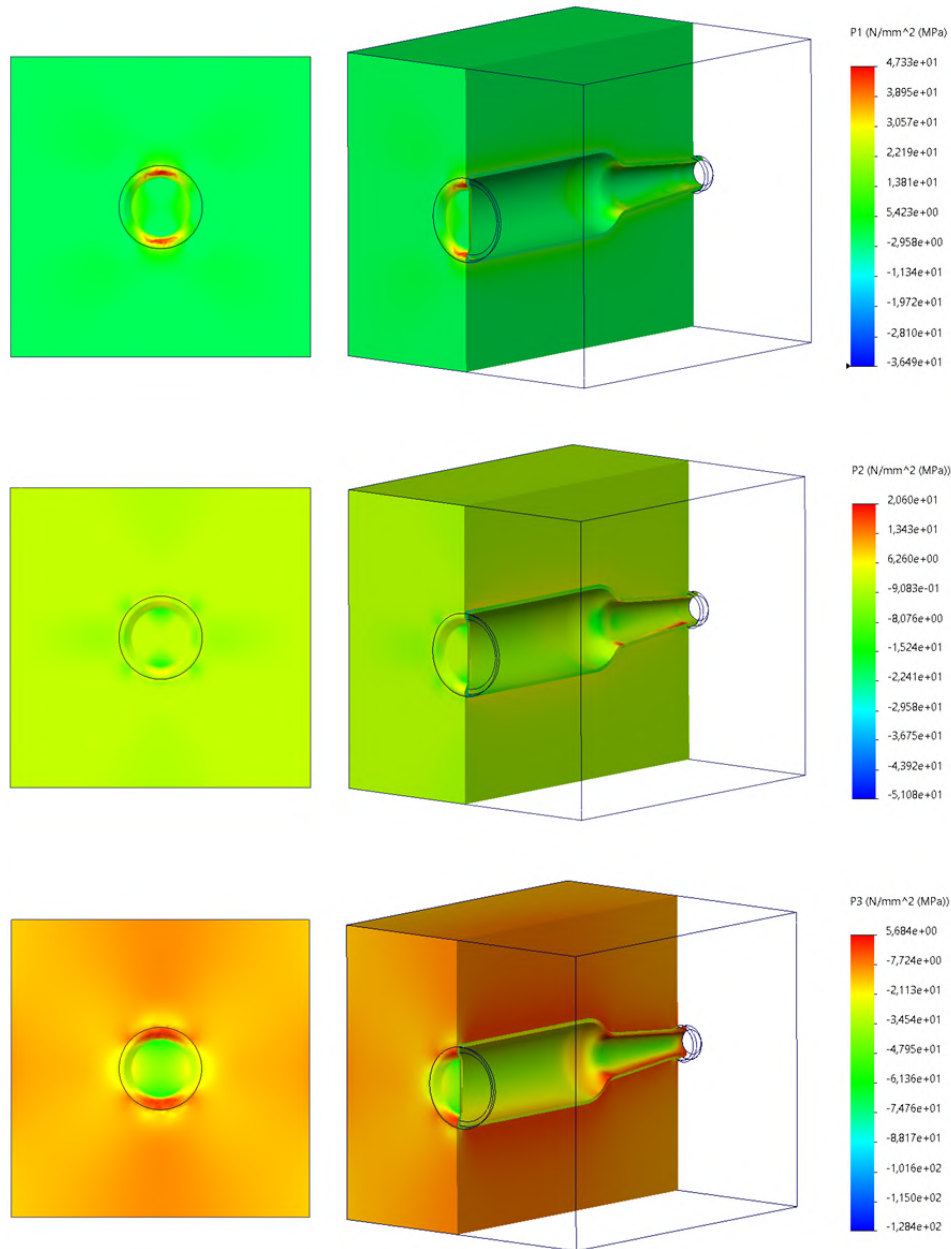


Figure 8.20: Principal stresses of GBEB

A stress factor is introduced to express the relationship between the applied load [MPa] onto the GBEB and the stress occurring in the GBEB. This factor is derived by dividing the peak stresses present in the brick $\sigma_{peak,GBEB}$ by the applied stress on top of the brick $\sigma_{applied,GBEB}$ as depicted in Equation 8.11. The stress factor K_{stress} for the peak tensile and compressive stresses occurring for each principal stress have been calculated and recorded in Table 8.13.

$$K_{stress} = \frac{\sigma_{peak,GBEB}}{\sigma_{applied,GBEB}} \quad (8.11)$$

Table 8.13: FEA Results of Principal Stresses: Referring to Laboratory Performance of Bricks

	Principal Stress	$\sigma_{peak,tensile}$	$\sigma_{peak,compressive}$
	P1	47.33 MPa	-36.49 MPa
FEA Results:			
	P2	20.50 MPa	-51.08 MPa
$\sigma_{applied,GBEB} = 11.16 \text{ MPa}$			
	P3	5.68 MPa	-128.4 MPa
Stress Factor K:			
	P1	4.25	-3.27
$\sigma_{peak,GBEB} / \sigma_{applied,GBEB}$			
	P2	1.84	-4.58
	P3	0.51	-11.51

Since the predominant tensile stress occurs in the bottle, the tensile strength of the glass bottle defines the resistance of the GBEB. Utilizing the linear property of the linear elastic calculation, one can determine the stress applied on top of the earth bottle brick, resulting in the governing stress within the bottle. Consequently, the applied load on the brick leading to the approximate breaking stress in the glass represents the characteristic resistance of the brick. Moreover, since the dominant tensile stress occurs at the knurl height of the longneck bottle, and the FEM model does not account for knurls, one might anticipate an increase in stresses at this location due to the knurl effect (refer to *Section 8.5 Effect of Knurls*). Hence, an additional factor, K_{knurls} , is introduced to address this consideration.

$$\sigma_{Rck,GBEB} = \frac{\sigma_{Rck,bottle}}{K_{knurls}} * \frac{\sigma_{applied,GBEB}}{\sigma_{peak,GBEB}} \quad (8.12)$$

When filling in Equation 8.11 into Equation 8.12 a new Equation 8.13 is retrieved which defines the characteristic resistance of the brick in relationship with the characteristic strength of the longneck beer bottle.

$$\sigma_{Rck,GBEB} = \frac{\sigma_{Rck,bottle}}{K_{stress} * K_{knurls}} \quad (8.13)$$

8.6.2. FEA of Laboratory Performance

In the previous subsection a method has been derived in order to calculate the characteristic resistance of the Glass Bottle Earth Brick. Now the characteristic resistance is calculated for the laboratory experiment and compared with the results from the compressive test.

The compressive tests conducted in the laboratory typically lasted between 30 seconds and one minute. The stresses derived from fracture analysis for Samples 2 and 3 amounted to approximately 59.62 MPa and 42.27 MPa, respectively. Please refer to Section 8 for the experimental study. Examination of the surface conditions and their approximate breaking stress detailed in Appendix D reveals that for a load duration of 1 minute, these stress levels correspond to surface conditions ranging around flute valley RT (56.5 MPa) and Mild abrasions OW (34.5 MPa).

To determine the characteristic resistance of the bottle, we consider the approximate tensile breaking stress ($\sigma_{Rck,bottle}$) of soda-lime glass under conditions similar to 'Flute valley RT' for a load duration of 1 minute, which is documented as 56.5 MPa in Appendix D. Substituting this value into Equation 8.13 yields the following results:

In case of no knurl effect where $K_{knurls} = 1.0$:

$$\sigma_{Rck,GBEB} = \frac{56.5}{4.25 * 1.0} = 13.29 [MPa]$$

In case of knurl effect where $K_{knurls} = 1.5$:

$$\sigma_{Rck,GBEB} = \frac{56.5}{4.25 * 1.5} = 8.86 [MPa]$$

Figure 8.21 displays the experimental data points represented by black dots, please refer to Chapter 6. Additionally, two vertical lines are plotted to indicate the values obtained from the Finite Element Analysis (FEA) as defined earlier.

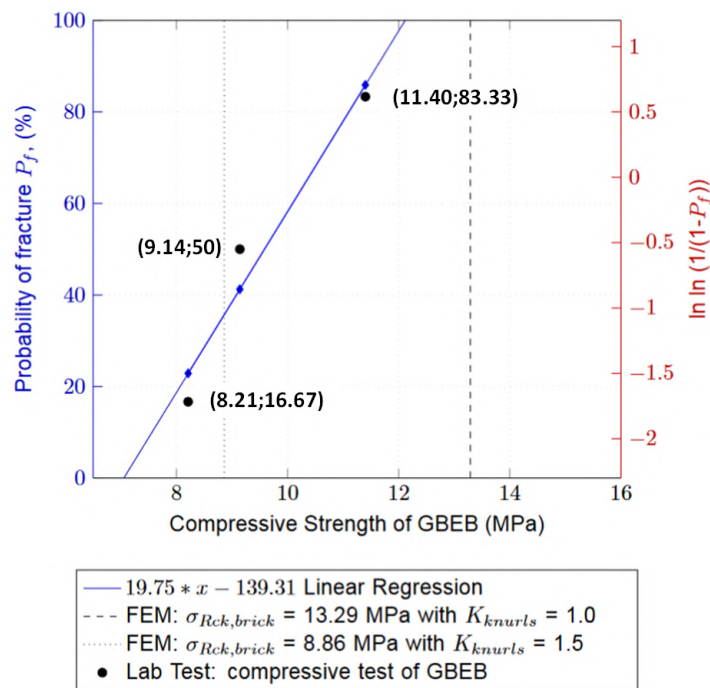


Figure 8.21: Compressive strength of GBEB: comparison of FEA and Laboratory performance

Table 8.14 provides a comprehensive summary of compressive strength values corresponding to various failure probabilities obtained from the Linear Regression Weibull plot, including probabilities of 5%, 0.8%, and 0.12%. Additionally, the table compares these findings with results from the Finite Element Analysis (FEA), considering both scenarios with and without the incorporation of a knurl effect to address potential stress increase between the knurls. Analysis of these data reveals that neglecting the influence of knurls leads to an overestimation of the compressive strength of the GBEB. This emphasizes the critical necessity of integrating a factor for knurls into the assessment process.

Table 8.14: Failure Probabilities: comparison of FEA and Laboratory performance

	Pf	%	Mpa
	0.05	5	7.3
<i>Lin. Regr.</i>	0.008	0.8	7.09
	0.0012	0.12	7.06
$K_{knurls} = 1.5$	0.357	35.675	8.86
$K_{knurls} = 1.0$	1	100	13.29

8.6.3. Longterm resistance of the GBEB

In preceding sections, a methodology was developed to approach the characteristic resistance of the GBEB. Upon comparing Finite Element Analysis (FEA) outcomes to laboratory experiment results, it became evident that disregarding the influence of knurls results in an overestimation of the compressive strength.

Now, the long-term resistance of the GBEB is computed for a 50-year load duration incorporating a factor K_{knurls} of 1.5, indicating a 50% stress increase between knurls. Considering the re-purposing of longneck glass beer bottles, a surface condition of 'Severe abrasions' is assumed. Its corresponding approximate breaking stress for a load duration 'long' is 11.7 MPa, as detailed in Appendix D. For further details, refer to *Subsection 8.2.2 Material Properties of Soda-Lime Container Glass*.

Substituting these values in Equation 8.13, the characteristic strength ($\sigma_{Rck,GBEB}$) of the GBEB with repurposed bottles for a design load of 50 years results in:

$$\sigma_{Rck,GBEB} = \frac{11.7[MPa]}{4.25 * 1.5} = 1.84 [MPa]$$

Incorporating a material factor (γ_M) the design resistance ($\sigma_{Rd,GBEB}$) of the GBEB with repurposed bottles for a design load of 50 years results in:

$$\sigma_{Rd,GBEB} = \frac{1.84[MPa]}{1.8} = 1.02 [MPa]$$

8.6.4. Visual comparative analysis: FEM Model versus compression test results

Despite existing uncertainties and areas requiring further exploration within the model, certain similarities emerge between expected behaviors in the FEM model and observations from the compressive test.

Beginning with the 2D model depicting the glass ring encased in earth mortar (please refer to *Subsection 8.3.2 FEM: DIANA FEA 10.7*). In Figure 8.22 c the Cauchy Total Stresses SXX in-plane principal components are illustrated. This Figure reveals red colors denoting tensile stresses in the SXX direction. Given glass's susceptibility to tension, cracks are anticipated in regions experiencing tensile stresses, perpendicular to the stress direction. Furthermore, these tensile stresses predominantly occur on the bottle's interior, aligning with reality as depicted in Figure 8.22 a, where cracks are evident internally. Conversely, compressive stresses are anticipated on the bottle's interior, represented by blue circles, where no cracks are present. However, when captured with flash, as shown in Figure 8.22 b, cracks appear on the bottle's exterior within the red circle regions. This observation corresponds to the DIANA model, where blue stresses (compression) occur on the interior surface and green/yellow stresses (representing tension) are found on the exterior (red circle).

Turning to the 3D FEM model, it is anticipated that the brick will fail at the base of the glass, a phenomenon observed in Samples 2 and 3. A comparative analysis is presented in Figure 8.23.



Figure 8.22: Comparative Analysis: 2D FEM Model versus Physical Compression Test Results

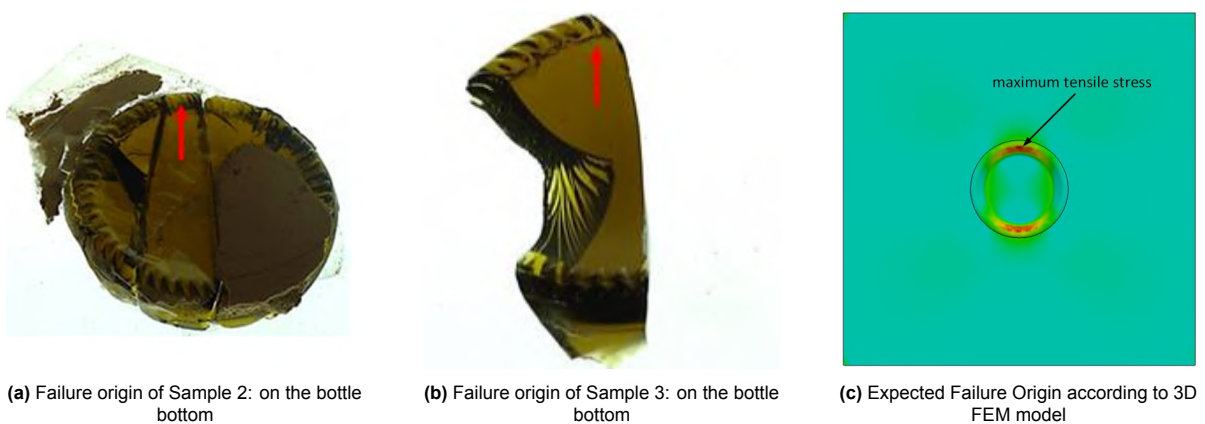


Figure 8.23: Comparative Analysis: 3D FEM Model versus Physical Compression Test Results

8.7. Bottle Arrangement within the Brick

8.7.1. alternating vs. non-alternating placement in bricks

The 3D Finite Element Method (FEM) model, established in DIANA FEA based on the descriptions provided in Subsection 8.3.2 *FEM: SolidWorks 2023*, is employed to analyze the distribution of reaction forces on the Glass Bottle Earth Brick (GBEB) in both alternating and non-alternating bottle arrangements. Subsequently, the impact of these arrangements on the principal stresses in the glass bottle is examined. Specifically, attention is given to the outer surface of the bottle bottom, the inner surface of the bottom bottle, and the interior along the length of the bottle.

Reaction Forces: Alternating vs. Non-Alternating

To analyze the FEA results effectively, a Python code is written to manage all the data. This code plots all the reaction forces at the location of the loaded face alongside the bottle section. Consequently, along the x-axis, you observe the length of the brick, while the z-axis represents the distribution of the total applied force on the brick. Figure 8.24 displays the reaction force on each node along the brick's loaded surface for alternating and non-alternating the bottles. A side-view of the GBEB of both arrangements is presented where on top the reaction forces are plotted which are illustrated in Figure 8.25.

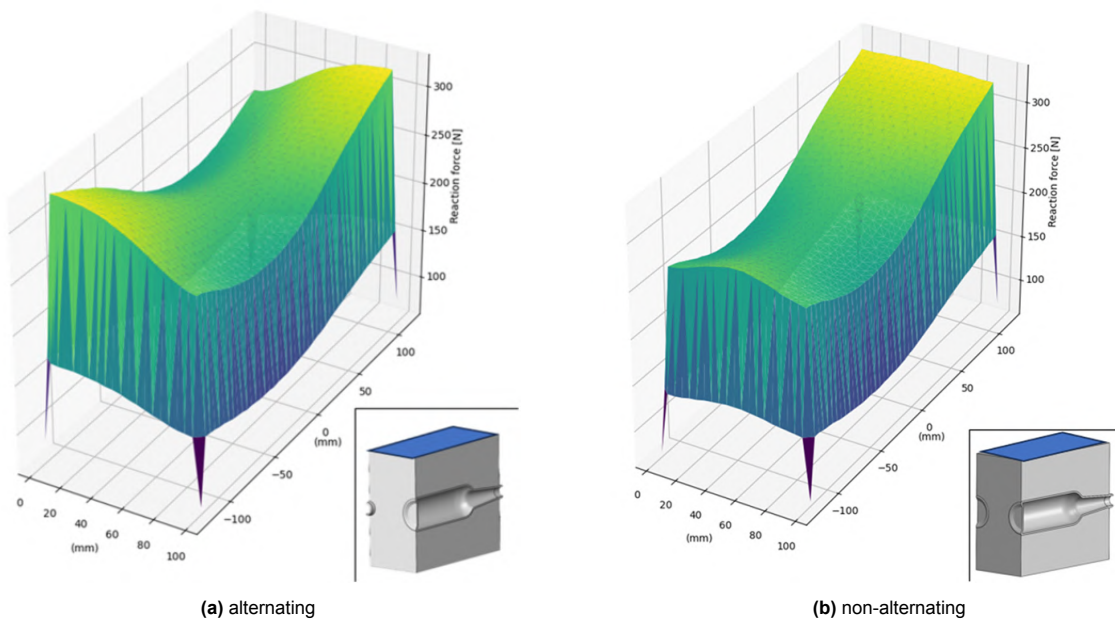


Figure 8.24: 3D bar plot illustrating the distribution of the reaction force [N] for uniform displacement

Based on stress analysis, the brick exhibits greater rigidity in specific areas due to bottle asymmetry. Consequently, when force is applied atop the brick, reaction forces are elevated in stiffer regions. Examining the results of the non-alternating bottle configuration, it's evident that the reaction forces at the bottle neck height are higher, indicating a stiffer section. In regions where there is less earthen mix, for instance where the bottom of a bottle is placed, one can clearly see a drop in reaction force.

Looking at the side views of Figure 8.25, alternating bottle openings appears logical, resulting in a more symmetric cross-section when viewed from the side. However practicality with building the non-alternating version could be more preferable, as it is a more symmetrical force distribution over the length of the wall. Overall, when building, a balance can be achieved by rotating the new layer of bricks.

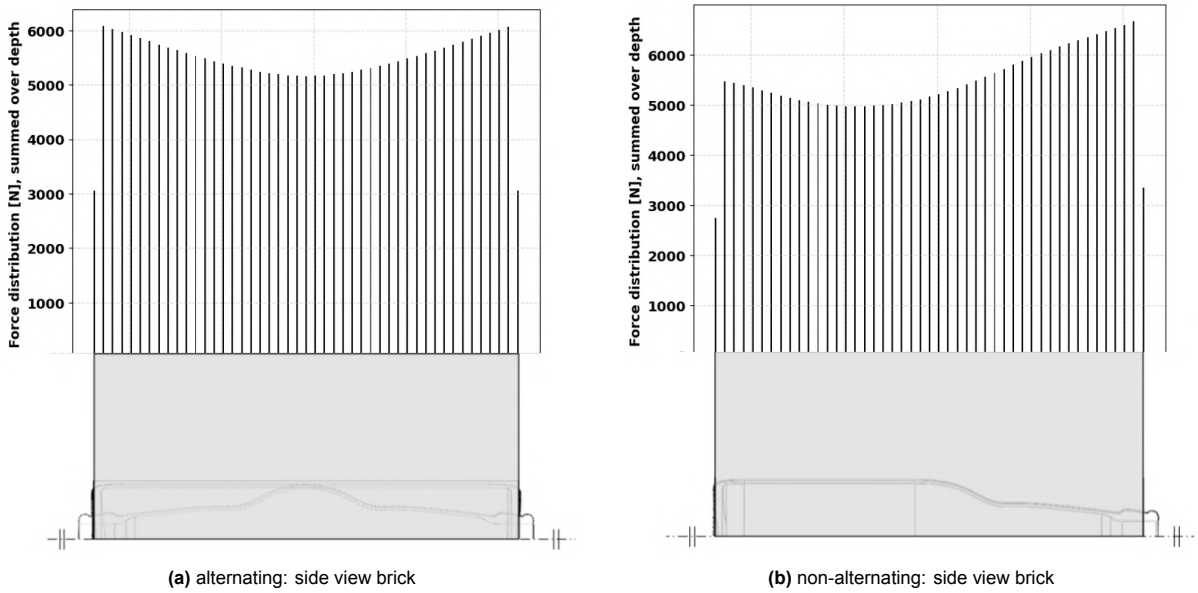


Figure 8.25: Distribution of Reaction Forces [N] over the Length of the Brick: Alternating vs. Non-Alternating

Principal stresses in longneck beer bottle: alternating vs. non-alternating

The impact of both alternating and non-alternating the bottle arrangements on the principal stresses in the glass bottle is examined. The principal stresses P1, P2 and P3 in the glass bottles at different locations are plotted in Figures 8.27, 8.28 and 8.29. Note that a positive and negative value stands for tensile and compressive stresses, respectively. In particular, focus is directed towards examining the external surface of the bottle’s bottom (Figure 8.26 a) , the internal surface of the bottom bottle (Figure 8.26 b), and the inner region extending along the length of the bottle (Figure 8.26 c). For a detailed description of the Finite Element Method and it’s assigned material properties, please refer to Section 8.3 *Finite Element Model (FEM)* and Section 8.2 *Material Properties*, respectively.

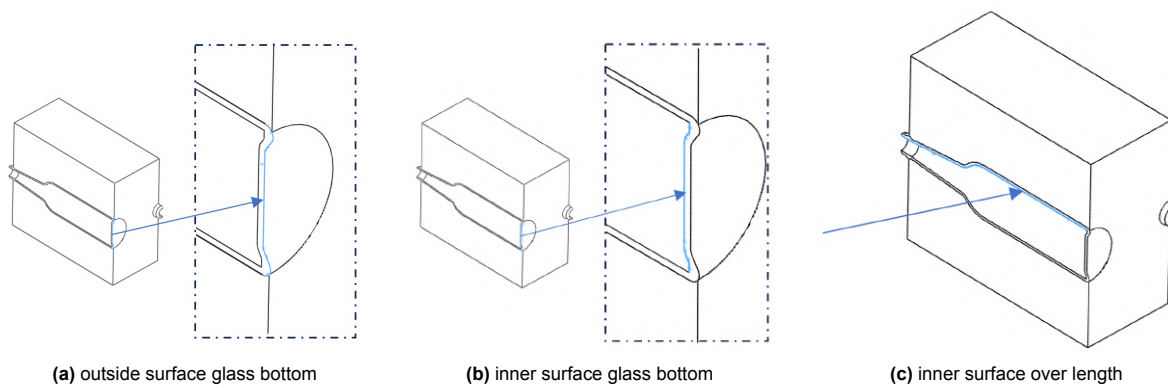


Figure 8.26: Overview of stress plot locations

In Figure 8.27, the principal stresses over the outside bottom of the bottle is plotted. Figure 8.26 a provides a visualization indicating the specific region where these stresses are plotted. Over the x-axis the width of the bottle bottom is plotted, over the y-axis the stress occurring in the bottle is divided by the stress applied on top of the brick. In Figure 8.27 a, one can see that the relative tensile peak stress is the highest around knurl height. This location is governing for failure. However, no significant difference is visible between alternating or not. Same for Figure 8.27 b, no significant difference between stresses can be perceived. In Figure 8.27 c, P3 is plotted, there is a significant difference in principal stresses between alternating and not. Not alternating the bottles show an increase in the compressive stresses over the bottom bottle.

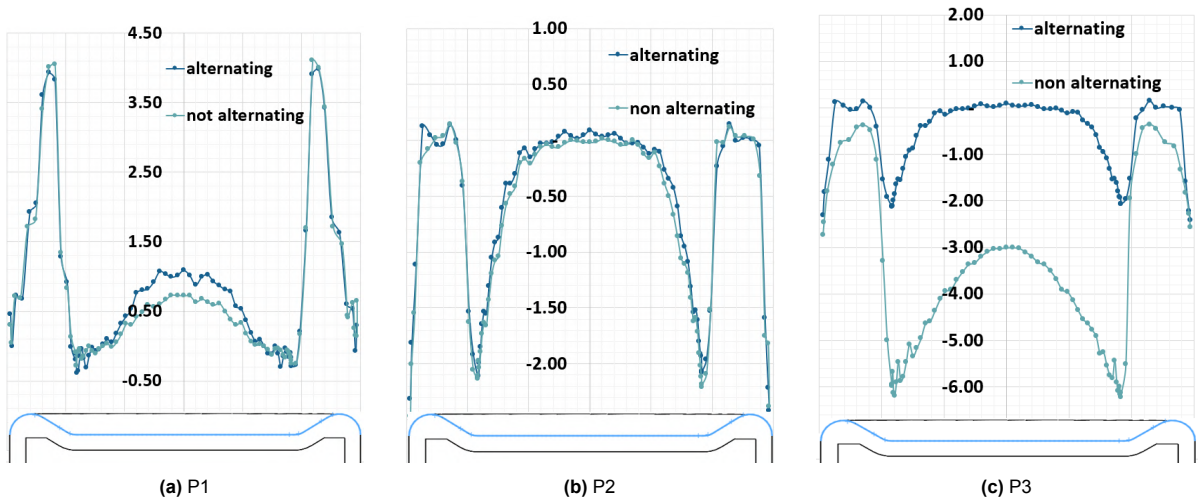


Figure 8.27: The relative peak stresses ($\sigma_{peak,bottle}/\sigma_{applied,GBEB}$) from principal stresses (P1, P2, P3) over the length of the bottom bottle on the outside surface (blue)

In Figure 8.28, the principal stresses over the inside bottom of the bottle is plotted. Figure 8.26 b provides a visualization indicating the specific region where these stresses are plotted. When looking at the inside bottle bottom stresses, no significant differences in stresses are observed for all the principal stresses. In Figure 8.28 a, one can see a slighter decrease in peak tensile stresses. Here, it is clear that the alternating variant slightly diminishes the tensile stresses. When looking at the stress plots over the length of the bottle.

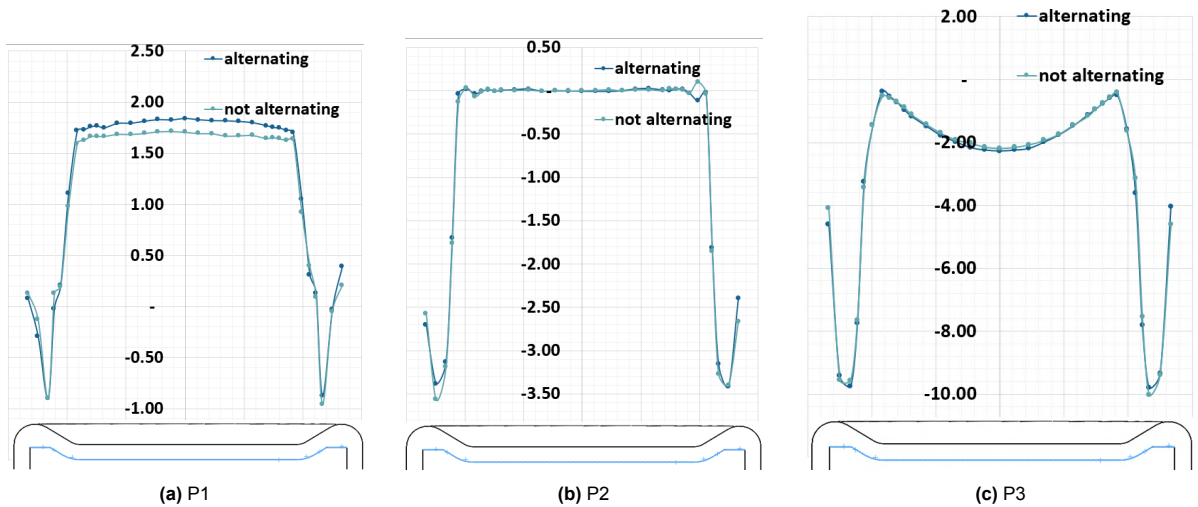


Figure 8.28: The relative peak stresses ($\sigma_{peak}/\sigma_{applied}$) from principal stresses (P1, P2, P3) over the length of the bottom bottle on the inside surface (blue)

In Figure 8.29, the principal stresses over the inner surface length of the bottle is plotted. Figure 8.26 c provides a visualization indicating the specific region where these stresses are plotted. As for P1, there is no clear difference visual between alternating or not alternating the bottles as can be seen in Figure 8.29 a. However, upon examining Figure 8.29 b, which illustrates the second principal stress, a distinct difference is perceived between the alternating and non-alternating conditions. It is worth noting that while the general shape of the stress plot remains similar, the alternating variant exhibits a visibly shorter period. Also in Figure 8.29 c, the alternating variant the general shape of the stress plot remains similar, however the alternating variant exhibits a phase shift to the left when comparing to the non-alternating variant.

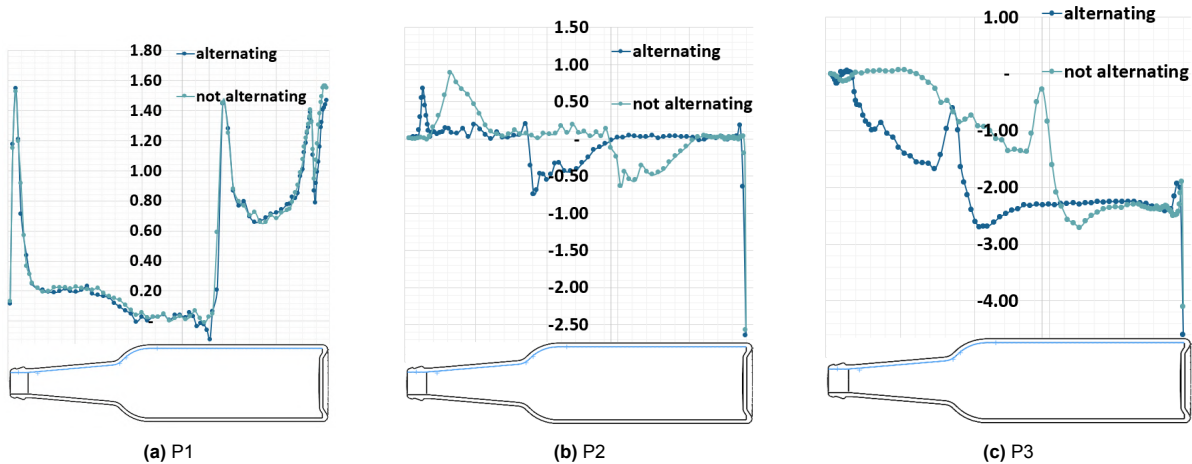


Figure 8.29: The relative peak stresses ($\sigma_{peak,bottle}/\sigma_{applied,GBEB}$) from principal stresses (P1, P2, P3) over the length of the bottle on the inside surface (blue)

To conclude, a notable difference between the alternating and non-alternating arrangement is evident for P3 along the outer surface bottom, where compressive stress notably increase (Figure 8.27 c) . Along the inner length of the bottle, distinctions in P2 and P3 are noted (Figure 8.29). However, while peak stresses exhibit no significant variance, differences are more apparent in phase shifts and periods. Overall, it's inconclusive whether alternating or non-alternating conditions are preferable for stress management, as the significant stresses —where tensile stress peaks in P1 (Figure 8.27 a) — show no perceivable difference between the two conditions.

8.7.2. Influence of horizontal distance between bottles

Initially, the stress distribution is investigated using the 2D Finite Element Method (FEM) model established in DIANA FEA (see Subsection 8.3.2). This exploration focuses on two scenarios where bottles are positioned both in close proximity and at greater distances from each other. The 3D Finite Element Method (FEM) model, established in SolidWorks based on the descriptions provided in Subsection 8.3.1 *FEM: SolidWorks 2023*, is employed to analyze influence of horizontal distance between the bottles on the stress distribution of the GBEB. Subsequently, the impact of these arrangements on the principal stresses in the glass bottle is examined. Specifically, attention is given to the outer surface of the bottle bottom, the inner surface of the bottom bottle, and the interior along the length of the bottle. An overview of these stress plot locations can be viewed in Figure 8.26.

2D FEA: DIANA 10.7

Two scenarios are analyzed using the 2D DIANA model, where the bottles have a 'large' and a 'close' center-to-center distance. A downward deformation of -0.1 mm is applied at the top, with a chosen mesh size of 1 mm. Note that positive stresses show tension and negative stresses show compression. For detailed information on the model set-up, including material properties and boundary conditions, please refer to Subsection 8.3.2 and Section 8.2 *Material Properties*.

Figure 8.30 illustrates the principal stresses P1 where the bottles have a 'large' c.t.c distance (left) and where the c.t.c. is 'small' (right). Notably, within the earth mortar, the maximum compressive stress is anticipated to occur at the left and right sides of the circle, approximately at the center height of the hole (dark blue). This stress concentration diminishes as the distance from the hole increases, and is negligible at two diameters distance. Placing holes too closely together may worsen these stress concentrations, which is unfavorable for the earth mixture. However, when looking at the tensile stresses occurring in the glass (red), one can see that these decrease when increasing the c.t.c. distance. Moreover, as the distance between them increases, the tensile stresses in the earth mortar also increase. The tensile stresses from both bottles will intersect, resulting in a mutual reinforcement.

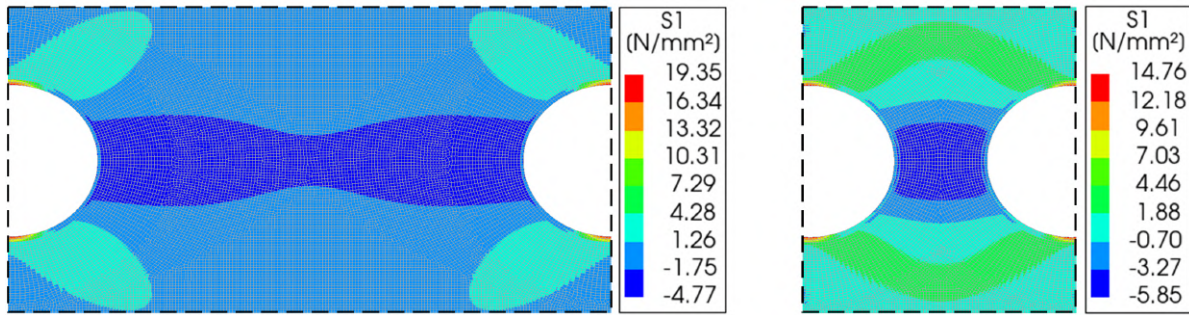


Figure 8.30: Principal Stresses P1 for 'large' (left) and 'small' (right) bottle distance, 2D model DIANA FEA

Figure 8.31 illustrates the principal stresses P2 where the bottles have a 'large' c.t.c distance (left) and where the c.t.c. is 'small' (right). Notably, within the earth mortar, the maximum compressive stress is anticipated to occur at the left and right sides of the circle, approximately at the center height of the hole (yellow). When increasing the c.t.c distance, these compressive stresses will intersect each-other and increase. As for the tensile stresses in the earth mortar (red), these will decrease when increasing the c.t.c. of the bottles. Similarly for the compressive stresses in the glass (blue) which will also decrease when decreasing the bottle distance.

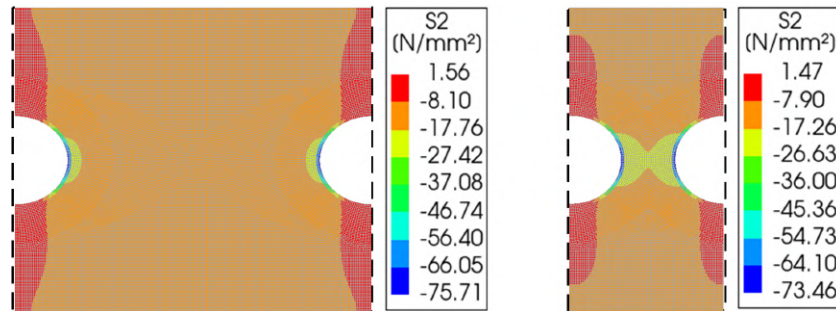


Figure 8.31: Principal Stresses P2 for 'large' (left) and 'small' (right) bottle distance, 2D model DIANA FEA

In conclusion, when looking at the simplified 2D model, increasing the internal distance may enhance the bottle's resistance by reducing the occurrence of tensile stresses in the glass. However, this could be unfavorable to the resistance of the earth mixture, as it would lead to an increase in tensile stresses. Therefore, this presents a dilemma, as the tensile strength of both components is significantly lower than their compressive strength, thus governing the overall outcome.

8.7.3. 3D FEA: SolidWorks 2023

Stress distribution for different internal distances between the bottles are analysed using the 3D SolidWorks FEM model. The alternating variant will be investigated with c.t.c. distances ranging from 70 mm up to 300 mm, which is illustrated in Figure 8.32. A downward displacement of -0.1 mm is applied at the top of the brick with a chosen mesh size of 7 mm. Note that a positive and negative value stands for tensile and compressive stresses, respectively. In particular, focus is directed towards examining the external surface of the bottle's bottom (Figure 8.26 a), the internal surface of the bottom bottle (8.26 b), and the inner region extending along the length of the bottle (8.26 c). For detailed information on the model set-up, including material properties and boundary conditions, please refer to Subsection 8.3.1 and Section 8.2 *Material Properties*.

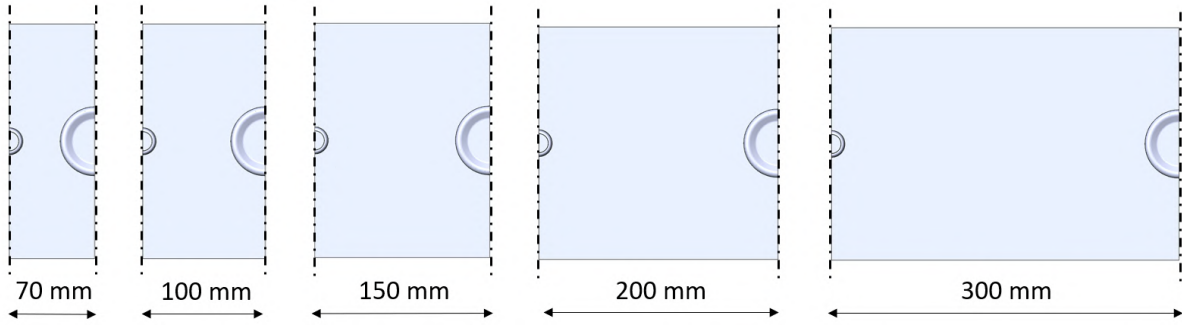


Figure 8.32: Overview of the horizontal distance between bottles ranging from 70 mm up to 300 mm

In Figure 8.33, the principal stresses over the outside bottom of the bottle is plotted. Over the x-axis the width of the bottle bottom is plotted, over the y-axis the stress occurring in the bottle is divided by the stress applied on top of the brick. In Figure 8.33 a, one can see that the relative tensile peak stress is the highest around knurl height. This location is governing for failure. However, no significant difference is visible when increasing the c.t.c. distance as the relative peak stress fluctuates between 3.5 and 4.2. Additionally, when looking at principal stresses P2 and P3, no significant difference in stresses is visible. However, it seems that for P2 (Figure 8.33 b), the compressive stress decreases in the middle of the bottle bottom.

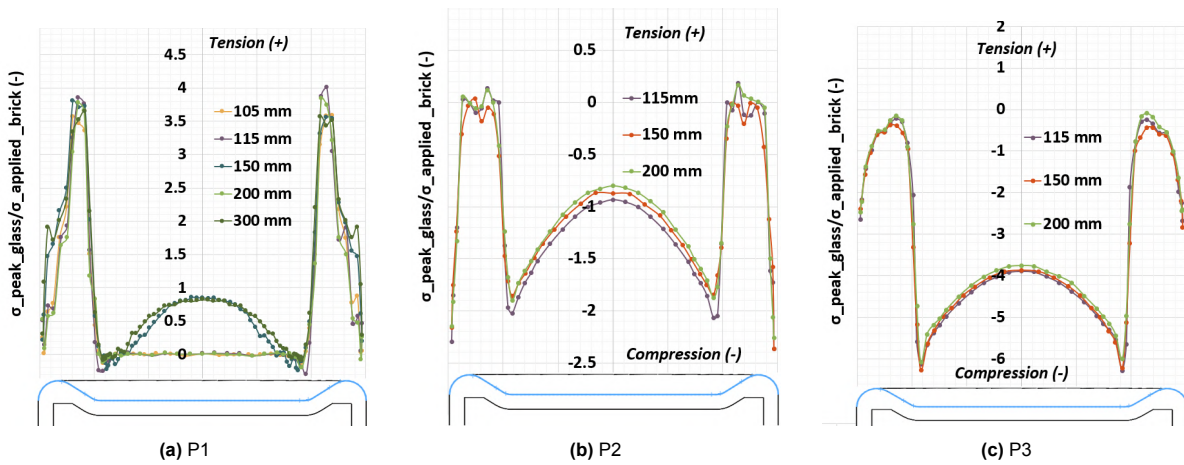


Figure 8.33: The relative peak stresses ($\sigma_{peak,glass}/\sigma_{applied,brick}$) from principal stresses (P1, P2, P3) over the length of the bottom bottle on the outside surface (blue) for alternating vs not alternating for different center-to-center distances

In Figure 8.34, the principal stresses over the inner surface bottom of the bottle is plotted. No significant difference is visible when changing the c.t.c. distance between the bottles. However, when looking at the peak smallest stresses in Figure 8.34, it seems that increasing the distance decreases the compressive stresses. The same is observed for P3 as can be seen in Figure 8.34 c.

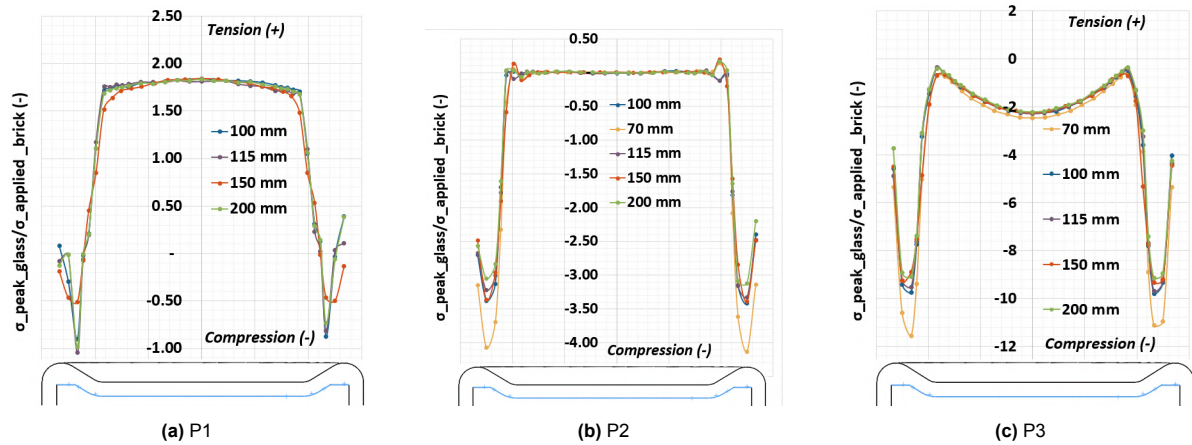


Figure 8.34: The relative peak stresses ($\sigma_{peak}/\sigma_{applied}$) from principal stresses (P1, P2, P3) over the length of the bottom bottle on the inside surface (blue) for different center-to-center distances

In Figure 8.35, the principal stresses over the inner surface of the bottle over the length is plotted. As for P1, no change in stress distribution is visible when altering the c.t.c. distance. However, upon examining Figure 8.35 b, which illustrates the second principal stress, a distinct difference is perceived in stress distribution when varying the bottle distance. It's notable that although the overall shape of the stress plot remains similar, reducing the distance between the bottles' centers exhibits a noticeably shorter period. Also in Figure 8.35 c, the general shape of the stress plot remains similar, however increasing bottle distance exhibits a phase shift to the right. It seems that there is also an upward vertical shift when increasing the bottle's distance.

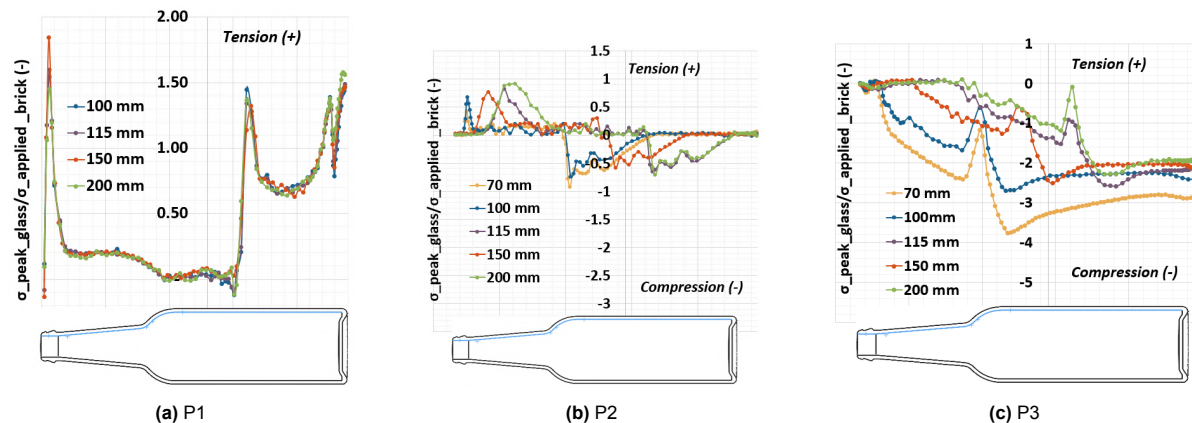


Figure 8.35: The relative peak stresses ($\sigma_{peak}/\sigma_{applied}$) from principal stresses (P1, P2, P3) over the length of the bottle on the inside surface (blue) for different center-to-center distances

Only along the inner length of the bottle, distinct variations in stress distribution in P2 and P3 are observed (see Figure 8.35). Differences are more apparent in phase shifts and periods of the stress distribution over the length of the bottle. However, while peak stresses show no significant difference, it may suggest that increasing the distance between bottles could marginally benefit the bottle's resistance. Overall, it remains inconclusive which bottle distance is preferable for stress management, as significant stresses — where tensile stress peaks in P1 (Figure 8.33 a) — shows no significant difference with changes in bottle distances.

Table 8.15 provides supplementary details regarding the center-to-center distance between the bottles and the applied force as a result of the -0.1 mm applied displacement.

Table 8.15: Exploring the Impact of Horizontal Bottle Distance: Results from 3D FEM Analysis

<i>c.t.c. distance</i>	100	115	150	200
<i>min. distance</i> ¹	37.7	52.7	87.7	137.7
<i>Applied Force [MPa]</i>	11.06	11.33	11.74	12.09
<i>Area of loading [mm²]</i>	23000	26450	34500	46000

¹ Smallest netto distance between two bottles assuming the maximum bottle diameter of 62.3 mm

9

Design of Glass Bottle Earth Brick Masonry (GBEB)

9.1. Introduction

The structural design of masonry constructions relies on established standards such as Eurocode, Indian, British, and Australian codes, among others. In cases where there is no dedicated design code for glass bottle earth brick (GBEB) masonry, existing masonry design codes are utilized for the construction of this type of masonry.

Masonry is comprised of two distinct materials: the masonry unit and the mortar. These materials generally exhibit varying strength and deformation characteristics. Consequently, when a masonry assembly is uniformly compressed, the stresses experienced by the two materials differ. The resistance of masonry walls is influenced by factors such as the effects of eccentricities, and material properties of the masonry.

Ultimately, the design of load-bearing walls involves determining the compressive strength of the masonry to support the specified design loads. The Eurocode 6 (BS EN 1996-1-1:2019) gives the design procedure for unreinforced masonry, which is based on the limit state design principles. Several standards, including EN 16612, ASTM E1300, and NEN 2608, among others, specify the requirements and determination methods for the load-bearing capacity and deformations of predominantly statically loaded soda-lime flat glass. A comparison of these standards and their method of defining the tensile design strength of soda lime glass can be read in Subsection 8.2.2. At the ultimate limit state, the principle of the masonry wall design can be expressed as follows.

$$N_{Ed} \leq N_{Rd} \quad (9.1)$$

Where,

N_{Ed} is the design value of the vertical load on the wall

N_{Rd} is the design value of the vertical resistance of the wall

The design value of the vertical resistance is expressed as follows.

$$N_{Rd} = \Phi * t * f_d \quad (9.2)$$

Where,

Φ is the capacity reduction factor accounting for slenderness and load eccentricity

t is the wall thickness

f_d is the design compressive strength of the masonry

9.1.1. Limit states and load combinations

A case-study calculation is conducted as an example for an application. For this calculation it is assumed the building has a service life of 50 years. Action Category A is chosen, which implies a domestic, residential area. For the calculation the European Standard is used (EN 1990).

Every structure has to comply with two limit states which are related to the reliability (ULS) and usability (SLS) of the structure. The Ultimate Limit State (ULS) is used to check structural safety, whereas the Serviceability Limit State (SLS) is used to check usability. The ULS according to the Eurocode *EN 1990* is prescribed as in Equation 9.3. The SLS according to the Standard *EN 1990*, is prescribed as in Equation 9.4.

$$\gamma_G * G_k + \gamma_{Q:1} * Q_{1;k} + \sum (\gamma_{Q:i} * \Psi_{0;i} * Q_{i;k}) \quad (9.3)$$

Where,

γ_G is partial factor for permanent loads

G_k is total permanent load

$\gamma_{Q:1}$ is partial factor for variable loads

$Q_{1;k}$ is characteristic value of the leading variable load

$\Psi_{0;i}$ is factor for combination of variable load i with the leading variable load

$Q_{i;k}$ is characteristic value of variable load i

$$G_k + \gamma * Q_{1;k} + \sum (\Psi_{0;i} * Q_{i;k}) \quad (9.4)$$

Where,

G_k is total permanent load

$Q_{1;k}$ is characteristic value of the leading variable load

$\Psi_{0;i}$ is factor for combination of variable load i with the leading variable load

$Q_{i;k}$ is characteristic value of variable load i

The load factors for permanent (γ_G) and variable (γ_Q) loads complied with the CC2 construction class for Ultimate Limit State (ULS) are taken as in Table 9.1.

Table 9.1: Ultimate Limit State (ULS): Load Factors CC2 according to EN 1990

Design Situation	permanent load		variable loads	other
	unfavourable	favourable	leading	
1	1.35	0.9	-	1.5
2	1.2	0.9	1.5	1.5

An overview of the factors for combination $\Psi_{0;i}$ can be found in Table 9.2.

Table 9.2: $\Psi_{0;i}$ -factors for buildings according to EN 1990 Table NB.2 - A1.1

Category	Load	Ψ_0	Ψ_1	Ψ_2
A	residential areas	0.4	0.5	0.3
H	roofing	0	0	0

9.1.2. Masonry unit

Chapter 8, titled "*Investigations on Stress Concentrations of a Long Neck Beer Bottle Casted in Earth-Based Mortar*", provided valuable insights into the optimal arrangement of bottles within the brick. It was observed that alternating the placement of bottles effectively distributes reaction forces along the

depth of the brick. However, a symmetrical pattern over the width without alternating the bottles may be more preferable in practical applications. Moreover, the variations in peak stresses with increasing center-to-center distance of the bottles were found to be too minor, limiting the ability to draw definitive conclusions from this aspect of the study.

Following experimental and numerical investigations, a method has been devised to assess the design strength of a GBEB as can be reread in Section 8. The experiments focused on a relative large sample containing a single bottle, see Figure 9.1a b. Notably, the simplified 3D FEM model used in the study does not incorporate knurls, necessitating the inclusion of a factor denoted as K_{knurls} . It is of interest to explore a brick design where the earth mortar around the bottles is minimized to prioritize increasing the number of bottles. This brick should be easily handled without requiring expensive machinery and should not be overly heavy.

In summary of these findings, a masonry unit referred to as the 'Eco' GBEB has been developed, as illustrated in Figure 9.1a. For the full technical drawing, please refer to Appendix E. The center-to-center distance has been set at 105 mm. Based on the study examining the impact of varying internal distances between the bottles, it has been determined that this distance results in relatively low peak stress for a small center-to-center distance. Regarding the height of the brick, a dimension of 85 mm has been selected, considering the wall effect, with the largest aggregate size in the earth mix being 2 mm. Thus, the 85 mm dimension results from the upper boundary bottle diameter of 62.3 mm, with an additional 3*2 mm added on the top and bottom, resulting in a total height of 74 mm. To accommodate potential manufacturing errors, this has been rounded up to 85 mm. A summary of the properties of both the 'Eco' GBEB and the brick utilized in the experimental and numerical investigations, referred to as the 'sturdy' GBEB, is provided in Table 9.4.

Assumptions

Following assumptions are made:

- Partial safety factor for the material is taken as $\gamma_M = 1.8$ (material factor for float glass according to EN 16612)
- The tensile strength of soda lime glass with a surface condition of severe abrasions and a load duration of 50 years is taken as 11.7 MPa (based on data by AGR, see Section 8.2)
- The K_{knurls} factor taking stress increases between knurls into account is taken as $K_{knurls} = 1.5$ (see Section 8.6)
- The tensile and compressive strength of the SCEBM is taken as 3.42 MPa and 11.77 MPa, respectively (based on experimental investigations, see Section 6.4)
- The mass density of the SCEBM is taken as $\rho_{SCEBM} = 1950 \text{ kg/m}^3$ (based on experimental investigations, see Section 6.4)
- The elastic modulus of the SCEBM is taken as $E_{SCEBM} = 25000 \text{ MPa}$ (representing the anticipated critical value, see Section 8.4)
- The Poisson's ratio of the SCEBM is taken as $\nu_{SCEBM} = 0.2$ (representing the anticipated critical value, see Section 8.4)
- The shear modulus of the SCEBM is defined as $G = E/2*(1+\nu)$ and taken as $G_{SCEBM} = 10417 \text{ MPa}$
- Dry stacking is currently assumed due to the absence of investigations into the selection of an appropriate mortar and bonding options.

Masonry unit properties

The Eco Glass Bottle Earth Brick (GBEB) will have following properties:

- The geometry of the GBEB has a 315 mm length, 230 mm width and height of 85 mm, see Figure 9.1a.
- The mass of the GBEB will be approximately 5 kg, where the mass of one longneck beer bottle is 300 grams.

- The GBEB consists out of repurposed long neck beer bottles of 330 ml, with a 'severe abraded' surface condition (see Appendix D, approximate tensile breaking stress for different surface conditions)
- The stress factor K_{stress} , which shows the relationship between the applied force on the brick and the governing stress in the brick is defined as $\sigma_{peak,bottle} / \sigma_{applied,brick}$
- The bottom bottle at knurl height, is the governing location of failure, as observed by laboratory experiments (Subsection 7.4) and Finite Element Analysis (FEA) findings (Section 8))

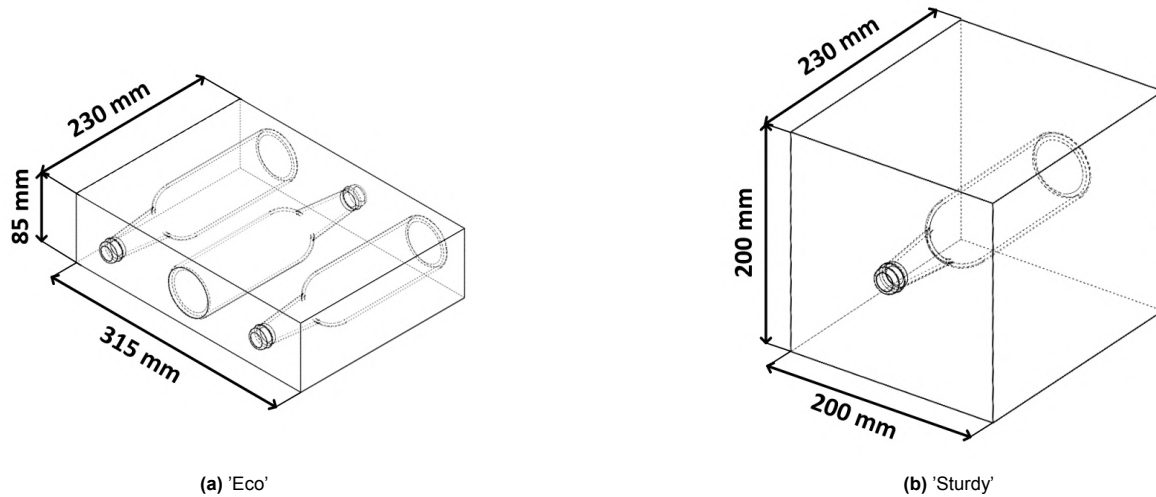


Figure 9.1: Geometry of GBEB: 'Eco' and 'Sturdy'

Table 9.3: Properties of different types of GBEB: 'Eco' and 'Sturdy'

GBEB	'Eco' ¹	'Sturdy' ²
<i>mass of one brick [kg]</i>	±8	±14
<i>mass/volume of brick [kg/m³]</i>	1299	1522
<i>horizontal c.t.c. bottles [mm]</i>	105	200
<i>number of bottles/ m² wall</i>	±112	±25
<i>design resistance [MPa]</i>	0.96	1.02

¹ see Appendix E for technical drawing, FEM results and calculation of design resistance

² see Appendix G for technical drawing, FEM results and calculation of design resistance

9.2. Case Study: Earth Bottle Brick Masonry Design Using Limit State Method

Standard codes are used for the design of masonry structures, however in absence of dedicated codes for earth block masonry, the existing masonry codes are used as a guidance. Generally masonry consists of two different materials being the brick and the mortar. As for this case, the assumption is made that the brick and the mortar have the same characteristics, as the earth bounding the bottle is an earth

based mortar.

The design of a load bearing wall using the limit state method will be performed in this section. The standard *Eurocode-6 (BS EN 1996-1-1:2005+A1:2012)* will be used as a guideline. The slenderness and load eccentricity will decrease the compressive strength of the masonry wall, which a factor Φ is taken into account. The basic principle for the load bearing wall design will be that the design load doesn't exceed the design load resistance.

9.2.1. Example three storey load bearing masonry building

A simple floor plan for a four storey load bearing Earth Based Bottle masonry is shown in Figure 9.2. This floor plan is part of a hostel complex, located close to Bangalore city, India. The roof and floor slabs are continuous reinforced concrete in-situ construction with a slab thickness assumed to be 150 mm, as can be seen in Figure 9.3. The design of a critical wall is colored yellow, and named wall C. Additionally, the loads from the roof and floor that are transferred to the wall will be calculated, along with the mass of the wall. Subsequently, the ultimate limit state for wall C will be determined. An overview of the calculations steps can be seen in Table 9.4. An overview of the design stresses and stresses in the wall are given in Table 9.5.

This case study serves as a simplified example with following assumptions:

- The capacity reduction factor taking eccentricity and slenderness into account is taken as $\Phi = 0.7$
- As $h < 10\text{m}$, wind loading is assumed to be negligible
- The residential building will assume a CC2

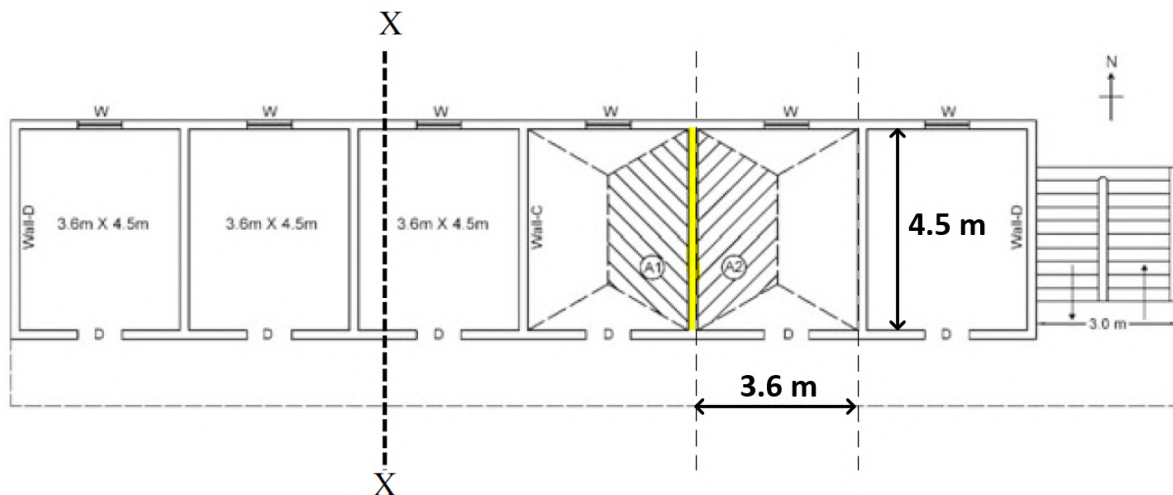


Figure 9.2: Floor plan example calculation case study

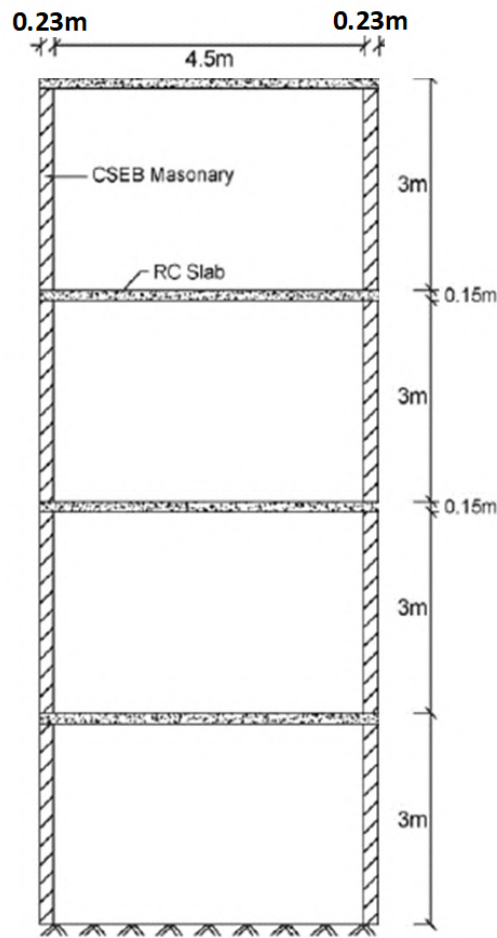


Figure 9.3: Cross section at XX

Roof loading

The roof consists out of a reinforced concrete slab with a thickness of 150 mm including weatherproofing and ceiling finishes. The masonry wall length considered is 4.5 meters. A load width of 3.6 meters is taken.

Dead load

The bulk density of the roof and finishes: $25 \text{ [kN/m}^3\text{]}$

Dead load of the roof to the wall: $0.15 \text{ [m]} * 25 \text{ [kN/m}^3\text{]} * 3.6 \text{ [m]} = 13.5 \text{ [kN/m]}$

Variable load

The variable load in the roof : 1.0 kN/m^2 (Category H: roof angle $0 \leq \alpha \leq 15$)

Variable load of the roof transferred to the wall: $1 \text{ [kN/m}^2\text{]} * 3.6 \text{ [m]} = 3.6 \text{ [kN/m]}$

Floor loading

The floor consists out of a reinforced concrete slab with a thickness of 150 mm including flooring finishes. The length of the masonry wall considered is 4.5 meters.

Dead load

The bulk density of the floor and finishes: $25 \text{ [kN/m}^3\text{]}$

Dead load of the floor transferred to the wall: $0.15 \text{ [m]} * 25 \text{ [kN/m}^3\text{]} * 3.6 \text{ [m]} = 13.5 \text{ [kN/m]}$

Variable load

The variable load: $1.75 \text{ [kN/m}^2\text{]}$ (NEN-EN 1991-1-1+C1+C11:2019)

Variable load of the floor transferred to the wall: $1.75 \text{ [kN/m}^2\text{]} * 3.6 \text{ [m]} = 6.3 \text{ [kN/m]}$

Wall loading

The Glass Bottle Earth Brick (GBEB) has a thickness of 230 mm, for design purposes a 12 mm plaster layer on each side of the wall is incorporated. The bulk density of the finish is assumed to be 20 kN/m^3 . The length of the masonry wall considered is 4.5 meters and a thickness of 230 millimeters. The floor height equals 2.85 meters. The bulk density of the 'eco-brick' with three bottles incorporated is approximately 12.74 kN/m^3 .

Dead load

Dead load of the wall: $12.74 \text{ [kN/m}^3\text{]} * 0.23 \text{ [m]} * 2.85 \text{ [m]} + 2 * 20 \text{ [kN/m}^3\text{]} * 0.012 \text{ [m]} * 2.85 \text{ [m]} = 9.72 \text{ [kN/m]}$

Table 9.4: Calculation of the vertical loading on wall C

Floor	kN/m	Design Load	kN/m	U.C.	(-)
3th floor		ULS 1		33.26/154.56 =	<u>0.22</u>
Dead load roof	13.5	$1.35 \times 23.33 + 1.5 \times 0 \times 3.6 =$	<u>31.35</u>		
Dead load wall	9.72	ULS 2			
<u>Total dead load</u>	<u>23.33</u>	$1.2 \times (23.22) + 1.5 \times (3.6) =$	<u>33.26</u>		
Variable load Roof	3.6				
2th floor		ULS 1		66.47/154.56 =	<u>0.43</u>
Dead load floor	13.5	$1.35 \times 46.44 + 1.5 \times 0.4 \times 6.3 + 1.5 \times 0 \times 3.6 =$	<u>66.47</u>		
Dead load wall	9.72	ULS 2			
Dead load from above	23.22	$1.2 \times (46.44) + 1.5 \times (6.3) =$	<u>65.18</u>		
<u>Total dead load</u>	<u>46.44</u>				
Variable load floor	6.3				
Variable load from above	3.6				
<u>Total variable load</u>	<u>9.9</u>				
1th floor		ULS 1		102.49/154.56 =	<u>0.66</u>
Dead load floor	13.5	$1.35 \times 69.66 + 1.5 \times 2 \times 0.4 \times 6.3 + 1.5 \times 0 \times 3.6 =$	<u>101.69</u>		
Dead load wall	9.72	ULS 2			
Dead load from above	46.44	$1.2 \times (69.99) + 1.5 \times (12.6) =$	<u>102.49</u>		
<u>Total dead load</u>	<u>69.66</u>				
Variable load floor	6.3				
Variable load from above	12.6				
<u>Total variable load</u>	<u>18.9</u>				
Ground floor		ULS 1		136.73/154.56 =	<u>0.89</u>
Dead load floor	13.5	$1.35 \times 92.88 + 1.5 \times 0.4 \times 3 \times 6.3 =$	<u>136.73</u>		
Dead load wall	9.72	ULS 2			
Dead load from above	69.66	$1.2 \times (92.88) + 1.5 \times 2 \times 6.3 + 1.5 \times 0.4 \times 6.3 =$	<u>134.14</u>		
<u>Total dead load</u>	<u>92.88</u>				
Variable load floor	6.3				
Variable load from above	6.3				
<u>Total variable load</u>	<u>18.9</u>				

Table 9.5: Stresses wall C and brick strength

Floor	Design Load	Design Stress	GBEB 'Eco' Strength*	U.C.	(-)
	kN/m	MPa	MPa		
3th floor	33.26	0.15	0.67	0.15/0.67 =	0.16
2th floor	66.47	0.29	0.67	0.21/0.67 =	0.31
1th floor	102.49	0.45	0.67	0.32/0.67 =	0.48
Ground floor	136.73	0.59	0.67	0.59/0.67 =	0.89

*Incorporating a reduction factor for slenderness and eccentricity $\Phi = 0.7$: $0.7 * 0.96$ [MPa] = 0.67 [MPa]

9.3. Case Study: Final Takeaways

The challenge with tackling this case study lies in the limited research and information regarding the Glass Bottle Earth Block (GBEB) itself. Many material properties remain unknown, and it's unknown which mortar is suitable for connecting these bricks or whether dry connecting them is feasible. Furthermore, there's a lack of data on appropriate safety factors for both the loads and materials due to the absence of design standards and tests. Despite the lower strength compared to traditional building materials, the GBEB can still serve as a load-bearing masonry unit for low-rise buildings. As illustrated in Table 9.5, the stresses anticipated in the wall remain relatively low. Additionally, addressing situations where only half of a brick is required and its impact on structural behavior warrants further examination. Which is definitely a factor to consider when utilizing bricks with an uneven amount of glass bottles.

Discussion, Conclusions and Recommendations

10

Discussion and Conclusion

The three sub-questions formulated at the beginning of the thesis will be addressed in the Discussions section. Following this, an answer to the main question will be formed in the Conclusion section, utilizing insights gained from these sub-questions.

10.1. Discussion

10.1.1. Glass Bottles: Exploring Their Role in Wall Configuration Case Studies

The first sub-question of this thesis is assessed:

What specific types of bottles are relevant for this research, and how have they been utilized in case studies focusing on wall configurations?

The review of literature highlights a growing tendency to incorporate glass bottles into earth-based constructions, driven by their mutual advantages of environmental sustainability and cost-effectiveness. Typically, in wall construction, bottles are arranged horizontally, creating a captivating effect where light filters through them. However, the irregular shapes of glass bottles pose challenges when connecting them with mortar during wall construction.

An innovative approach aims to improve construction efficiency and quality by pouring mortar between the bottles instead of applying it manually. Additionally, using molds to create bricks with embedded bottles facilitates easier stacking and faster execution. Prefabricating blocks with pre-positioned bottles in controlled environments enhances efficiency, construction speed and ease. This method, highlighted in case studies focusing on earth-based construction with glass bottles, contributes to manual building without the need for expensive and complex machinery. As it is stacked as masonry, it also contributes to the need of a more familiar building method.

Moreover, insights from the hollow glass market in Brazil suggest that long neck beer bottles constitute a significant portion, although specific data on disposal rates remain estimated. Nonetheless, industry experts agree that amber long neck beer bottles are among the most commonly consumed in Brazil.

In conclusion, the orientation of amber long-neck beer bottles in horizontal positions and their connection using a liquid, self-compacting earth-based mortar represents an effective approach, tackling several challenges when constructing with bottles identified through case studies.

10.1.2. Interconnecting Glass Bottles: Methods and Load Response in Several Arrangements

The second sub-question of this thesis is assessed:

What method can be employed to interconnect these bottles, and how do they respond to loading within this arrangement?

In the course of experimental investigations, a self-compacting earth-based mortar mixture is developed using locally sourced Dutch soil from Emmen. Five distinct mixture formulations are examined, incorporating both artificial and natural soil components. The mechanical characteristics of the earth-based mortar blends are assessed through compressive and flexural strength tests, alongside a mini slump flow test to measure workability. Projections indicate that the chosen earth mixture reaches an average compressive strength of 12.1 MPa after 28 days, an average flexural strength of 3.67 MPa after 7 days, and a flow diameter of 23.05 mm.

Subsequently, a prototype brick featuring a horizontally positioned longneck beer bottle is fabricated, unveiling compressive strengths ranging between 8.21 and 11.40 MPa after 28 days of curing. Upon conducting failure analysis, mirror fracture patterns pinpoint failure origins at the bottle's bottom, with mirror stresses at failure measuring 608 kg/cm² (59.62 MPa) and 431 kg/cm² (42.27 MPa) for two samples. SEM-EDS analysis exposes iron and aluminium residue at fracture origins, indicating that the cleavage damage was likely introduced during the application of the earth mixture to the bottles.

Through numerical investigations utilizing Finite Element Methods (FEM), a comprehensive grasp of stress propagation and behavior within a glass bottle wall confined by earth-based mortar is achieved. The study unveils that altering the Poisson's ratio and elastic modulus of the earth-based mortar impacts peak stresses, particularly at the bottle's base, with higher values correlating to heightened stress levels. While modifications in friction due to glass abrasion and earth composition insignificantly affect stress levels, modeling the brick with the bottle from laboratory experiments aligns with anticipated peak stresses. However, the FEM model's simplification disregards knurls, potentially overestimating strength, highlighting the necessity of considering knurls to accurately predict peak stresses.

Further investigations delve into the optimal arrangement of bottles within bricks, showcasing that alternating bottle placement yields a more symmetrical stress distribution over the length of the bottle whereas not alternating the bottles show a more symmetrical stress distribution in the other direction. Examination of varying horizontal center-to-center distances of the bottles show no significant difference in peak stresses. It may suggest that increasing the distance between bottles could marginally benefit the bottle's resistance. Overall, it remains inconclusive which bottle distance is preferable for stress management, as significant stresses — where tensile stress peaks — shows no significant difference with changes in bottle distances.

Diverse standards adopt varied approaches in determining the design tensile strength of floating glass. However, all building codes are founded on flat glass and not container glass. Comparative analysis of load duration factors across different standards (EN 16612, NEN 2608, ASTM E1300) and data provided by AGR American Glass Research based on container glass reveals a similar relationship, suggesting that the influence of the load duration factor approaches an asymptotic relationship. Following a load duration of 50 years and including material safety factors, a design tensile strength of the glass bottle with severe abrasions is expected to be between 6.5 MPa and 7.31 MPa.

10.1.3. Limitations and Challenges

The last sub-question of this thesis is assessed:

What are the limitations and challenges of re-purposing glass bottles in a structural wall?

The research on brick bottle masonry with earth based mortar has identified several limitations. Firstly, the mold used for production requires upgrading to ensure fast and easy production. The sensitivity of

the bottle to movement and floating, as it is not securely held in place by the mold, poses a challenge. Additionally, the current exploration of only one type of bottle limits the choices available for implementation. Finally, the bottle openings may create ideal conditions for insect incubation, suggesting a need for closure.

While the combination of earth mixture with bottles aligns with sustainability goals, the composition of the earth mixture includes ingredients like a PCE plasticizer and a cement/soil ratio of 12%, which are not environmental friendly materials. Further efforts to enhance sustainability could be explored. Additionally there are still numerous unknowns about this material, requiring additional research to determine the effectiveness of the earth mixture as a building material for connecting bottles. Factors such as sensitivity to erosion, shrinkage, stability of the mixture, and material properties have not been thoroughly examined.

Lack of available codes for self-compacting earth-based mortar and container glass necessitates the proposal of a design formula based on existing codes, taking following into account:

1. The surface condition of the bottle and thus the damaged state
2. A load-duration factor
3. A material factor
4. A factor incorporating the effect of knurls: peak stresses and tolerances

It is clear that the knurls have an effect on the strength of the bottle brick, yet the precise nature of this effect remains unknown.

In conclusion, the limitations encompass challenges in mold design, bottle sensitivity, limited bottle choices, potential insect habitats, composition of the earth mixture, and unknowns in material properties. These limitations highlight the need for further research to address these issues and refine the methodology for a more comprehensive understanding of the feasibility of brick bottle masonry. An example of a case study is conducted, showing that for now, the bricks are limited for low rise buildings. Lastly, safety needs to be assessed. Investigating post breakage and seeing how glass charts can be held together at failure. Besides, the bottom of the bottle is exposed, which can be a vulnerable surface.

10.2. Conclusion

In this section, an answer on the main research question is formed:

How can the structural feasibility of re-purposing beer bottles as a load-bearing wall structure be ensured?

A potential solution is to prefabricate bricks with embedded bottles. Given the complex geometry and gaps between bottles, a self-compacting earth-based mortar is designed. This mortar utilizes aggregates from local soil, with a maximum grain diameter of 2 mm. Based on the compressive strength of three samples, an average compressive strength of 12.09 MPa is anticipated after 28 days.

The expected design resistance of a proposed brick incorporating three bottles is assessed. With dimensions of 85mm x 315mm x 230mm (height x width x depth) and a weight of approx. 8 kg, the brick is expected to have a design strength of 0.96 MPa over a 50-year load duration. Although it may not seem like much, the stresses occurring in load-bearing walls remain relatively low. A case study conducted during the early design stages demonstrated the feasibility of constructing a four-level building. This indicates that load-bearing walls could serve as viable components for low-rise buildings.

However, there remains insufficient data to make definitive conclusions. Therefore, it is advisable to increase the number of samples tested to establish a characteristic strength that aligns with standards. Additionally, comparing these results with findings from other studies will enhance confidence in the

findings. Moreover, conducting a wider range of tests will provide insights into material properties and help validate the assumptions made.

Research Recommendations

This section proposes research recommendations aimed at advancing the understanding and application of self-compacting earth-based mortar and glass bottle earth bricks, paving the way for more eco-friendly and resilient building practices.

11.1. Self Compacting Earth Based Mortar

11.1.1. Optimizing mixture design

In order to optimize the mixture design for earth-based mortar, several key considerations should be addressed. First and foremost, increasing the sample size and conducting additional tests are essential steps to assess various properties such as electrical resistivity, water capillary absorption, drying shrinkage, stability of the mixture, and its resistance to environmental influences like erosion. Moreover, understanding material properties such as Elastic Modulus and Poisson's Ratio is crucial for effective design. Sustainable methods to enhance the tensile behavior of the mixture would also be interesting to explore. Additionally, considering the incorporation of local Brazilian fibers like sisal or banana fibers to augment material properties and evaluating their impact on flowability, yielding, and stabilization of the earth mortar can be ways to make the building material even more sustainable and increase its resistance. Enhancing the environmental sustainability of the mixture is also paramount. Researching methods for the solidification of the mortar using bio-sourced polymers and exploring environmentally friendly or natural superplasticizers to increase flowability are essential steps.

11.1.2. Investigating granulometry distribution and soil composition

Another significant aspect is investigating granulometry distribution and soil composition. Determining the preferable granulometry and soil composition for the application of self-compacting earth-based mortar is necessary. Exploring methods to achieve desired properties, such as mixing different types of soil or adding specific granulates, is crucial. Furthermore, developing strategies for handling soil unsuitable for mortar, including the addition of commercially available aggregates like bentonite clay or adjusting local soil composition, is important for successful implementation.

11.1.3. Moisture content influence

Understanding the influence of moisture content is another critical aspect. Investigating how moisture content affects material properties such as Poisson's ratio and Elastic modulus, exploring moisture absorption properties of the earth mixture, and studying how environmental conditions, including increased humidity, affect the hardening and mechanical properties of earth mortar are important considerations.

11.1.4. Alignment with building standards

Finally, aligning with building standards is crucial for ensuring compliance and reliability. Exploring integration with existing building standards and determining the suitability of earth-based formulas for

this application, considering similarities with concrete properties, are necessary steps to ensure the success of the optimized mixture design. By addressing these aspects comprehensively, it is possible to develop an optimized mixture design for earth-based mortar that meets both performance requirements and environmental sustainability goals.

11.2. Glass bottles

Investigating the impact of knurls on stress concentrations in the discussed configuration is a crucial area of research. Additionally, exploring methods to close bottle openings and assessing their influences to determine if closure is necessary is essential. Testing bottles with severe abrasions and comparing the results with those from bottles with mild abrasions can provide valuable insights into the effects of wear and tear on bottle strength. Monitoring potential decreases in glass quality during production of the bricks, especially when scaling up, is crucial. It is also important to monitor potential decreases in glass quality during exposure to environmental conditions.

Determining the appropriate factor of safety and material factor is fundamental for ensuring the reliability and durability of the bottles. Assessing the infrastructure of bottle collection and storage to potentially improve bottle quality and strengths is another important aspect that warrants investigation. Besides, setting up a system to clean the bottles and remove the labels effectively can increase the practicality of the application.

Reevaluating the bottle configuration and exploring other possibilities can lead to innovative solutions for enhancing bottle performance. Investigating post-breakage behavior and safety, such as introducing methods to ensure that glass shards stay together, such as by introducing a coating, is critical for mitigating risks associated with broken bottles.

Finally, exploring other bottle types can provide alternative options that may offer improved structural characteristics and performance. These research recommendations are essential for advancing our understanding of bottle performance and safety, as well as for informing design and manufacturing practices.

11.3. Glass Bottle Earth Brick (GBEB)

11.3.1. Assumption verification

It is essential to verify assumptions, particularly regarding the friction coefficient's effect on stress distribution and amplitude. One approach is to consider casting strain gauges in a sample to compare with strains found in the FEM model. Refining FEM models to better define interface conditions between the bottle and brick and to understand the effect of stress concentrations due to the presence of knurls is also necessary.

11.3.2. Brick design and optimization

Developing a practical and sustainable mold is crucial, considering the sensitivity to movement of the bottles during casting. Additionally, optimizing brick design and exploring possibilities for adding reinforcement can be interesting and enhance its competitiveness as a building material. Additionally, determining appropriate stacking methods, whether dry stacking or with mortar, and selecting suitable mortar types are essential considerations. Exploring applications beyond bricks, such as larger prefab panels or monolithic walls, can lead to innovative uses and enhance its competitiveness as a building material.

11.3.3. Further research

Conducting additional research on masonry techniques and performing appropriate tests will provide valuable insights into the performance and durability of the GBEB wall. Additionally, investigating thermal insulation properties and overall building physics is necessary to ensure thermal comfort for occu-

pants.

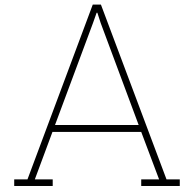
References

- [1] H. Varum A. M. Matos. "Self-Compacting Earth-Based Composites: Mixture Design and Multi-Performance Characterisation". In: *Buildings* 12, 612. 12 (2022). DOI: <https://doi.org/10.3390/buildings12050612>.
- [2] S W Lee et al. "The Use of Oil Palm Fiber as Additive Material in Concrete". In: *IOP Conf. Series: Materials Science and Engineering* 431 (2018). DOI: [doi:10.1088/1757-899X/431/4/042012](https://doi.org/10.1088/1757-899X/431/4/042012).
- [3] All About Architecture. *Making a house out of Beer Bottles in Tamil Nadu, India*. URL: <https://architecturerealestate.wordpress.com/2021/04/08/making-a-house-out-of-beer-bottles-in-tamil-naduindia-2/> (visited on 06/28/2023).
- [4] artlife. *How to Make a Bottle Building*. URL: <https://www.instructables.com/How-to-make-a-Bottle-Building/> (visited on 06/27/2023).
- [5] "Asia-Pacific recycled glass market forecast 2022-2030". In: *Inkwood research* (2021).
- [6] P. W. de Haan B. S. Aldinger. *Color Atlas of Glass Container Defects Hardcover*. Blurb, 2019, p. 154.
- [7] E. AGAHZADEH B.Y. PEKMEZCİ R. KAFESÇİOĞLU. "IMPROVED PERFORMANCE OF EARTH STRUCTURES BY LIME AND GYPSUM ADDITION". In: *METU JFA* (2012), pp. 205–221. DOI: [10.4305/METU.JFA.2012.2.9](https://doi.org/10.4305/METU.JFA.2012.2.9).
- [8] Kenai S. Benhaoua W. Grine K. "Performance of Stabilized Earth with Wheat Straw and Slag". In: *MRS Advances* (2020). DOI: [DOI:10.1557/adv.2020.174](https://doi.org/10.1557/adv.2020.174).
- [9] Wood B. et al. Bhargava A. Wang F. "Studies of polyethylene-coated tin oxide films on glass bottles." In: *Surface and Interface Analysis* 29 (2000), pp. 663–670.
- [10] Government of Brazil. *Presidente institui o sistema de logística reversa para embalagens de vidro*. 2022. URL: <https://www.gov.br/secretariageral/pt-br/noticias/2022/dezembro/presidente-institui-o-sistema-de-logistica-reversa-para-embalagens-de-vidro> (visited on 11/07/2023).
- [11] brazilsustainableindustry. *Proper step by step glass disposal*. 2022. URL: <https://brazilsustainableindustry.com.br/sustainable-hints/proper-step-by-step-glass-disposal/> (visited on 10/16/2023).
- [12] Hoekman L. C. "COATING COMPOSITION FOR GLASS CONTAINERS (EP 3 502 077 A1)". In: *European Patent Office* (2019).
- [13] C. Jacintho C. A. dos Santos L. I. Librelotto. "Building with earth – Brazil's most popular raw earth building techniques and the opinion of experienced builders." In: *Key Engineering Materials* 600 (2014), pp. 123–131.
- [14] CETIE. "EGlass Finish Glossary and Nomenclature". In: *DT23.02* ().
- [15] Signes C.H. et al Clausell J.R. Quintana-Gallardo A. "Environmental evaluation of a self-compacted clay based concrete with natural superplasticisers." In: *Mater. Struct. Mater. Et Constr.* 54 (2021), pp. 1–16.
- [16] Heineken Collection. "The WOBO: a futuristic bottle". In: ().
- [17] CRAterre. URL: <http://craterre.org/> (visited on 09/27/2023).
- [18] C. Perlot et al. D. Gallipoli A. W. Bruno. "A geotechnical perspective of raw earth building". In: *Acta Geotechnica* 12 (2017), pp. 463–478. DOI: [10.1007/s11440-016-0521-1](https://doi.org/10.1007/s11440-016-0521-1).
- [19] P. Walker D. Maskell A. Heath. "Laboratory scale testing of extruded earth masonry units". In: *Mater. Des.* 45 (2013), pp. 359–364.
- [20] M. W. Davis. *The Wiley Encyclopedia of Packaging Technology*. Vol. 3rd ed. John Wiley and Sons, Inc. 2009, p. 1353.

- [21] R. Dinger. "One dimensional packing of spheres". In: *Am. Ceram. Soc. Bull* Part II (2000), pp. 83–91.
- [22] EPA. *Glass: Material-Specific Data*. 2022. URL: <https://www.epa.gov/facts-and-figures-about-materials-waste-and-recycling> (visited on 05/09/2023).
- [23] feve.org. *Feve The European Container Glass Federation*. 2020. URL: <https://feve.org> (visited on 04/26/2023).
- [24] feve.org. *Food Packaging Forum*. 2022. URL: <https://www.foodpackagingforum.org/news/associations-report-european-packaging-recycling-rates> (visited on 04/26/2023).
- [25] M. Frerking. "Cast Earth: A Revolutionary Building Concept". In: *buildingstandards* (2000), pp. 37–39.
- [26] Patano C. G. "The Role of Coatings and Other Surface Treatments in the Strength of Glass". In: *European Patent Office* [slides] (). <https://gmic.org/wp-content/uploads/2016/06/The-Role-of-Coating-and-Other-Surface-Treatments-in-the-Strength-of-Glass-Carlo-Pantano.pdf>.
- [27] R. D. Southwick G. L. Smay J. S. Wasyluk. *A critical assessment of lubricating and damage-preventive glass coatings*. Third Proceeding of the Symposium. pp.39. The Eitel Institute for Silicate Research, 1982.
- [28] Sibelco Deutschland GmbH. *Sibelco Ceramic Bodies*. 2023. URL: <https://ceramicsbodies.sibelcotools.com/> (visited on 10/09/2023).
- [29] gov.br Presidência da República. *Title of the Website*. 2022. URL: <https://www.gov.br/secretariageral/pt-br/noticias/2022/dezembro/presidente-institui-o-sistema-de-logistica-reversa-para-embalagens-de-vidro> (visited on 07/05/2023).
- [30] Gueguen Y. Guin J. P. "Mechanical Properties of Glass". In: *Springer Handbook of Glass* (2019), pp. 227–272.
- [31] T. Drupsteen et al. H. Moorris M. Allen. *Engineering Design of Earth Buildings*. NZS 4297:1998. Private Bag 2439, Wellington 6020: Standards New Zealand, 1998.
- [32] T. Drupsteen et al. H. Moorris M. Allen. *Materials and workmanship for earth buildings*. NZS 4298:1998. Private Bag 2439, Wellington 6020: Standards New Zealand, 1998.
- [33] J. Hann. "Annealing of glass containers and hollowware". In: *Glass International* (2013), pp. 222–28.
- [34] Dr. Ing. J. Harder. *Glass recycling – Current market trends*. 2018. URL: <https://www.recovery-worldwide.com/en/artikel/glass-recycling-current-market-trends-3248774.html> (visited on 05/09/2023).
- [35] Mitchell KK Herzog A. "Reactions accompanying the stabilization of clay with cement". In: *Highway Research Record No. 36, Highway Research Board, National Research Council, Washington, D. C.* 36 (1963).
- [36] W. Hu. "Glass container knurling study". In: *Glass Worldwide* (2022), pp. 88–90.
- [37] W. Hu. "Glass container knurling study - part 2". In: *Glass Worldwide* (2022), pp. 152–154.
- [38] F. Rahimi K. Bakhshandeh I. Rajabi. "Investigation of Stress Concentration Factor for Finite-Width Orthotropic Rectangular Plates with a Circular Opening Using Three-Dimensional Finite Element Model". In: *Journal of Mechanical Engineering* 54.2 (2008), pp. 140–147.
- [39] blogpost by K. Johnson. *Questions about stained glass bottle bricks for cordwood walls*. 2018. URL: <https://permies.com/t/140181/Bricks-beer-bottles-adobe-stabilized> (visited on 11/06/2023).
- [40] R. Keable J.; Keable. "Rammed Earth Structures: A Code of Practice". In: *Practical Action Publishing* (2011).
- [41] L. Keefe. "Earth Building: Methods and Materials, Repair and Conservation". In: (2005).
- [42] L. Keefe. *Earth Building Methods and Materials, Repair and Conservation*. 1th ed. p.7. London: Taylor and Francis, 2005.

- [43] Wasyluk J. S. Kepple J. B. "Fracture of Glass Containers." In: *Fractography of Glass* 1st ed. Vol. 1 (1994). https://doi.org/10.1007/978-1-4899-1325-8_7, pp. 207–252.
- [44] Normando P. Barbosa Khosrow Ghavami Romildo D. Toledo Filho. "Behaviour of composite soil reinforced with natural fibres". In: *Cement and Concrete Composites* 21 (1999), pp. 39–48.
- [45] I. Kostakis and K. P. Tsagarakis. "Social and economic determinants of materials recycling and circularity in Europe: an empirical investigation". In: *The Annals of Regional Science* 68 (2022). <https://doi.org/10.1007/s00168-021-01074-x>, pp. 263–281.
- [46] Robertson G. L. *Food Packaging: Principles and Practice*, Third Edition. <https://doi.org/10.1201/b21347>. CRC Press, 2012.
- [47] Smay G. L. "Effect of coatings on adhesion of labels of glass containers." In: *Glass Worldwide* 69 (2017). https://americanglassresearch.com/sites/default/files/effect_of_coatings_w_hitepaper_jan2017_gw.pdf, pp. 68–70.
- [48] Winnefeld et al Landrou G. Brumaud C. "Lime as an Anti-Plasticizer for Self-Compacting Clay Concrete." In: *Materials* 9 (2016), p. 330.
- [49] B. Lawson. "Building Materials Energy and The Environment". In: (1996).
- [50] V. Soebarto M. Gomaa W. Jabi. "Digital manufacturing for earth construction: A critical review." In: *J. Clean. Prod.* (2022), p. 338.
- [51] Chen L. Ma C. Chen B. "Variables controlling strength development of self-compacting earth-based construction." In: *Constr. Build. Mater.* 123 (2016), pp. 336–345.
- [52] Y. Maachi. "Exploring the potential reuse of glass bottles in structural columns: Investigating the Structural Behaviour of Glass Columns Containing Glass Bottles through FE-modelling and Physical testing". In: *[Master's thesis]* (2022). [TU Delft, Netherlands], p. 174.
- [53] MASSFIX. *Contribuindo para um futuro mais limpo*. URL: <http://www.massfix.com.br/> (visited on 11/07/2023).
- [54] Olagnon C et al Moevus M Jorand Y. "Earthen construction: an increase of the mechanical strength by optimizing the dispersion of the binder phase." In: *Mater. Struct* 49 (2015), pp. 1555–1568. DOI: 10.1617/s11527-015-0595-5.
- [55] Armin L. Müller-Simon H. Jorg W. "Practical strength of glass containers Part 1. Influence of the type of defect." In: *Glastechnische Berichte* 67(5) (1994), pp. 134–142.
- [56] Yokokura S. Nakawaga M. Amano T. "Development of lightweight returnable bottles". In: *Journal of Non-Crystalline Solids* 218 (1997), pp. 100–104.
- [57] Nadia Saiyouri Nathalie Kouta Jacqueline Saliba. "Fracture behavior of flax fibers reinforced earth concrete". In: *Engineering Fracture Mechanics* 241 (2021). DOI: <https://doi.org/10.1016/j.engfracmech.2020.107378>.
- [58] Habert G. Ouellet-Plamondon C. "Proof of concept of self-compacting clay concrete to scale-up earth construction. In Proceedings of the American Society of Agricultural and Biological Engineers Annual International Meeting 2014 (ASABE 2014), Montreal, QC, Canada, 13–16 July 2014." In: (2014).
- [59] Habert G. Ouellet-Plamondon C.M. "Self-Compacted Clay based Concrete (SCCC): Proof-of-concept." In: *J. Clean. Prod.* 117 (2016), pp. 160–168.
- [60] A. Pinel, Yves Jorand, and Olagnon et al. "Towards poured earth construction mimicking cement solidification: demonstration of feasibility via a biosourced polymer". In: *Materials and Structures* 50 (Oct. 2017), p. 224. DOI: 10.1617/s11527-017-1092-9.
- [61] J Morel et al. Q. B. Bui S. Hans. "First exploratory study on dynamic characteristics of rammed earth buildings". In: *Engineering Structures* 33.12 (2011). DOI:10.1016/j.engstruct.2011.08.004, pp. 3690–3695.
- [62] Penlington R. "Surface engineering in the glass container industry". In: *Vacuum* 56 (2000), pp. 179–183.

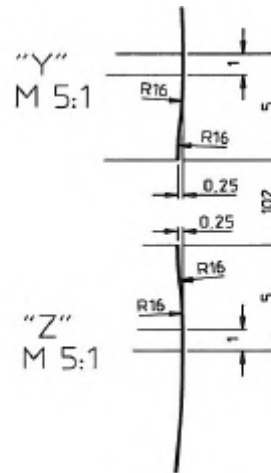
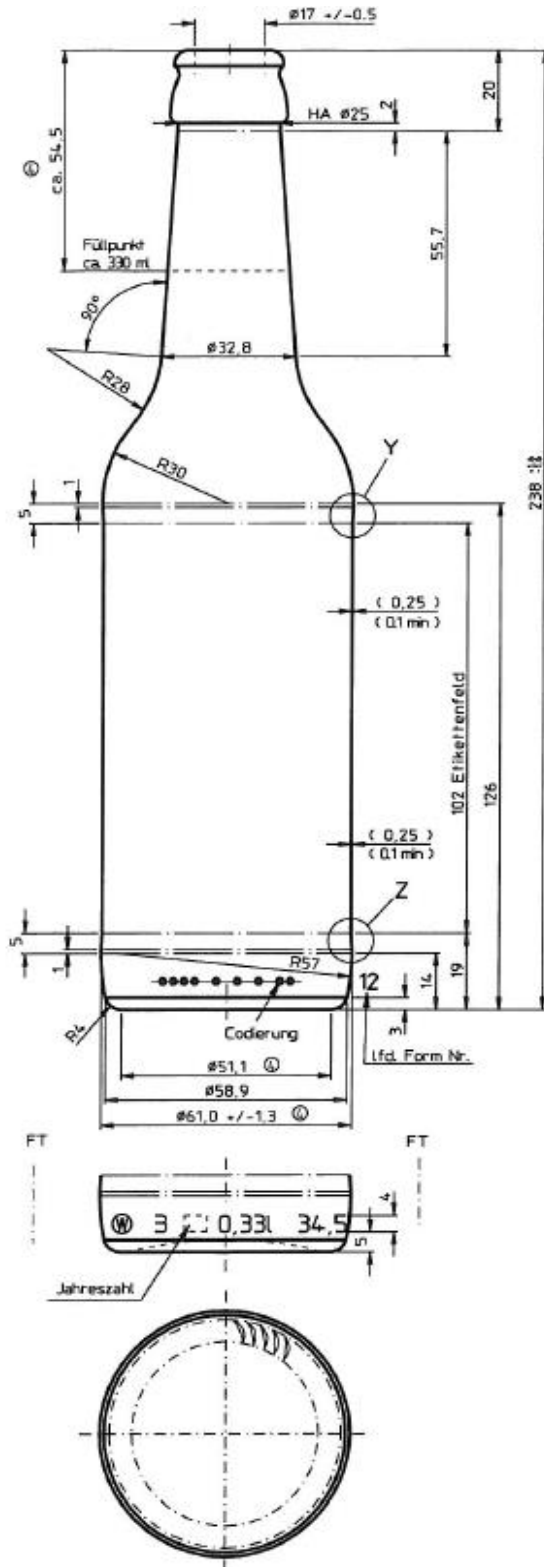
- [63] P. Capellato et al. R. d. C. M. Alves M. G. A. Ranieri. "LOW ENVIRONMENTAL IMPACT CONSTRUCTION: FRAGILITIES AND POTENTIALITIES OF HYPERADOBE AS A SOLUTION FOR THE BRAZILIAN HOUSING DEFICIT". In: *REVES- Revista Relações Sociais* 04 N.01 (2021).
- [64] Recycle across america. *Recycling is in a serious crisis*. 2023. URL: <https://www.recycleacrossamerica.org/recycling-facts> (visited on 04/28/2023).
- [65] B. V. Venkatarama Reddy. *Compressed Earth Block and Rammed Earth Structures*. 1th ed. Springer, 2022. DOI: <https://doi.org/10.1007/978-981-16-7877-6>.
- [66] Presidência da República Secretaria-Geral Subchefia para Assuntos Jurídicos. "DECRETO N° 11.300, DE 21 DE DEZEMBRO DE 2022". In: (2022). D11300.
- [67] Negahdari Z. et al. Roos C. Rosin A. "Hot-end coating: Strengths, risks and alternatives". In: *Glass International* 37 (2014), pp. 13–15.
- [68] A. Hibouche et al S. Imanzadeh A. Jarno. "Ductility analysis of vegetal-fiber reinforced raw earth concrete by mixture design". In: *Construction and Building Materials* 239 (2020). DOI: <https://doi.org/10.1016/j.conbuildmat.2019.117829>.
- [69] S. Avudaiappan et al S. M. Kavitha Venkatesan G. "Mechanical and flexural performance of self compacting concrete with natural fiber". In: (July 2020). DOI: DOI:10.7764/RDLC.19.2.370.
- [70] Saxco. *Anatomy of a bottle*. URL: <https://www.saxco.com/resources/reference-guides/packaging-fundamentals-bottle-anatomy/> (visited on 07/06/2023).
- [71] H. Schroeder. "Modern earth building codes, standards and normative development". In: (2012), p. 38.
- [72] H. Schroeder. "Modern earth building codes, standards and normative development". In: *Modern Earth Buildings*. Ed. by Matthew R. Hall, Rick Lindsay, and Meror Krayenhoff. Woodhead Publishing Series in Energy. Woodhead Publishing, 2012, pp. 72–109. ISBN: 978-0-85709-026-3. DOI: <https://doi.org/10.1533/9780857096166.1.72>. URL: <https://www.sciencedirect.com/science/article/pii/B9780857090263500046>.
- [73] G. L. Smay. "Effect of coatings on adhesion of labels to glass containers". In: *[GLASS WORLD-WIDE]* 69 (2017). [], pp. 68–70.
- [74] Smay et al. Southwick R. Wasylyk J. *The mechanical properties of films for the protection of glass surfaces*. Volume 77. Thin Solid Films, 1981.
- [75] CHOLADA K. SUCHADA P. J. TRÄNKLER and W. SCHÖLL. "THE ROLE OF FORMAL AND INFORMAL SECTORS IN SOLID WASTE MANAGEMENT OF DEVELOPING COUNTRIES". In: *The Title of the Journal* 1.2 (2000), pp. 123–456.
- [76] T. D. Khong Y. D. Tong T. D. X. Huynh. "Understanding the role of informal sector for sustainable development of municipal solid waste management system: A case study in Vietnam". In: *Waste Management* 124 (2021), pp. 118–127.



Beer bottle Longneck 33 cl, brown, 26
mm Brouwland



017.525.7 Beer bottle Longneck 33 cl, brown, 26 mm



Weight	Ca. 300 gr
Refillable	Yes
CO2 content	4-6 g/L
Internal pressure T101	12 bar
Axial loading	5 kp
Temperature shock	42°C
Filling temperature	6-8°C

Brouwland

Korpelsesteenweg 86 • B-3581 Beverlo - Belgium
 Tel. +32 11 40 14 08 • Fax. +32 11 89 03 09
 info@brouwland.com • www.brouwland.com

B

Technical Data Sibelco Deutschland
GmbH

Characteristics

GR - T is a red earthenware body for casting.
Available as blended powder.

Firing Colour	rose - terracotta
Recommended Firing Temperature Range	1000 - 1150 °C

Technical Data

Unfired

Moisture	0,6% powder							
Chemical Analysis	SiO ₂	TiO ₂	Al ₂ O ₃	Fe ₂ O ₃	CaO	MgO	K ₂ O	Na ₂ O
	66,6%	1,20%	19,0%	4,00%	5,80%	0,50%	2,60%	0,30%
Loss of Ignition	9,7%							
Wet to Dry Shrinkage	4,5% casting							

Fired

Specimen Firing Temperature [°C]	1040	1100
Coefficient of Thermal Expansion [x10 ⁻⁶ /°C]		
	20 - 400 °C	7,1
	20 - 500 °C	7,8
	20 - 600 °C	8,9
Dry to Fired Shrinkage [%]	0,8	0,9
Water Absorption [%]	10,0	8,5

Casting Advice

Dolaflux B 11 : Giessfix 162	1 : 2		
Optimum Amounts	0,30%	-	0,36%
First deflocculant and afterwards, add the powder under slow stirring to the water.			
Specific Weight to Achieve	1780	-	1800 g/l
GR - T needs about 44 l water per 100 kg powder to achieve s.w. of 1790 g / l.			
Test the casting advice in own production first remembering the mentioned amounts are depending			

- use the right amount of deflocculant to achieve optimum casting time
- if castthickness is too small, use less deflocculant
- don't use more than 10 - 15 % of scrap (above the fresh made slip)

The technical data quoted on this sheet is indicative only. Any sale is by sample and is governed by our general conditions of sale.

**KERAMISCHE MASSEN**

Sibelco Deutschland GmbH
 Sälzerstraße 20
 56235 Ransbach-Baumbach
 DEUTSCHLAND

Tel.: +49 2623 8828-0
 Fax: +49 2623 8828-92
 E-Mail: kontakt@sibelco.de

15.06.2015



C

SEM-EDS analysis results

C.1. Composition of Raw Earth

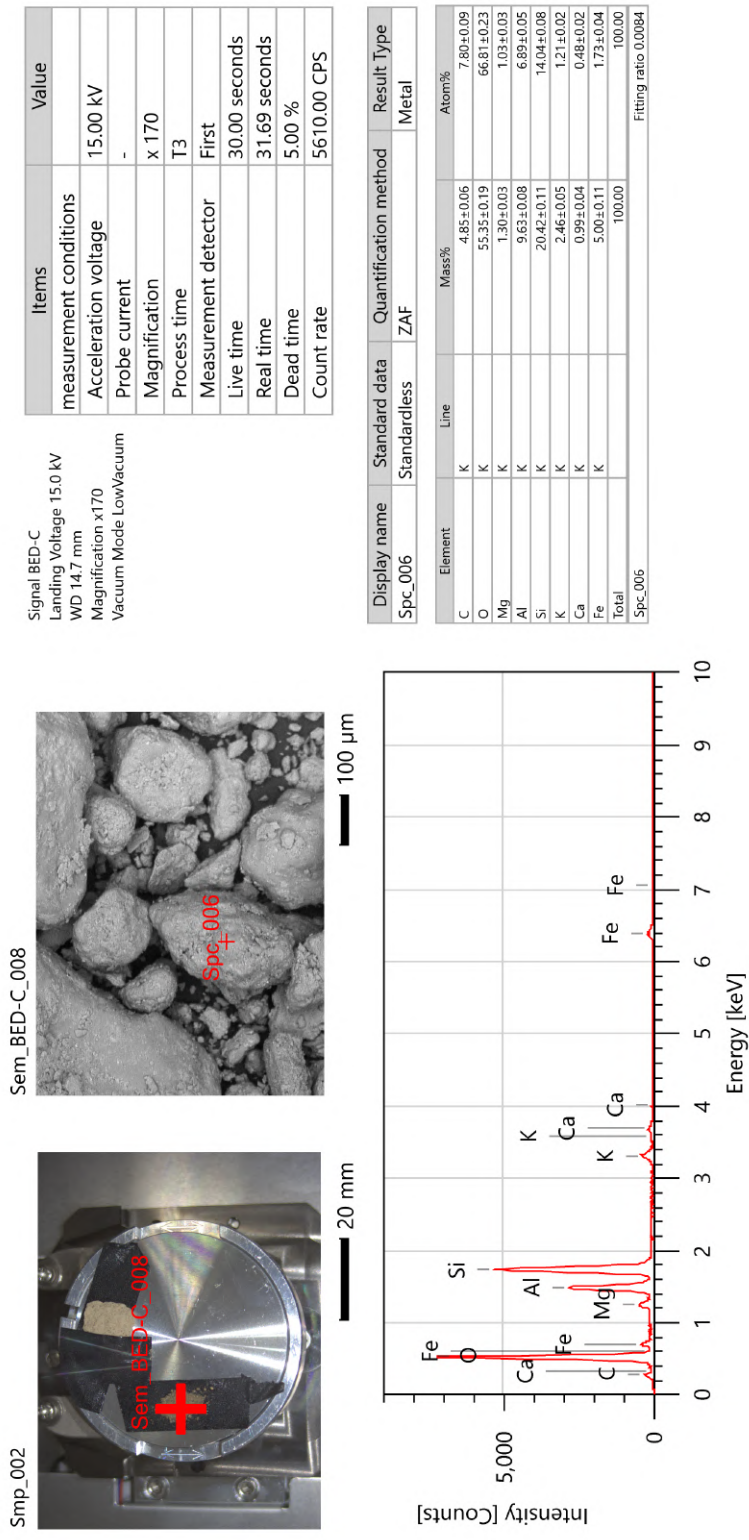


Figure C.1: SEM-EDS analysis results with the compositions determined for the earth

C.2. Composition of Earth Based Mortar

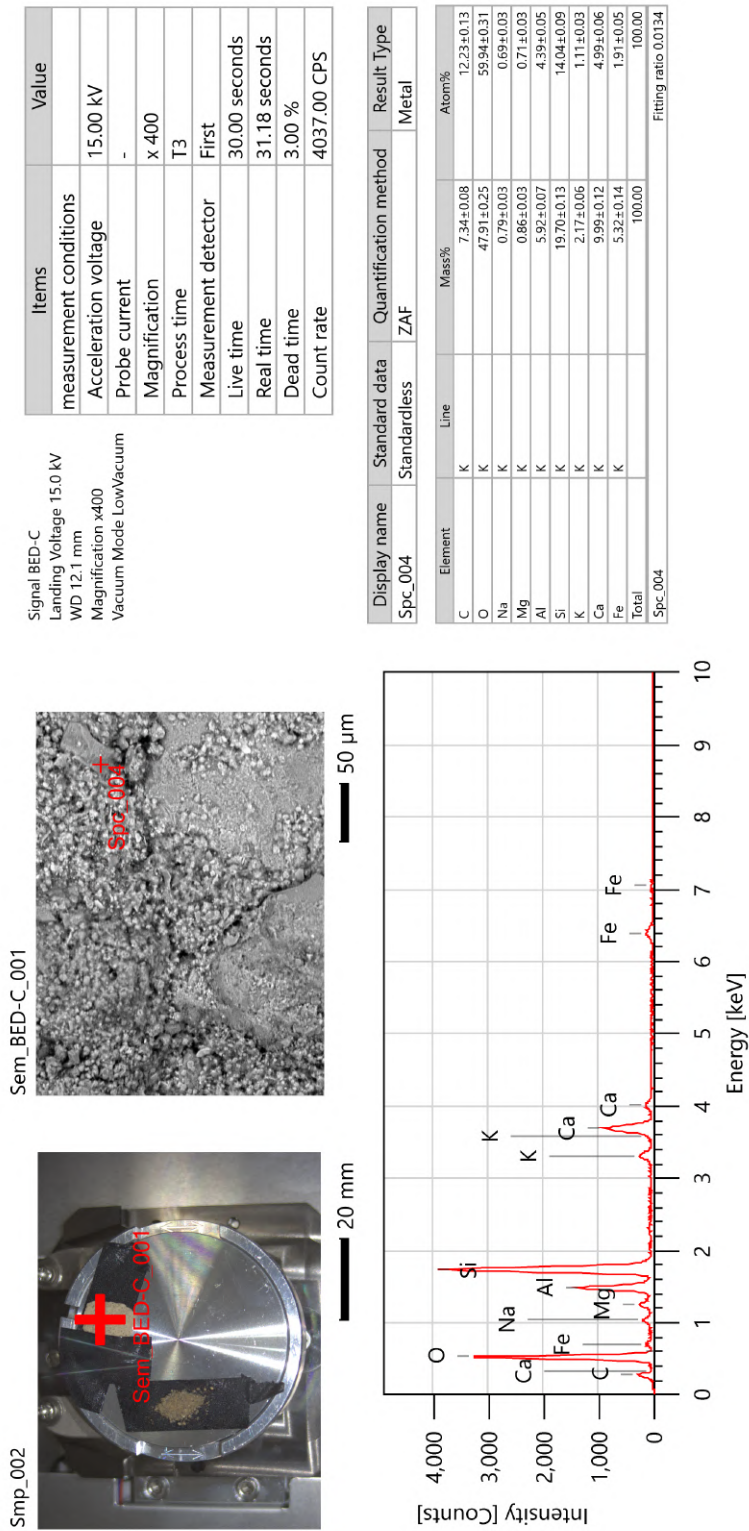


Figure C.2: SEM-EDS analysis results with the compositions determined for the Earth Based Mortar

C.3. Sample 2: Cleavage Scratch

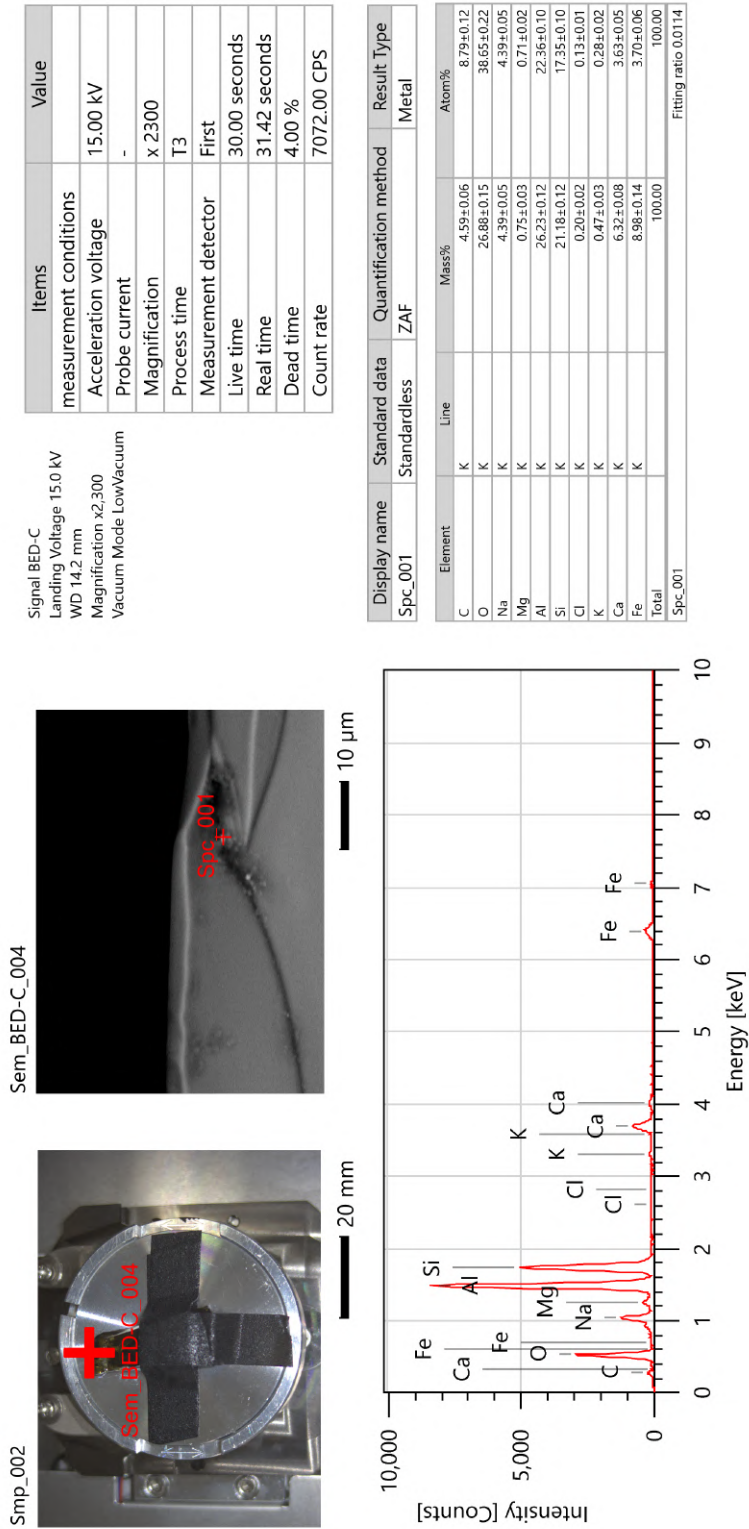


Figure C.3: SEM-EDS analysis results with the compositions determined for the glass next to the cleavage scratch of sample 2

C.4. Sample 2: Next to Cleavage Scratch

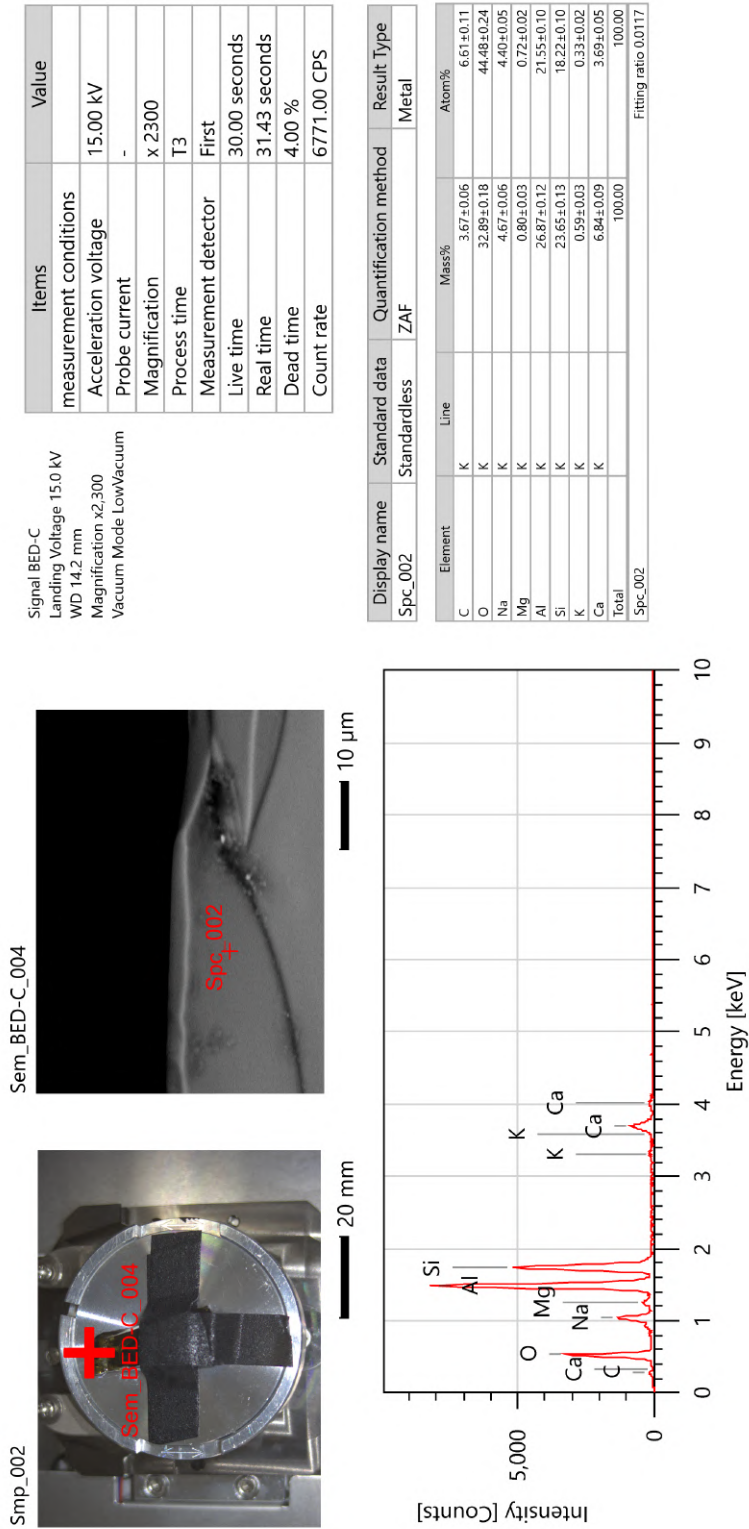


Figure C.4: SEM-EDS analysis results with the compositions determined for the glass next to the cleavage scratch of sample 2

C.5. Sample 3: Cleavage Scratch

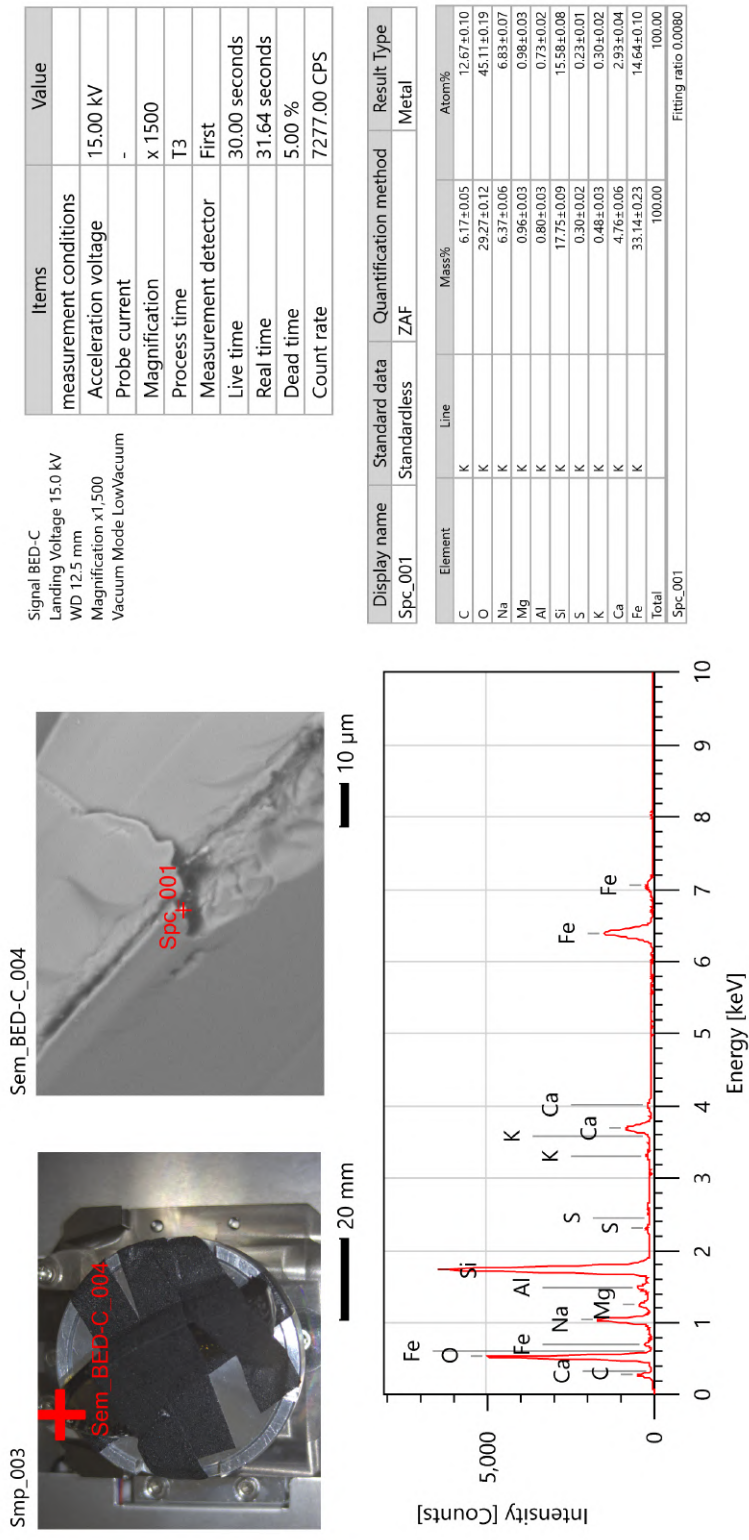


Figure C.5: SEM-EDS analysis results with the compositions determined for the Earth Based Mortar

D

APPROXIMATE TENSILE BREAKING
STRESSES OF SODA LIME GLASS (psi)

APPROXIMATE TENSILE BREAKING STRESSES OF SODA LIME GLASS (psi)																							
SURFACE CONDITION	psi																						
	<1ms	1s	2s	3s	5s	10s	15s	20s	30s	1min	5min	10min	15min	20min	30min	1hr	10hr	12hr	1day	3day	1wk	long	
Pristine inside BB	####	####	95250	92250	88500	84000	81750	80250	78000	75000	68250	66750	65250	63750	62250	60000	54750	53250	51750	50250	48000	45000	
Pristine inside PB	40000	26800	25400	24600	23600	22400	21800	21400	20800	20000	18200	17800	17400	17000	16600	16000	14600	14200	13800	13400	12800	12000	
Flute valley OW	24462	16390	15533	15044	14433	13699	13332	13087	12720	12231	11130	10886	10641	10396	10152	9785	8929	8684	8439	8195	7828	7339	
Mild abrasions	20000	13500	12700	12300	11800	11200	10900	10700	10400	10000	9100	8900	8700	8500	8300	8000	7300	7100	6900	6700	6400	6000	
Flute valley RT	16390	10981	10408	10080	9670	9178	8933	8769	8523	8195	7457	7294	7130	6966	6802	6556	5982	5818	5655	5491	5245	4917	
Mild abr OW	10000	6750	6350	6150	5900	5600	5450	5350	5200	5000	4550	4450	4350	4250	4150	4000	3650	3550	3450	3350	3200	3000	
Moderate abr OW	8000	5400	5080	4920	4720	4480	4360	4280	4160	4000	3640	3560	3480	3400	3320	3200	2920	2840	2760	2680	2560	2500	
Mod Sev abr RT	6700	4500	4254	4120	3953	3752	3651	3584	3484	3350	3048	2981	2914	2850	2780	2680	2445	2378	2311	2244	2144	2250	
Severe abrasions	5000	3350	3175	3075	2950	2800	2725	2675	2600	2500	2275	2225	2175	2125	2075	2000	1825	1775	1725	1675	1600	1700	
Deep bruises	3000	2000	1905	1845	1770	1680	1635	1605	1560	1500	1365	1335	1305	1275	1245	1200	1095	1065	1035	1005	960	650	
Cracks	1500	1000	952	922	885	840	817	802	780	750	682	667	652	640	622	600	547	532	517	502	480	470	
kg/cm2																							
SURFACE CONDITION	kg/cm2																						
	<1ms	1s	2s	3s	5s	10s	15s	20s	30s	1min	5min	10min	15min	20min	30min	1hr	10hr	12hr	1day	3day	1wk	long	
	Impact	crowning		Thermal						Pressure testing					Pasteurizer							Warehouse	
Pristine inside BB- inside surfa	10546	7066	6697	6486	6222	5906	5748	5642	5484	5273	4798	4693	4588	4482	4377	4218	3849	3744	3638	3533	3375	3164	
Pristine inside PB- inside surfa	2812	1884	1786	1730	1659	1575	1533	1505	1462	1406	1280	1251	1223	1195	1167	1125	1026	998	970	942	900	844	
Flute valley OW- region betwee	1720	1152	1092	1058	1015	963	937	920	894	860	783	765	748	731	714	688	628	611	593	576	550	516	
Mild abrasions- bottle just fab	1406	949	893	865	830	787	766	752	731	703	640	626	612	598	584	562	513	499	485	471	450	422	
Flute valley RT- between flutes	1152	772	732	709	680	645	628	616	599	576	524	513	501	490	478	461	421	409	398	386	369	346	
Mild abr OW- Strength compara	703	475	446	432	415	394	383	376	366	352	320	313	306	299	292	281	257	250	243	236	225	211	
Moderate abr OW- Strength com	562	380	357	346	332	315	307	301	292	281	256	250	245	239	233	225	205	200	194	188	180	176	
Mod Sev abr RT- Strength of a re	471	316	299	290	278	264	257	252	245	236	214	210	205	200	195	188	172	167	163	158	151	158	
Severe abrasions	352	236	223	216	207	197	192	188	183	176	160	156	153	149	146	141	128	125	121	118	112	120	
Deep bruises	211	141	134	130	124	118	115	113	110	105	96	94	92	90	88	84	77	75	73	71	67	46	
Cracks	105	70	67	65	62	59	57	56	55	53	48	47	46	45	44	42	38	37	36	35	34	33	
Mega Pascal																							
SURFACE CONDITION	Mega Pascal																						
	<1ms	1s	2s	3s	5s	10s	15s	20s	30s	1min	5min	10min	15min	20min	30min	1hr	10hr	12hr	1day	3day	1wk	long	
Pristine inside BB	1034.2	692.9	656.7	636.0	610.2	579.2	563.6	553.3	537.8	517.1	470.6	460.2	449.9	439.5	429.2	413.7	377.5	367.1	356.8	346.5	330.9	310.3	
Pristine inside PB	275.8	184.8	175.1	169.6	162.7	154.4	150.3	147.5	143.4	137.9	125.5	122.7	120.0	117.2	114.5	110.3	100.7	97.9	95.1	92.4	88.3	82.7	
Flute valley OW	168.7	113.0	107.1	103.7	99.5	94.4	91.9	90.2	87.7	84.3	76.7	75.1	73.4	71.7	70.0	67.5	61.6	59.9	58.2	56.5	54.0	50.6	
Mild abrasions	137.9	93.1	87.6	84.8	81.4	77.2	75.2	73.8	71.7	68.9	62.7	61.4	60.0	58.6	57.2	55.2	50.3	49.0	47.6	46.2	44.1	41.4	
Flute valley RT	113.0	75.7	71.8	69.5	66.7	63.3	61.6	60.5	58.8	56.5	51.4	50.3	49.2	48.0	46.9	45.2	41.2	40.1	39.0	37.9	36.2	33.9	
Mild abr OW	68.9	46.5	43.8	42.4	40.7	38.6	37.6	36.9	35.9	34.5	31.4	30.7	30.0	29.3	28.6	27.6	25.2	24.5	23.8	23.1	22.1	20.7	
Moderate abr OW	55.2	37.2	35.0	33.9	32.5	30.9	30.1	29.5	28.7	27.6	25.1	24.5	24.0	23.4	22.9	22.1	20.1	19.6	19.0	18.5	17.7	17.2	
Mod Sev abr RT	46.2	31.0	29.3	28.4	27.3	25.9	25.2	24.7	24.0	23.1	21.0	20.6	20.1	19.7	19.2	18.5	16.9	16.4	15.9	15.5	14.8	15.5	
Severe abrasions	34.5	23.1	21.9	21.2	20.3	19.3	18.8	18.4	17.9	17.2	15.7	15.3	15.0	14.7	14.3	13.8	12.6	12.2	11.9	11.5	11.0	11.7	
Deep bruises	20.7	13.8	13.1	12.7	12.2	11.6	11.3	11.1	10.8	10.3	9.4	9.2	9.0	8.8	8.6	8.3	7.5	7.3	7.1	6.9	6.6	4.5	
Cracks	10.3	6.9	6.6	6.4	6.1	5.8	5.6	5.5	5.4	5.2	4.7	4.6	4.5	4.4	4.3	4.1	3.8	3.7	3.6	3.5	3.3	3.2	

Figure D.1: APPROXIMATE TENSILE BREAKING STRESSES OF SODA LIME GLASS (psi)

E

GBEB: 'Eco'

E.1. Technical Drawing

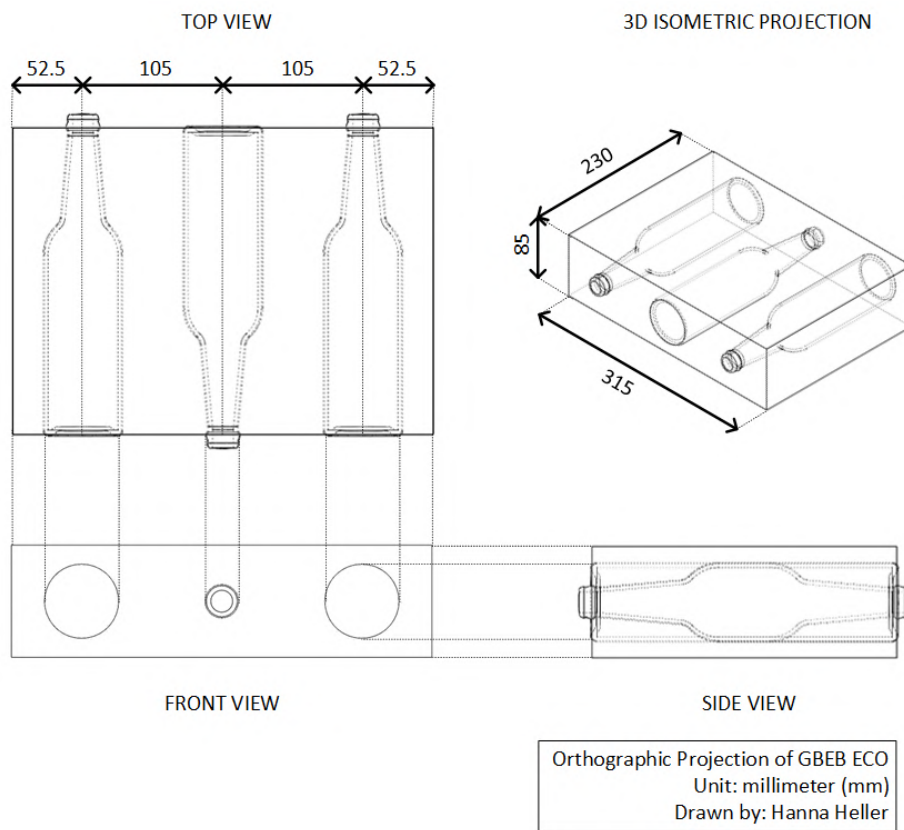


Figure E.1: Orthographic Projection of GBEB 'Eco'

E.2. FEM: Principal Stresses

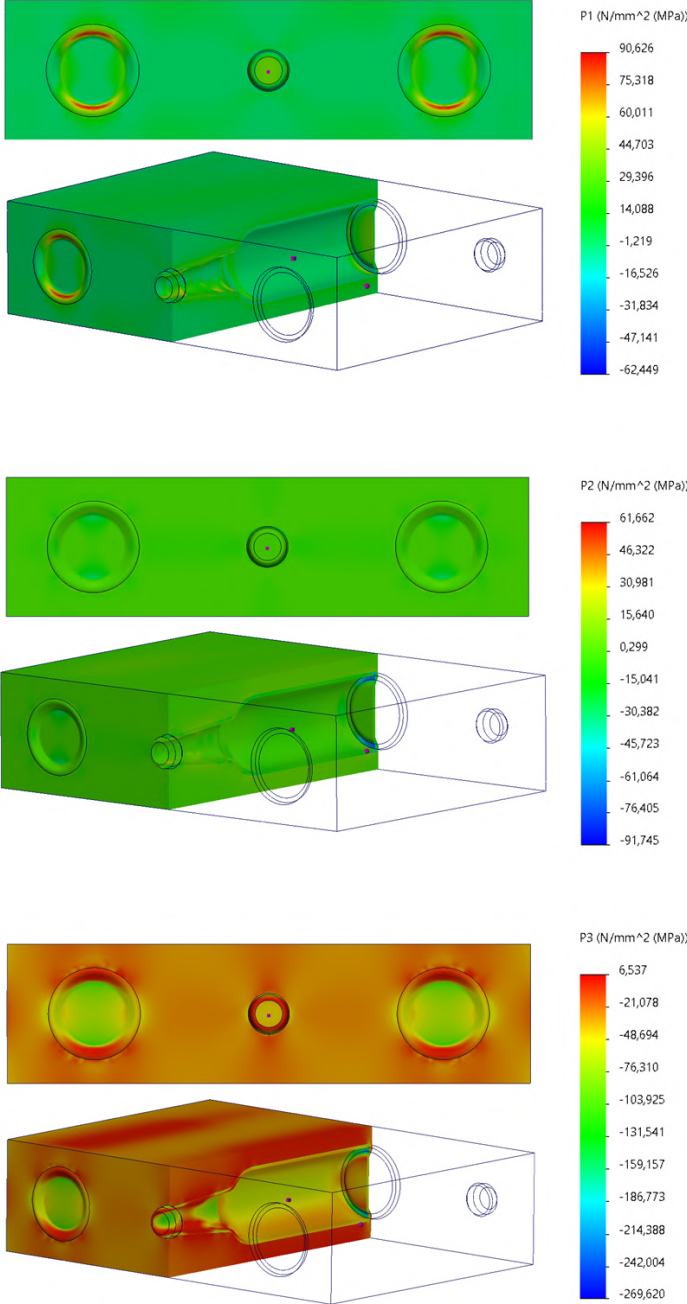


Figure E.2: Principal Stresses of GBEB 'Eco'

E.3. Design Resistance

In order to define the design resistance, the same method and formula's are used as in Subsection 8.6.

The stress factor K_{stress} is primarily defined as the ratio of the maximum tensile stress experienced by the glass bottle to the stress induced on the brick due to the applied displacement.

$$K_{stress} = \frac{\sigma_{peak,bottle}}{\sigma_{applied,brick}}$$

Which is filled in as:

$$K_{stress} = \frac{90.63 [MPa]}{20.05 [MPa]} = 4.52[-]$$

The design resistance of the brick is then calculated by dividing the approximate tensile breaking stress of soda-lime glass with severe abrasions (11.7 MPa, see Appendix D) by the previously defined stress factor K_{stress} , knurl factor K_{knurls} (see Subsection 8.6), and material factor γ_M .

$$\sigma_{Rd,brick} = \frac{\sigma_{Rd,bottle}}{K_{stress} * K_{knurls} * \gamma_M}$$

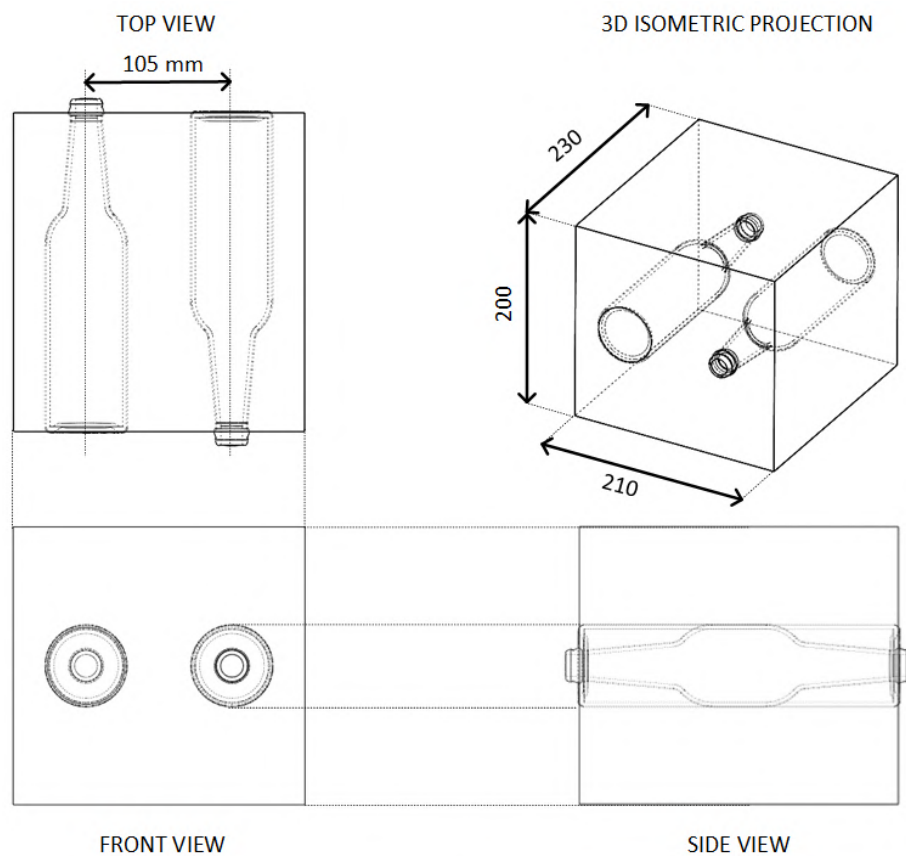
Which is filled in as:

$$\sigma_{Rd,brick} = \frac{11.7 [MPa]}{4.52 * 1.5 * 1.8} = 0.96 [MPa]$$

F

GBEB: 'Eco-Sturdy'

F.1. Technical Drawing



Orthographic Projection of GBEB ECO-STURDY
Unit: millimeter (mm)
Drawn by: Hanna Heller

Figure F.1: Orthographic Projection of GBEB 'Eco-Sturdy'

F.2. FEM: Principal stresses

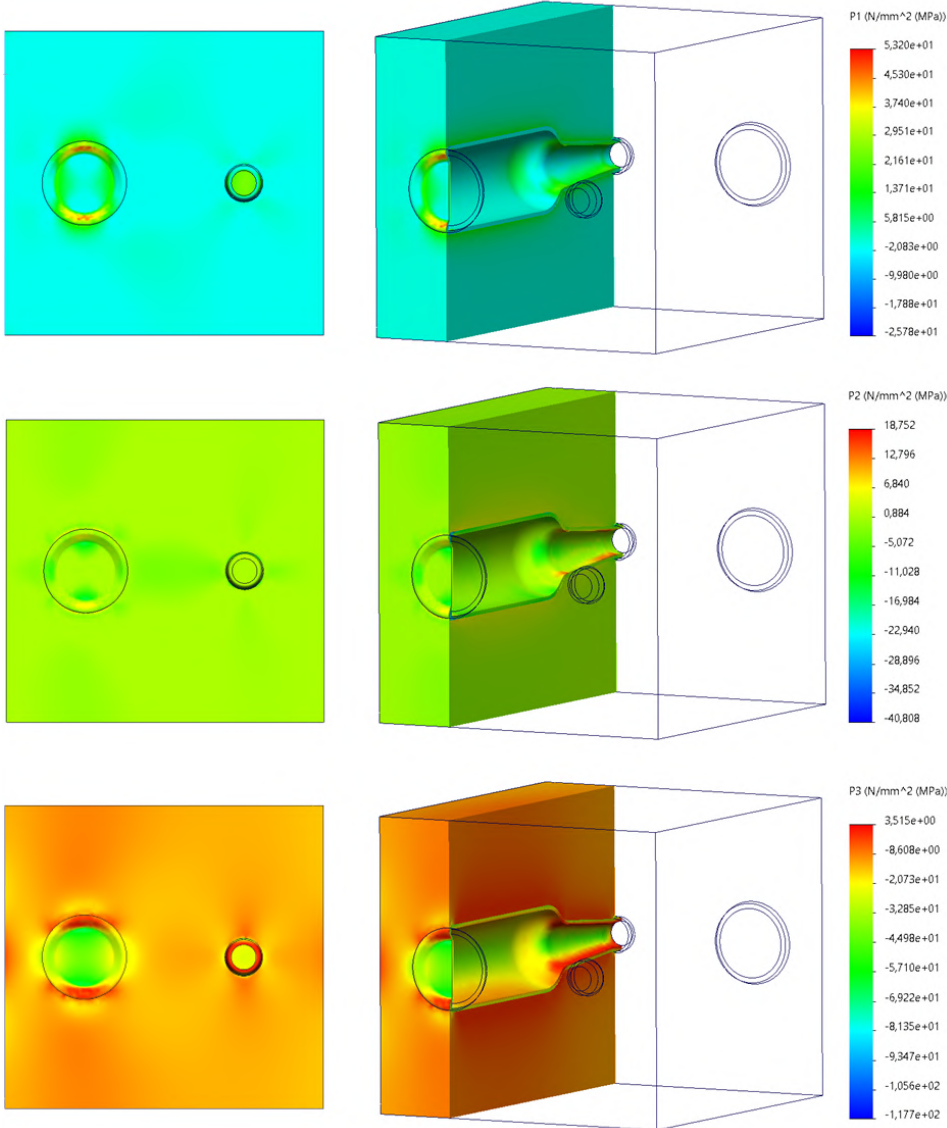


Figure F.2: Principal stresses of GBEB 'Eco-Sturdy'

F.3. Design Resistance

In order to define the design resistance, the same method and formula's are used as in Subsection 8.6.

The stress factor K_{stress} is primarily defined as the ratio of the maximum tensile stress experienced by the glass bottle to the stress induced on the brick due to the applied displacement.

$$K_{stress} = \frac{\sigma_{peak,bottle}}{\sigma_{applied,brick}}$$

Which is filled in as:

$$K_{stress} = \frac{53.20 [MPa]}{9.90 [MPa]} = 5.38 [-]$$

The design resistance of the brick is then calculated by dividing the approximate tensile breaking stress of soda-lime glass with severe abrasions (11.7 MPa, see Appendix D) by the previously defined stress factor K_{stress} , knurl factor K_{knurls} (see Subsection 8.6), and material factor γ_M .

$$\sigma_{Rd,brick} = \frac{\sigma_{Rd,bottle}}{K_{stress} * K_{knurls} * \gamma_M}$$

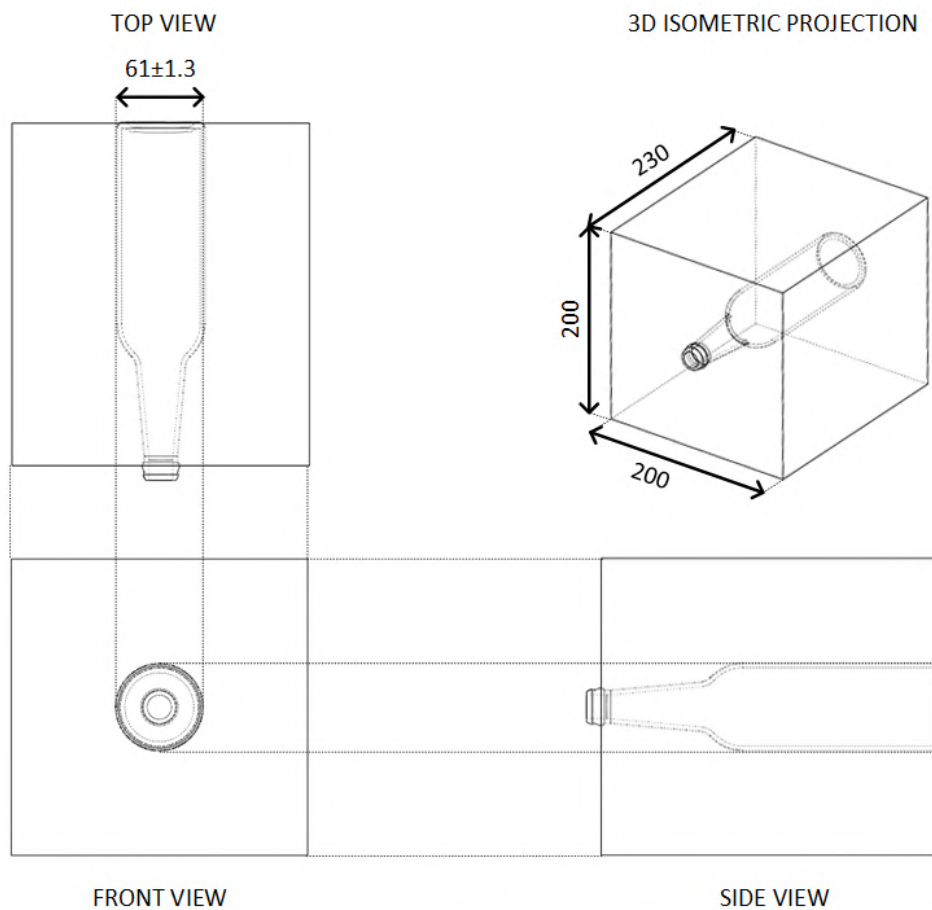
Which is filled in as:

$$\sigma_{Rd,brick} = \frac{11.7 [MPa]}{5.38 * 1.5 * 1.8} = 0.81 [MPa]$$

G

GBEB: 'Sturdy'

G.1. Technical Drawing



Orthographic Projection of GBEB STURDY
Unit: millimeter (mm)
Drawn by: Hanna Heller

Figure G.1: Orthographic Projection of GBEB 'Sturdy'

G.2. FEM: Principal Stresses

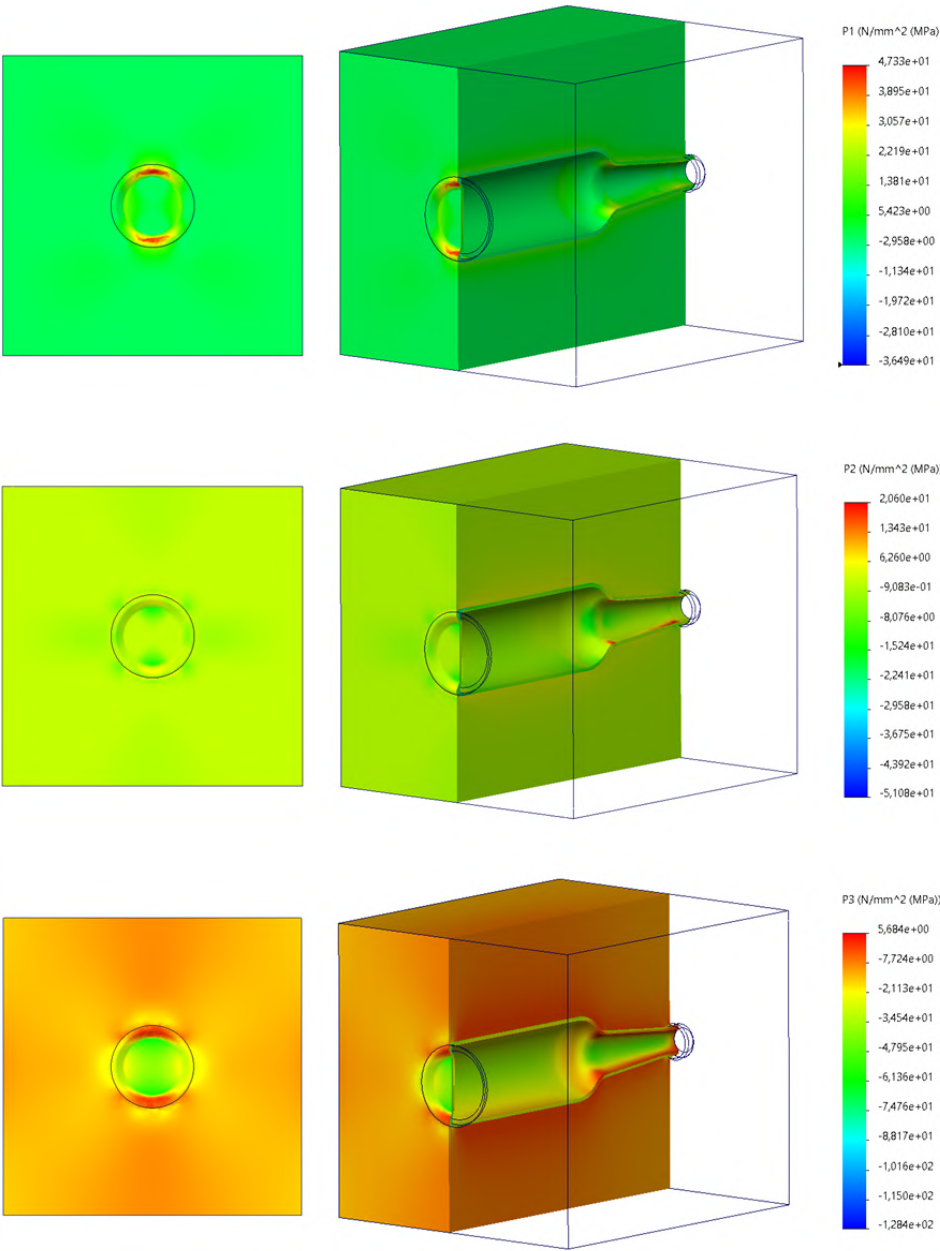


Figure G.2: Principal stresses of GBEB 'Sturdy'

G.3. Design Resistance

In order to define the design resistance, the same method and formula's are used as in Subsection 8.6.

The stress factor K_{stress} is primarily defined as the ratio of the maximum tensile stress experienced by the glass bottle to the stress induced on the brick due to the applied displacement.

$$K_{stress} = \frac{\sigma_{peak,bottle}}{\sigma_{applied,brick}}$$

Which is filled in as:

$$K_{stress} = \frac{47.33 [MPa]}{11.16 [MPa]} = 4.25 [-]$$

The design resistance of the brick is then calculated by dividing the approximate tensile breaking stress of soda-lime glass with severe abrasions (11.7 MPa, see Appendix D) by the previously defined stress factor K_{stress} , knurl factor K_{knurls} (see Subsection 8.6), and material factor γ_M .

$$\sigma_{Rd,brick} = \frac{\sigma_{Rd,bottle}}{K_{stress} * K_{knurls} * \gamma_M}$$

Which is filled in as:

$$\sigma_{Rd,brick} = \frac{11.7 [MPa]}{4.25 * 1.5 * 1.8} = 1.02 [MPa]$$